Mirian Cristina Feiten

Functional and structural studies of lipase from *Candida antarctica* (CalB) treated in pressurized fluids

Thesis for the award of the degree "Doctor of Philosophy" in Food Engineering, submitted to the Graduate Program in Food Engineering of Technology Center of Federal University of Santa Catarina.

Supervisor: José Vladimir de Oliveira, Ph.D.
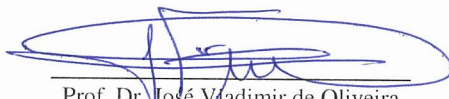Co-Supervisors: Marco Di Luccio, Ph.D.
Karine Fernanda dos Santos, Ph.D.

Florianópolis
2018

"FUNCTIONAL AND STRUCTURAL STUDIES OF LIPASE FROM *Candida antartica* (CalB) TREATED IN PRESSURIZED FLUIDS"

Por

Mirian Cristina Feiten

Tese julgada para obtenção do título de **Doutor em Engenharia Alimentos**, área de Concentração de **Desenvolvimento de Processos da Indústria de Alimentos,** e aprovada em sua forma final pelo Programa de Pós-graduação em Engenharia de Alimentos da Universidade Federal de Santa Catarina.

_____
Prof. Dr. José Vladimir de Oliveira
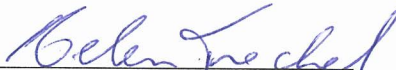**Orientador**

_____
Prof. Dr. Marco Di Luccio
Coorientador

_____
Dra. Karine Fernanda dos Santos
Coorientadora

_____
Prof. Dr. Bruno Augusto Mattar Carciofi
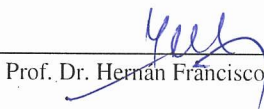**Coordenador**

Banca Examinadora:

_____
Prof. Dr. Marco Di Luccio

_____
Profa. Dra. Helen Treichel

_____
Prof. Dr. Hernán Francisco Terenzi

_____
Profa. Dra. Sandra Regina Salvador Ferreira

Florianópolis, 19 de fevereiro de 2018.

ACKNOWLEDGMENTS

RESUMO

Lipase B de *Candida antartica* (CalB) é um dos biocatalizadores mais utilizados em síntese orgânica devido à sua capacidade de atuar em diversos substratos, apresentar ampla especificidade pelo substrato e enantiosseletividade, tolerância a meios não aquosos e resistência à desativação térmica. CalB foi caracterizada, tratada em fluidos pressurizados e sua estrutura determinada por cristalografia de raios X antes e após o tratamento em alta pressão. Dicroísmo circular, fluorimetria diferencial de varredura, espectrometria de massas e cromatografia por exclusão de tamanho − espalhamento de luz a múltiplos ângulos foram algumas das técnicas utilizadas para caracterizar a CalB. A lipase é composta por 50,9% de α-hélices e folhas-β paralelas e antiparalelas, e apresentou uma temperatura de fusão máxima de 65,1 °C em TrisHCl 50 mM pH 8,4. Cristais da CalB purificada por filtração em gel, não tratada em alta pressão, difrataram a 1,7 Å e, resolvendo a estrutura por substituição molecular, foi verificado que a α5 não está presente na nossa molécula, provavelmente devido à presença de um ligante no sítio ativo (Ser105). Também foi possível modelar na estrutura da CalB duas moléculas de N-acetilglucosamina (NAG) ligadas a Asn74, seguidas por três moléculas de manose. Esta é a primeira estrutura da CalB que mostra um estado intermediário enzima/substrato ligado determinada até o momento. Uma atividade de hidrólise residual específica de 132% foi observada quando a CalB foi exposta em dióxido de carbono (CO_2) a 35 °C, 75 bar por 1 hora. A atividade de hidrólise da CalB foi de 142% quando tratada com gás liquefeito de petróleo (GLP) a 65 °C, 30 bar e 1 hora, e os cristais da CalB purificada após exposição a essas condições difrataram a 2,15 Å. Cristais da CalB purificada após exposição a 160 bar, 35 °C e 1 hora em CO_2 (atividade residual de 89%) difrataram a 2,3 Å. Não foi possível modelar um substrato ligado a Ser105 na CalB tratada com CO_2 e a densidade eletrônica foi suficiente apenas para alocar duas moléculas de NAG ligadas a Asn74. Por outro lado, foi possível modelar um ligante na Ser105 em três das seis moléculas da unidade assimétrica da CalB tratada com GLP e apenas uma molécula de NAG foi modelada anexada a Asn74. Os tratamentos com CO_2 ou GLP efetivamente mudam a conformação da proteína, ao ponto que a CalB é mais propensa a perder seu ligante e seus açúcares, seja concomitantemente com o tratamento ou durante a etapa de filtração em gel, promovendo, portanto, outras

possibilidades de empacotamento do cristal. Considerando a falta de estudos sobre modificações estruturais de enzimas causadas pelo tratamento sob alta pressão, os resultados atuais são inéditos na literatura especializada e podem ajudar a entender os fenômenos de ativação e desativação da CalB em CO_2 e GLP, bem como estimular a aplicação de tais técnicas a outras enzimas de interesse.

Palavras-chave: cristalografia 1. estrutura tridimensional 2. lipase 3. fluido pressurizado 4. dióxido de carbono 5. gás liquefeito de petróleo 6.

RESUMO EXPANDIDO

Introdução
Lipase B de *Candida antartica* (CalB) é um dos biocatalizadores mais utilizados em síntese orgânica devido à sua capacidade de atuar em diversos substratos, apresentar ampla especificidade e enantiosseletividade, tolerância a meios não aquosos e resistência à desativação térmica. O uso de fluidos pressurizados como solventes para reações bioquímicas pode ser uma rota promissora no sentido de eliminar resíduos de solventes líquidos convencionais dos produtos da reação. Além de aumentar as taxas de transferência de massa, os processos industriais em condições próximas ao ponto crítico do fluido são vantajosos em termos de consumo de energia, facilidade de recuperação dos produtos e minimização da formação de produtos secundários indesejados. Vários estudos têm relatado alterações na atividade catalítica de enzimas submetidas a tratamentos em altas pressões, porém poucos trabalhos aprofundam a análise estrutural destas enzimas. Como existe uma infinidade de aplicações de enzimas em sistemas reacionais em gases pressurizados, possivelmente um maior conhecimento das características e do comportamento destas enzimas nestes solventes significaria um aprimoramento destas aplicações.

Objetivos
Como uma pesquisa detalhada na literatura especializada apontou uma falta de estudos sobre modificações estruturais de enzimas causadas pelo tratamento sob alta pressão, o objetivo principal desta tese é caracterizar a CalB, uma lipase amplamente utilizada nas indústrias alimentícia, química e farmacêutica, investigar seu comportamento em fluidos pressurizados e elucidar sua estrutura tridimensional, comparando as estruturas e analisando possíveis mudanças conformacionais que possam ocorrer devido ao tratamento em alta pressão.

Metodologia
Dicroísmo circular (CD), fluorimetria diferencial de varredura (DSF), espectrometria de massas (MS) e cromatografia por exclusão de tamanho – espalhamento de luz a múltiplos ângulos (SEC-MALS) foram algumas das técnicas utilizadas para caracterizar a CalB quando da realização do Doutorado Sanduíche na Freie Universität Berlin (FUB). Os experimentos de alta pressão foram realizados no Laboratório de Termodinâmica e Tecnologia Supercrítica do Departamento de Engenharia Química e de Alimentos (EQA) da

Universidade Federal de Santa Catarina (UFSC). A CalB foi submetida a tratamentos com dióxido de carbono supercrítico (SC-CO$_2$) e gás liquefeito de petróleo comprimido (GLP) e o efeito foi mensurado pela diferença na atividade de hidrólise da enzima antes e após o tratamento. As estruturas tridimensionais da CalB não tratada, tratada com SC-CO$_2$ e tratada com GLP foram determinadas via cristalografia de raios-X na FUB, e então comparadas.

Resultados e Discussão

Dados de CD indicaram que a CalB é composta por 50,9% de α-hélices e folhas-β paralelas e antiparalelas, e apresentou, via DSF, uma temperatura de fusão (T$_m$) máxima de 65,1 ℃ em TrisHCl 50 mM pH 8,4. Cristais da CalB purificada por filtração em gel, não tratada em alta pressão, difrataram a 1,7 Å e, resolvendo a estrutura por substituição molecular, foi verificado que a α5 não está presente na nossa molécula, provavelmente devido à presença de um ligante no sítio ativo (Ser105). Também foi possível modelar na estrutura da CalB duas moléculas de N-acetilglucosamina (NAG) ligadas a Asn74, seguidas por três moléculas de manose. Esta é a primeira estrutura da CalB que mostra um estado intermediário enzima/substrato ligado determinada e depositada até o momento no Protein Data Bank (PDB). Uma atividade de hidrólise residual específica de 132% foi observada quando a CalB foi exposta em SC-CO$_2$ a 35 ℃, 75 bar por 1 hora. A atividade de hidrólise da CalB foi de 142% quando tratada com GLP a 65 ℃, 30 bar e 1 hora, e os cristais da CalB purificada após exposição a essas condições difrataram a 2,15 Å. Cristais da CalB purificada após exposição a 160 bar, 35 ℃ e 1 hora em SC-CO$_2$ (atividade residual de 89%) difrataram a 2,3 Å. Não foi possível modelar um substrato ligado a Ser105 na CalB tratada com SC-CO$_2$ e a densidade eletrônica foi suficiente apenas para alocar duas moléculas de NAG ligadas a Asn74. A estrutura da CalB tratada em SC-CO$_2$ encontra-se no estado fechado. Acreditamos que a CalB não tenha o substrato ligado à Ser105 (1) após o tratamento com SC-CO$_2$ ou (2) após a filtração em gel, ou apenas muito poucas moléculas do cristal estão ligadas ao substrato, o que não produz uma densidade eletrônica clara no sítio ativo. Por outro lado, foi possível modelar um ligante na Ser105 em três das seis moléculas da unidade assimétrica da CalB tratada com GLP (monômeros A, B e C) e apenas uma molécula de NAG foi modelada anexada a Asn74 em todos os monômeros. Acreditamos que o sítio ativo também não está totalmente ocupado pelo substrato em todas as moléculas do cristal da CalB tratada com GLP. Análises de SEC-MALS revelaram que a CalB encontra-se no estado monomérico em solução, mesmo na presença do

substrato ou após o tratamento em fluidos pressurizados. Portanto, as duas ou seis moléculas da unidade assimétrica encontradas nas estruturas de raios-X são devidas apenas ao empacotamento do cristal. Acreditamos, no entanto, que os tratamentos com CO_2 ou GLP efetivamente alteram a conformação da proteína, ao ponto que a CalB é mais propensa a perder seu ligante e seus açúcares, seja concomitantemente com o tratamento ou durante a etapa de filtração em gel subsequente, promovendo, portanto, outras possibilidades de empacotamento do cristal.

Considerações finais

Considerando a falta de estudos sobre modificações estruturais de enzimas causadas pelo tratamento sob alta pressão, a investigação do comportamento da CalB em fluidos pressurizados e a determinação das estruturas tridimensionais da lipase tratada e não tratada, via cristalografia de raios X, representam um grande avanço na área. Ainda há muitas questões a serem abordadas, mas os resultados atuais são inéditos na literatura especializada e podem ajudar a entender os fenômenos de ativação e desativação da CalB em CO_2 e GLP, bem como estimular a aplicação de tais técnicas a outras enzimas de interesse.

Palavras-chave: cristalografia 1. estrutura tridimensional 2. lipase 3. fluido pressurizado 4. dióxido de carbono 5. gás liquefeito de petróleo 6.

ABSTRACT

CalB from *Candida antarctica* is one of the biocatalysts most used in organic synthesis due to its ability to act in several substrates, wide substrate specificity and enantioselectivity, tolerance to non-aqueous environment and resistance to thermal deactivation. CalB was characterized, treated in pressurized fluids and its structure was determined by X-ray crystallography before and after high-pressure treatment. Circular dichroism, differential scanning fluorimetry, mass spectrometry and size exclusion chromatography − multi-angle light scattering were some of the techniques used to characterize CalB. The lipase is composed of 50.9% of α-helix and parallel and antiparallel β-sheets, and showed a maximum melting temperature of 65.1 ℃ in 50 mM TrisHCl pH 8.4. Crystals of untreated gel-filtration purified CalB diffracted to 1.7 Å and, by solving the structure by molecular replacement it was noticed that α5 is not present in our molecule, probably due to the presence of a ligand at the active site (Ser105). It was also possible to model in the CalB structure two N-acetylglucosamine (NAG) molecules attached to Asn74, followed by three mannoses. This is the first CalB structure showing an intermediate bound-state enzyme up to date. Residual specific hydrolysis activity of 132% was observed when CalB was exposed to carbon dioxide (CO_2) at 35 ℃, 75 bar and 1 hour. CalB hydrolysis activity was 142% when treated with liquefied petroleum gas (LPG) at 65 ℃, 30 bar and 1 hour, and crystals of CalB purified after exposure to these conditions diffracted to 2.15 Å. Crystals of CalB purified after exposure to 160 bar, 35 ℃ and 1 hour in CO_2 (residual activity of 89%) diffracted to 2.3 Å. It was not possible to place a substrate bound to Ser105 in the CO_2 treated CalB and the electronic density was only enough to place two NAG molecules attached to Asn74. On the other hand, it was possible to place a ligand bound to Ser105 in three of the six molecules of the asymmetric unit of CalB treated with LPG and only one NAG molecule was modeled attached to Asn74. The treatments under CO_2 or LPG do change the protein conformation to the point that CalB is more prone to lose its ligand and its sugars, either concomitantly with the treatment or during the gel-filtration run, therefore promoting other crystal packing possibilities. Considering the lack of studies concerning structural modifications of enzymes caused by treatment under high pressure, the present results are unprecedented in the specialized literature, and may

help to understand CalB activation and deactivation phenomena in SC-CO_2 and LPG as well as to encourage the application of such techniques to other enzymes of interest.

LIST OF FIGURES

LIST OF TABLES

CONTENTS

1.   INTRODUCTION

Biocatalysis has exponentially grown in the last years mainly due to the molecular biology and protein engineering tools, which allow manipulating variables such as selectivity, stability, activity and tolerance to non-aqueous solvents. Currently, there are several enzymes known to act well in organic solvents or supercritical fluid systems in the absence of water. The advantages of supercritical fluids include higher substrate solubility, modification of the enzyme specificity and absence of undesirable hydrolytic reactions. Those features broaden the scale of the enzymatic reaction applications and expand the use of those reactions for chiral pharmaceutical compounds production and for enantioselective polymerization (OLIVEIRA; MANTOVANI, 2009).

Several medicines, amino acids, saccharides and polysaccharides, vitamins and esters are produced by enzymatic biotransformation in industrial scale. Essentially, all those reactions are carried out in aqueous reaction systems and occasionally in organic solvents. Although the chemical reactions in sub and supercritical fluids have been used in large scale operations in the 20th century, the employment of such fluids in large scale for biosynthesis is still under development. On the other hand, the studies related to enzymatic catalysis in pressurized fluids have promptly increased in the last years. There is clear evidence in the literature regarding pressurized fluids adequacy as enzymatic reaction medium (KNEZ; HABULIN; KRMELJ, 1998; OLIVEIRA; OLIVEIRA, 2000; 2001; KNEZ; HABULIN, 2002; DALLA ROSA et al., 2008; 2009; ESMELINDRO et al., 2008; HILDEBRAND et al., 2009; BRUSAMARELO et al., 2010; PRADO et al., 2012; SHIN et al., 2012).

The use of pressurized fluids as solvents for chemical and biochemical reactions may be a promising alternative to eliminate conventional solvent residues from the final products. Moreover, industrial processes performed under conditions near the solvent critical point can be advantageous in terms of energy costs, ease of product recovery and minimization of secondary products formation (KNEZ; HABULIN; KRMELJ, 1998; HABULIN; KNEZ, 2001).

The catalytic activity, specificity and stability of enzymes depend on their three-dimensional structures. Environmental conditions such as pH, temperature, ionic strength among others affect the enzyme structure and, consequently, its properties (LIMA et al., 2001). Therefore, it is important to highlight that the solvent can strongly affect the enzyme activity by its interaction with the support of immobilized enzymes or the residues of free enzymes. In this context, as a previous step to enzyme application as a biocatalyst, it is relevant to evaluate the enzyme behavior in these alternative solvents (FEIHRMANN, 2005; PRIMO et al., 2007).

The enzyme specificity is basically the interaction between the substrate or the inhibitor molecule and the enzyme active site, by hydrogen bond and/or van der Waals and electrostatic interactions (DIXON; WEBB, 1979).

The catalytic activity of enzymes is a function of their tertiary and quaternary structures. Enzyme proprieties can be modified by treatments (heating, pH changes, salt concentration, ions and cofactors, high pressure, ultrasound waves, magnetic field, etc.) which lead to impaired substrate binding, or an increase in enzymatic activity due to structural modifications (SCRIBAN, 1985; LEHNINGER; NELSON; COX, 1995).

There are several techniques documented in the literature to determine the secondary and tertiary structures of enzymes, each one with its own peculiarities. The spectroscopic techniques of Mössbauer, Raman, fluorescence, infrared, UV-visible and circular dichroism are used to determine a protein's secondary structure. To determine the three-dimensional structure of proteins, meaning locate the position of amino acid residues in space, X-ray crystallography, nuclear magnetic resonance (NMR) and cryo-electron microscopy (cryo-EM) are the methods of choice. Structural studies have the potential to reveal details about reaction mechanisms, such as the substrate binding mode at the active site of enzymes (STRYER, 1995; LEHNINGER; NELSON; COX, 1995).

Some studies have shown modification on the enzyme catalytic activity after treatment in pressurized fluids (OLIVEIRA et al., 2006a; 2006b; FRICKS et al., 2006; 2009; PRIMO et al., 2007; ANDRADE et al., 2008; EISENMENGER; REYES-DE-CORCUERA, 2009; FRANKEN et al., 2010; KUHN et al., 2010; 2011; 2013; MANERA et

al., 2011; BRAGA et al., 2012; LIU et al., 2012; SILVA et al., 2012; 2013a; 2013b; CHEN et al., 2013; SENYAY-ONCEL; YESIL-CELIKTAS, 2013; MELGOSA et al., 2015), but only a few studies have been carried out to deeply analyze structural changes that may have occurred (LIU; CHEN; WANG, 2013a; CHEN et al., 2013a; 2013b; MELGOSA et al., 2015). As there is a wide variety of enzyme applications in pressurized/supercritical fluids media, most likely a deeper knowledge of the characteristics and the behavior of enzymes in these solvents would mean a technological upgrade in such techniques.

The investigation of enzyme behavior in pressurized fluid systems is extremely relevant to enhance enzyme's catalytic activity/specificity and to increase enzyme stability during storage after the treatment, both properties that are essential for industrial application. Additionally, the determination of three-dimensional structures before and after enzyme treatment may help to elucidate its mechanisms of activation or deactivation, i.e., to reveal the effects of pressure treatment on the enzyme structure and possible changes in the catalytic activity after exposure to pressurized fluids.

1.1 OBJECTIVES

1.1.1 Main objective

As a detailed search in the specialized literature pointed out a lack of studies concerning structural modifications of enzymes caused by the treatment under high pressure, it is important to investigate the behavior of lipase B from *Candida antarctica* (CalB) in pressurized fluids, which is a lipase widely used in food, chemical and pharmaceutical industries. With that in mind, the main goal of this thesis is to characterize this enzyme of great industrial interest, to investigate its behavior in pressurized fluids and to elucidate its three-dimensional structure, comparing the structures and analyzing possible changes that might occur due to high-pressure treatment.

1.1.2 Specific objectives

Based on the main goal, the following specific aims were defined:

- Functional and structural characterization of the commercial lipase B from *Candida antarctica* (Lipozyme CALB L®);

- Investigation of the influence of process variables (temperature, pressure, time of exposure) on the hydrolysis activity of CalB, treated in pressurized fluids (supercritical carbon dioxide - CO_2 - and compressed liquefied petroleum gas - LPG);

- Stability evaluation of CalB, treated in the best condition with CO_2 and LPG, during storage at different temperatures;

- Three-dimensional structure determination, via X-ray crystallography, of CalB before and after treatment in pressurized fluids.

2.   LITERATURE REVIEW

This section presents a summary of the basic theory in which this research is based on, including the topics of lipases, pressurized fluids and the influence of high pressure treatments on the activity and stability of enzymes. There is an increased use of pressurized fluids as solvents for enzymatic reactions aiming to improve their activity and stability for later application in industrial catalysis.

2.1 ENZYMES

Enzymes are versatile biocatalysts, as they selectively catalyze reactions in short times and under mild temperature and pressure conditions. The major advantage of enzymes is that they catalyze molecular transformations with no parallel reactions occurrence − common in chemical synthesis − due to their specificity (DZIEZAK, 1991; PATEL, 2002; PIZARRO; PARK, 2003).

Enzymes are proteins biologically active responsible for catalysis of several biochemical reactions. In an enzyme, there is a region called "active site" which binds the substrate – the reagent molecule (which could be a small compound or a stretch of residues from another protein) – and reduces the energy required to the transition state that leads to the desired product. The binding between the active site and the substrate is extremely specific – the substrate must have certain surface features that allow its "fitting" to the enzyme's active site (BORZANI et al., 2001).

All the known enzymes are proteins and are composed by the same 20 amino acids covalently bound in different sequences. The aminoacid sequence has 4 structural levels. The primary structure is characterized by the linear sequence of amino acids and peptide bonds in the molecule; it is the simplest and the most important structural level, since the whole spatial arrangement of the molecule is derived from it. The secondary structure is characterized by the establishment of hydrogen bonds between amino acids in a protein chain; the most common secondary structure elements are the α-helix and the β-sheet. The tertiary structure is the "global" organization of a single polypeptide chain; it is the three-dimensional arrangement the protein assumes to perform its functions. A determinant factor for maintaining a globular tertiary structure is the hydrophobic effect, i.e., the side chains of non-polar amino acids are mostly "hidden" within the structure and the side

chains of polar residues are mostly exposed on the surface. Hydrogen bonds and salt bridges are also fundamental to stabilize the tertiary structure of proteins. The quaternary structure is characterized by the combination of two or more polypeptide chains into a structure with several subunits, an oligomer, resulting in an active unit LEHNINGER; NELSON; COX, 1995).

The industrial application of biocatalysts has been driven by the increased concerns with environmental pollution, product quality and cost reduction of some industrial sectors (HASAN; SHAH; HAMEED, 2006; SCHERER, 2010). The benefits offered by enzymes are: their specificity (which allows the control of products formed and minimization of undesirable side reactions), their operation under mild temperature and pressure conditions (the industrial plant can be operated with less capital and energetic costs, besides the minimization of product thermal degradation), and minimal waste production (less costs to treat the waste and negligible contribution of enzyme to the biological oxygen demand (BOD)).

2.2 LIPASES

The industrial interest for enzymatic technologies has gradually been increasing, mainly in the protein engineering areas in non-conventional reaction systems, which have considerably enhanced enzyme application as catalysts in industrial processes. Among those processes, the most interesting are esterification, transesterification and hydrolysis of lipids performed by lipases. The large biotechnological potential of lipases is mostly due to their interesting features: i) high stability in organic solvents; ii) high substrate specificity; iii) high enantioselectivity. The knowledge of those advantages has provided a desirable increase in the production and commercialization of lipases, resulting in a consistent development of alternative technologies for industrial application (CASTRO et al., 2004).

Lipases (triacylglycerol acyl hydrolases, E. C. 3.1.1.3) are a special group of esterases, classified as hydrolases, and act in ester bonds present in acylglycerols, releasing diacylglycerols, monoacylglycerols, fatty acids and glycerol. They act in substrates slightly soluble in water, in the water/lipid interface, hydrolyzing, mainly, acylglycerols of long chain (more than 10 carbon atoms) (CÔTÉ; SHARECK, 2008).

Lipases are able to catalyze hydrolysis of acylglycerols as well as synthesis of esters from glycerol and fatty acids of long chains (VILLENEUVE et al., 2000). The reaction equilibrium can be displaced towards the hydrolysis or synthesis by the water content of the reactive medium (Figure 1). These reactions present extremely high regioselectivity or enantioselectivity, which characterize lipases as an important group of biological catalysts.

Figure 1. General scheme of esterification and hydrolysis reactions. Source: CASTRO et al. (2004).
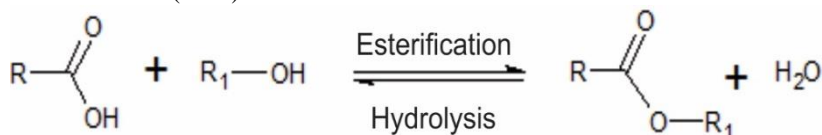
Lipases are commonly found in animal tissues (pancreas, liver and gastric mucosa) and vegetables (seeds, pulp and roots), and can also be produced by microorganisms (bacteria, filamentous fungi and yeast). From an economic and industrial point of view, lipases from microorganisms present advantages against those obtained from animal and vegetable sources, due to the ease of production and abundance of microorganisms able to synthesize them. Besides, lipases from animals or vegetables have high costs of isolation (CASTRO; ANDERSON, 1995). According to SOARES (2000), the microorganisms more often used for lipase production are fungus of *Rhizopus*, *Aspergillus* and *Mucor* gender, and yeast of *Candida* gender.

Most lipases present maximum activity in a temperature range between 30 and 40 ºC, although their thermal stability changes substantially depending on their source – microbial lipases may resist higher temperatures (65-70 ºC) (MACRAE; HAMMOND, 1985). The molecular mass of lipases is generally between 20 and 75 kDa (CARVALHO et al., 2003). In general, they are active in a wide pH range, presenting high activity between pH 5 and 9 with maximum activity between 6 and 8, and do not require cofactor (GHANEM; ABOUL-ENEIN, 2005).

Lipases can show specificity or selectivity to the substrate (chemo), to the position (regio) or to the isomer (stereo). Chemospecificity is related to the different activity rates shown by the same enzyme towards different substrates. Lipases may have specificity for tri-, di-, or monoacylglycerols or other fatty acid esters, obtained

from the same carboxylic acid molecule, and may be able to distinguish among fatty acids of different chain sizes. Regiospecificity is related to the different enzymatic activities shown by the same lipase towards the different positions of the fatty acid in the triacylglycerol. On the other hand, stereospecificity is related to the different activity rates shown by the same lipase towards the different isomers of a molecule (PINHEIRO, 1992; VILLENEUVE, 2003).

Lipases are able to catalyze a wide diversity of reactions such as hydrolysis, interesterification, alcoholysis, acidolysis, esterification, aminolysis. Figure 2 shows a scheme of the main reactions catalyzed by lipases. These enzymes are widely used in biotransformation processes because, among other features, they exhibit affinity to a large spectrum of substrates, versatility under different reaction environments (aqueous, organic or supercritical), high activity in reaction medium with no solvent and commercial availability (PANDEY et al., 1999).

Figure 2. Reactions catalyzed by lipases. Source: PAQUES; MACEDO (2006).

Due to the specificity, lipases are important in the organic synthesis or hydrolysis of enantioselective compounds in pharmaceutical, food, chemical and cosmetic industries (production of medicine; detergents; pesticides; flavors, sweeteners, modified carbohydrates and other food additives; oils and derivatives, biodiesel; leather; waste treatment) (BORNSCHEUER; KAZLAUSKAS, 1999; LEAL et al., 2002; BURKERT, 2002; BARON, 2003; BURKERT; MAUGERI; RODRIGUES, 2004; DALLA-VECCHIA; NASCIMENTO; SOLDI, 2004; BEVILAQUA, 2005; HASAN; SHAH; HAMEED, 2006; KADER; YOUSUF; HOQ, 2007; TREICHEL et al., 2010; MATSUDA, 2013).

In the last years, lipases have been increasingly used in biodiesel production, by transesterification of triglycerides and alcohols of short chain. The resulting long chain fatty acid esters have been used as fuel, since they do not generate sulfur oxides and particulates upon combustion (ISO et al., 2001). The increasing interest in alternative fuels is consequence of the petroleum shortage and environmental concerning (LEE; FOGLIA; CHANG, 2002).

Nowadays, the major obstacle to the use of lipases in industrial processes is related to their high costs; however, recent and constant advances in genetic engineering technology and enzyme immobilization indicate promising changes in this scenario in the near future (SAXENA et al., 2003a; 2003b).

2.3 LIPASE B FROM *Candida antarctica* (CALB)

Lipase B from *C. antarctica* (CalB) is one of the biocatalysts most used in organic synthesis, due to its ability to act in several substrates, tolerance to non-aqueous environment and resistance to thermal deactivation (McCABE; TAYLOR, 2004; LUTZ, 2004). CalB is an extracellular enzyme that is commercially available in a sorbitol-based solution (CALB L®) and immobilized in a resin via ionic bond (Novozym 435). CalB is extremely stereospecific for synthesis and hydrolysis of esters, mainly due to the small hydrophobic portion, which is a CalB peculiarity (IDRIS; BUKHARI, 2012). On the opposite way of most of lipases, CalB does not present interfacial activation phenomenon, and the active site access is made through a narrow channel covered by a small highly mobile helix (JAEGER; REETZ, 1998).

CalB has huge industrial applicability mainly due to its high stability and stereoselectivity, wide substrate specificity and enantioselectivity, which makes it superior to other lipases in biotransformation processes (RAZA; FRANSSON; HULT, 2001; JUN et al, 2013). CalB assumes an open or closed conformation depending on the surrounding medium. The open conformation shows a restricted entrance to the active site that can justify its high specificity. This open conformation exposes a highly hydrophobic pocket, which renders the enzyme unstable in homogeneous aqueous medium. Therefore, CalB is in a closed conformation in aqueous medium. However, in hydrophobic surfaces, the open conformation is favored, and the lipase may be easily adsorbed to oil droplets for example, even in low ionic strength (HERNANDEZ; GARCIA-GALAN; FERNANDEZ-LAFUENTE, 2011).

The first CalB structure was solved by X-ray crystallography, published in 1994 by UPPENBERG et al., at 1.55 Å resolution (Protein Data Bank (PDB) code: 1TCA, Figure 3). Basically, CalB is an α/β hydrolase, composed by 317 amino acids, arranged in 10 α-helices and 9 β-sheets. In the structure, there is one molecule in the asymmetric unit and a glycan, an N-acetyl glucosamine (NAG) attached to the asparagine 74.

Figure 3. 1TCA structure of lipase B from *Candida antarctica* solved at 1.55 Å by Uppenberg et al. (1994). (**A**) general view, (**B**) active site and lid, (**C**) N-glycosylation.

B

C
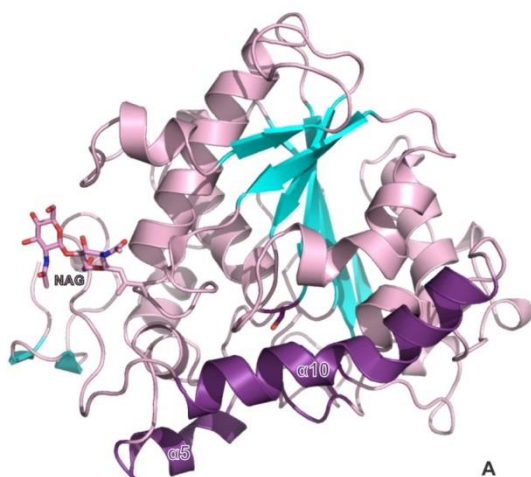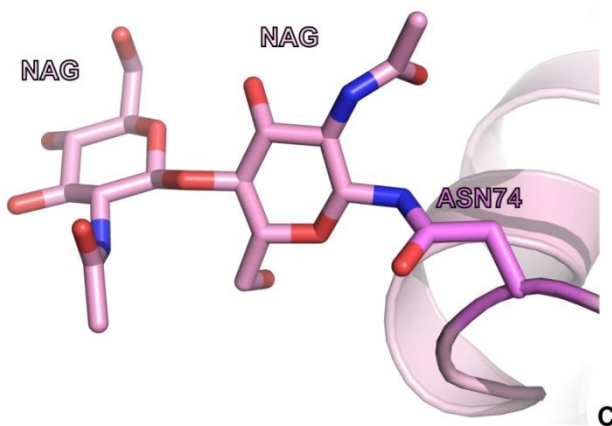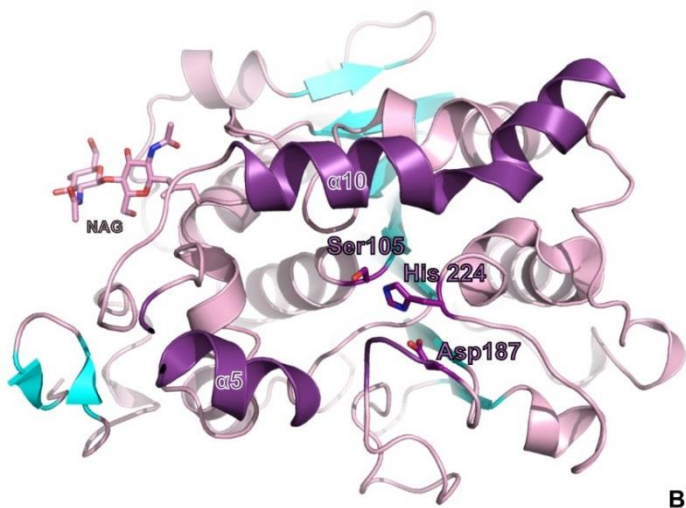
The catalytic triad is made up from serine 105 (Ser105), aspartate 187 (Asp187) and histidine 224 (His224). The active site is accessible to external solvent through a narrow channel of approximately 10 Å x 4 Å wide and 12 Å deep, as measured from the Oγ of Ser105 to the surface. Most of the channel is formed by three parts of the structure: helices α5 and α10 and a loop region which projects isoleucine 189 (Ile189) into

the channel. The channel walls are very hydrophobic and are lined with mostly aliphatic residues. This channel is covered by a "lid", which elements are highlighted in purple in Figure 3 (a) and (b). This lid can be open or closed depending on the enzyme cycle, and its conformation will define the access to the active site. The 1TCA structure represents the open state of the lipase.

Uppenberg's workgroup had extensively studied CalB from *C. antarctica* and crystallized it in different conditions (UPPENBERG et al., 1994a; 1994b; 1995). They solved the CalB structure with different ligands bound to its active site, showing wide conformation changes of its active site surrounding, which may explain the huge variation in the specificity that CalB presents towards a wide range of substrates.

A summary of all the CalB structures deposited in PDB up to date as well as the main features and differences among them are highlighted in Table 1. A careful inspection of the structures and corresponding articles published led us to some interesting findings: CalB is in the open state when α-helix 5 is present, which is formed by residues 140-147 and corresponds to a region of high mobility; and when these residues are arranged as an unfolded loop, the lipase is in the closed state (STAUCH; FISHER; CIANCI; 2015). The first CalB structures crystallized in the closed state are dated of 2014, twenty years later than the first CalB structure solved in the open state, 1TCA, showing that researches on such lipase structure and catalytic mechanism are in constant change and improvement, and that there is still a lot to be worked on and understood.

Table 1. Summary of CalB structures deposited in PDB.

PDB code	Crystallization condition	Space group	Resolution (Å)	Chains	State	Residues Gap	Glycosylation-Position	Ligand-Position	Reference
1TCA	50 mM sodium acetate pH 3.6; 20% PEG 4000 10% isopropanol	P 2₁ 2₁ 2₁	1.55	A	Open	-	NAG - ASN74	-	UPPENBERG et al., 1994b
1TCB	50 mM sodium acetate pH 3.6; 20% PEG 4000 10% isopropanol	P 1 2₁ 1	2.1	A,B	Open	-	[2] NAG - ASN74 A	β-octylglucoside (BOG) - HIS224 (A,B)	UPPENBERG et al., 1994b
1TCC	50 mM sodium acetate pH 5.5; 20% PEG 4000 10% isopropanol	P 1 2₁ 1	2.5	A,B	Open	-	[2] NAG - ASN74 A	β-octylglucoside (BOG) - HIS224 B	UPPENBERG et al., 1994b
1LBS	0.1 M sodium citrate/citric acid pH 4; 1.3 M ammonium sulfate; 10% dioxane	C 1 2 1	2.6	A,B,C, D,E,F	Open	-	[2] NAG - ASN74 (A,B,C,D,E,F)	N-hexilphosphonate ethyl ester (HEE) - SER105 (A,B,C,D,E,F)	UPPENBERG et al., 1995
1LBT	0.1 M sodium citrate/citric acid pH 4; 1 M ammonium sulfate; 10% dioxane	P 1 2₁ 1	2.5	A,B	Open	-	[2] NAG - ASN74 (A,B)	Methyl penta oxyethyl heptadecanoate (T80) - SER105 (A,B)	UPPENBERG et al., 1995

3W9B	0.1 M phosphate-citrate pH 4.2; 40% PEG 600	P 6$_5$	2.9	A,B,C, D	Open	-	-	[4] 3,6,9,12,15,18,21-heptaoxatricosane-1,23-diol (PE8) THR40 A/ SER105 B GLN157 B THR40 C / THR40 D GLN157 D	KIM et al., 2014
4ZV7	24% PEG 3350; 0.1M citric acid pH 5.5; 0.1M sodium acetate	P 6$_3$ 2 2	2	A	Open	-	[2] NAG - ASN74	-	STRZELCZYK et al., 2016
5GV5	Tris pH 8.5; 1.2 M ammonium dihydrogen phosphate	P 1 2$_1$ 1	2.89	A,B,C, D,E,F, G,H	Open	147 C 142-149 D 146-148 E	[4] NAG - ASN74 A,C [2] NAG - ASN74 B,D,E,F,G,H	[(1S)-2-(methoxycarbonylamino)-1-phenyl-ethoxy]-propyl-phosphinic acid (MSW) – SER105 A,B,C,D,E,F,G,H	PARK; LEE, 2017
5A71	200 mM sodium acetate pH 4.8; 20% PEG 4000; 10-13% 2-propanol	P 1	0.91	A,B	Closed B	-	[2] NAG - ASN74 A,B	[3] isopropyl alcohol ILE189 A,B ILE285 B	STAUCH; FISHER; CIANCI; 2015
5A6V	200 mM sodium acetate pH 4.8; 20% PEG 4000; 10-13% 2-propanol	P 1	2.28	A,B	Closed B	-	[2] NAG - ASN74 A,B	[2] isopropyl alcohol ILE189 A,B	STAUCH; FISHER; CIANCI; 2015
3ICV	0.1M Bis-Tris pH 5.5; 0.2M sodium chloride; 25% PEG 3350	P 3$_2$ 2 1	1.49	A	-	176-181	[2] NAG ASN108 SER229	2-[bis-(2-hydroxy ethyl) amino]-2-hydroxy methyl propane-1,3-diol (BTB) - GLU222	QIAN et al., 2009
3ICW	0.2M sodium	P 3$_2$ 2 1	1.69	A	-	176-	[2] NAG	Methyl hydrogen R hexyl	QIAN et al.,

	dihydrogen phosphate pH 4.5; 20% PEG 3350					183	ASN108 SER229	phosphonate (MMH) – SER139 Phosphate ion - SER284	2009
4K5Q	0.1M Bis-Tris pH 6.5; 0.2M sodium acetate; 25% PEG 3350	C 2 2 2$_1$	1.49	A	Closed	-	-	-	XIE et al., 2014
4K6G	0.1M Bis-Tris pH 6.5; 0.2M sodium acetate; 25% PEG 3350	P 1 2$_1$ 1	1.5	A,B	Closed	141-147 A	-	[2] 1,2-ethanediol (EDO) SER105 A VAL306 A	XIE et al., 2014
4K6K	0.1M Bis-Tris pH 6.5; 0.2M sodium acetate; 25% PEG 3350	P 2$_1$ 2$_1$ 2$_1$	1.6	A,B	-	141-146 A,B	-	1,2-ethanediol (EDO) [4] ALA18 A [2] ASN96 A [2] TYR203 A PRO317 B	XIE et al., 2014
4K6H	0.1M Bis-Tris pH 6.5; 0.2M sodium acetate; 25% PEG 3350	P 1 2$_1$ 1	1.6	A,B	Closed	-	-	1,2-ethanediol (EDO) LYS13 A SER105 A ILE314 A SER67 B SER105 B PRO198 B VAL306 B	XIE et al., 2014

CalB is a serine hydrolase and, as all α/β hydrolases, share the catalytic triad and have a common fold that is characterized by mostly parallel β-sheets surrounded by α-helices. Therefore, CalB shares a similar catalytic mechanism to all α/β hydrolases (Figure 4).

Figure 4. Catalytic mechanism of CalB showing the existence of an acylation and a deacylation step. The letters in the square boxes refer to the two substrates (A, B), the two reaction products (P, Q) and the free and covalently modified enzyme species (E and E*, respectively). Source: VELD, 2010.
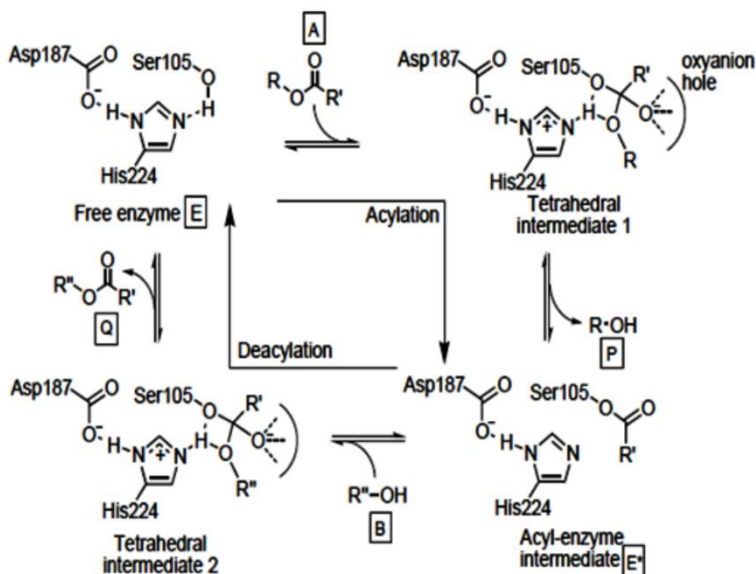
After the correct positioning of the substrate, a nucleophilic attack of Ser105 occurs in the substrate carbonyl group and a first tetrahedral intermediate is formed. In this intermediate, the proton from His224 is transferred to the substrate alkyl oxygen and the first product (alcohol) is released. As a result, the covalently bound acyl enzyme intermediate is formed. Then, a second tetrahedral intermediate is formed by attack of a nucleophilic substrate, which generally is water or alcohol, in the acyl-enzyme carbonyl group. The proton is transferred from the His224 to the Ser105 alkyl oxygen, restoring the carbonyl bond of the bound substrate. As a result, a weakly bound enzyme-product complex is formed and the free enzyme species is regenerated after

release of the reaction product, closing the catalytic cycle (VELD, 2010).

Because of the importance of CalB in organic synthesis, especially for the kinetic resolution of racemates, numerous approaches have been used to optimize the activity, specificity, selectivity and stability of CalB. This has been achieved either by changing the microenvironment of the enzyme or by optimizing the enzyme itself using random or site-directed mutagenesis (BLANK et al., 2006). Factors influencing the microenvironment are, for example, supports for immobilization (FERNANDEZ-LAFUENTE et al., 1998; CIPOLATTI et al., 2014, NICOLETTI et al., 2015; VALÉRIO et al., 2015), the content of water in an organic solvent (PIYATHEERAWONG et al., 2004) or the nature of the organic solvent itself (WESCOTT; KLIBANOV, 1994; OTTOSSON et al., 2002).

2.4 PRESSURIZED FLUIDS

In the last few decades, supercritical fluids (SCF) have been widely exploited in science and, less extensively, in the industry as potential solvents for reaction medium. Due to their physical and chemical features that can be finely tuned from gas to liquid-like properties, they have been used in diverse fields (KRAMMER; VOGEL, 2000; KNUTSON; SARKARI, 2004; KARMEE; CASIRAGHI; GREINER, 2008).

SCF are substances in a state above their temperature and pressure critical point. The critical temperature of a substance is defined as the temperature above which a pure substance cannot be liquefied, independently on the pressure applied. The critical pressure is defined as the gas saturation pressure when it is under its critical temperature. In the critical point, both gas and liquid phases coexist, i.e., there is just one-fluid phase (ALMEIDA FILHO, 2003). If the substance is under pressure but not above its critical temperature and critical pressure, it is a pressurized fluid or a compressed liquid.

In the supercritical state, near the critical region, the fluid physical-chemical properties have intermediate values of liquids and gases, such as density similar to liquid density, viscosity close to gas viscosity, diffusivity twice more than for liquids, and high compressibility and low superficial tension similar to gases (BRUNNER, 2005; MOURA et al., 2007).

Near the critical point, little changes in temperature or pressure can lead to significant changes in density and in properties dependent on the density, as the solubility, partition coefficient and dielectric constant (PALJEVAC et al., 2007). There is a direct relation between the SCF density and its solvation power that, due to the high compressibility, is extremely dependent on the pressure (CARRILHO; TAVARES; LANÇAS, 2001).

Pressurized fluids present several advantages over liquid solvents such as the high diffusivity that can speed the mass transfer in enzymatic reactions (DALLA ROSA, 2006). Among other advantages, it is possible to highlight: increase of reaction selectivity, high yields, reagent solubilization and ease of separation of products, reagents, catalysts and sub-products from the mixture (SUBRAMANIAN; McHUGH, 1988; SAVAGE et al., 1995).

The critical parameters of the fluids more commonly used in enzymatic reactions are listed in Table 2.

Table 2. Critical parameters of solvents. Source: Adapted from WEN; JIANG; ZHANG (2009).

Solvent	Molecular Mass (g/mol)	Critical Temperature (K)	Critical Pressure (MPa)
Carbon dioxide	44.01	304.1	7.38
Water	18.02	647.3	22.12
Methane	16.04	10.4	4.6
Ethane	30.07	305.3	4.87
Propane	44.09	369.8	4.25
Butane	58.12	425.15	3.75
Methanol	32.04	512.6	8.09
Ethanol	46.07	513.9	6.14
Acetone	58.08	508.1	4.70

Several aspects can be considered to better understand the pressurized fluid contribution to biotechnology, which justify pursuing the aim to master this new process, as presented as follows (OLIVEIRA, 1999):

• The conventional methods to produce compounds via enzymatic catalysis, in general, involve the use of organic solvents, which may be difficult to separate from the final product. When such process is carried out via pressurized fluid, that problem is solved, once the pressurized fluid, besides presenting similar properties to the organic solvents, also has the additional ability to ease the product separation in the end of the process – solvent is removed by a simple depressurization step.

- The use of pressurized fluids as solvents in enzymatic reactions also allows the control of the variables that regulate the reaction yields, the catalyst regeneration and the reaction rates.

- The replacement of a conventional solvent, such as hexane for example, by a pressurized fluid or SCF, leads to higher mass transfer rates due to their higher diffusivity and lower viscosity.

The most used SCF is carbon dioxide (CO_2), because it exhibits mild critical conditions (31 ºC and 73.8 bar) that are easily reached and compatible to enzymatic catalysis application, as well as favorable transport properties that can speed the mass transfer of enzymatic reactions (KNEZ; HABULIN, 2002; KUMAR; MADRAS; MADAK, 2004), besides to its low cost, non-toxicity, non-flammability and high availability in nature.

There are, however, limitations in the use of CO_2 as solvent for enzymatic reactions, due to its non-polarity and, therefore, its preference for dissolving hydrophobic compounds. Although water is usually required for enzymatic activity in SC-CO_2, irreversible denaturation of enzymes has been reported by a variety of aqueous enzymatic systems in the presence of pressurized CO_2 – detailed discussed in section 2.5. Thus, new alternatives have been sought to perform biotransformation with the use of other gases, such as fluorocarbons, propane, butane, ether, dimethyl ether and sulfur hexafluoride (SF_6) (KNEZ, 2009).

The use of liquefied petroleum gas (LPG) as a pressurized fluid is also considered promising. This gas is commercially used as cooking gas, and consists of a mixture of propane, n-butane, isobutane, ethane, and other minor gases. This gas has a slightly lower cost compared to carbon dioxide, but mostly if compared to either propane or n-butane.

2.5 PARAMETERS THAT INFLUENCE THE ENZYMATIC ACTIVITY

Proteins are delicate structures, maintained by interactions inside the protein chain (determined by the amino acid sequence) and the protein-solvent interactions. Changes in factors, such as pressure, temperature, ionic strength, pH, shear stress and solvent hydrophobicity can affect the enzyme structure and, therefore, its activity, stability and specificity, properties that depend on the enzyme three-dimensional structure (HENDRICKX et al., 1998; LIMA et al., 2001).

The catalytic activity of an enzyme is the property measured by the increase in the reaction rate, in mol s^{-1}, of a specified chemical reaction that the enzyme produces in a specific assay system (NC-IUB, 1979). The activity is expressed in units of activity. The definition considers a unit of activity as the amount of enzyme that catalyzes the transformation of one mol of substrate per second under defined assay conditions.

The enzyme stability and activity can vary according to their source, the solvent characteristics, the water content of the enzyme/support/reaction medium, and the process variables, meaning that different effects can be obtained depending on the characteristics of the system under study (FADILOGLU; ERKMEN, 2002; FRANKEN et al., 2010).

Usually, enzyme application is accompanied by the use of liquid organic solvents to enhance their stability and allow the proper contact between the substrates and the enzyme active site. However, the use of organic solvents has disadvantages such as their toxicity, difficulty of separation from products and use of a huge amount of solvent. With that in mind, considerable efforts have been done to carry out enzymatic reactions using "clean technologies'' conducted in sub and supercritical fluids (KNEZ; HABULIN; KRMELJ, 1998; KUMAR; MADRAS; MADAK, 2004; OLIVEIRA; OLIVEIRA, 2000; 2001; DALLA ROSA et al., 2008).

Pressurized fluids can affect the enzyme, rearranging their secondary and tertiary structure, leading to a new conformation different from the native one. These conformational rearrangements may be beneficial and lead to enhanced catalytic activity.

In a SCF, enzymes' structure are not usually affected by pressures up to 30 MPa (300 bar). Under pressures above 150 MPa (1500 bar) enzymes might be denatured. At extremely high pressures (>400 MPa) irreversible changes in the protein structure are possible. However, in the pressure range commonly applied in most of enzymatic processes (10-40 MPa), only slight and reversible changes can occur in the enzyme conformation and, most of them do not interfere in the general performance of the enzyme (CHEFTEL, 1995; KNEZ, 2009; REZAEI; TEMELLI; JENAB, 2007).

Among the factors that affect the enzymatic activity, the water content is one of the most important because enzymes require certain amount of water bound to them to keep their activity. Usually a small amount of water is enough to the reaction in SCF. Water affects the

enzyme action through the establishment of hydrogen bonds or facilitating the reagent diffusion that influence the reaction equilibrium (KNEZ, 2009). However, it is not the water solubility itself, but the water partition between the enzyme and the solvent what influences the enzyme stability (HABULIN; PRIMOZI; KNEZ, 2005).

At high water activities, protein structural changes can occur and even slight conformational changes can show an important effect on the enzyme activity. The water excess also can lead to the enzyme aggregation, reducing the superficial area available to the reaction (KNEZ, 2009).

The use of non-aqueous solvents for enzymatic reactions is attractive for several reasons. An enzyme in a non-aqueous solvent can show similar interactions enzyme/solvent as those of its native medium and, then, present higher activity if compared to pure water. The substrates can also be more soluble in a non-aqueous solvent, leading to higher reaction rates. The biomolecule thermostability in pressurized fluids, for example, is higher than in water and there is the possibility of solvent recycling (KAMAT et al., 1995; OLIVEIRA; OLIVEIRA, 2000).

The interactions enzyme/pressurized fluid that can affect the enzymatic activity include the partition of substrate, product and water between enzyme and solvent and direct interactions between the fluid and the enzyme that can inhibit or inactivate the enzyme by breakage of ionic, hydrophobic or hydrogen bonds/interactions. The less harmful solvents for enzymes are the more hydrophobic ones, because they interact less with the water required for the enzyme action. Hydrophilic solvents, i.e., solvents that contain greater amount of polar groups or groups able to establish hydrogen bonds, tend to take the essential water from the enzyme surroundings, leading to a loss of activity (KNEZ; HABULIN, 2002).

There are many studies performing enzymatic reactions in liquid or SC-CO_2 or other pressurized fluids such as propane and butane, due to their transport properties favorable to mass transfer. However, there is the inconvenient of the CO_2 polarity, as its hydrophilic characteristics can negatively affect the enzyme activity (OLIVEIRA et al., 2006a). The solvent influence has been interpreted based on different aspects, such as the change in the enzyme stiffness, caused by solvents of high dielectric constant, and ionic interactions in the protein. The solvent can stabilize the charges of the transition state through the modification of the active site polarity, as well as the variation of the total free energy,

that are related to different solvation energy of solvent. There is no consensus in the literature regarding the parameter choice to describe quantitatively the solvent effect in enzymatic reactions. However, the parameter most frequently used is log P_{oct}, defined as the logarithm of the solvent partition coefficient in the system octanol/water (DALLA-VECHIA; NASCIMENTO; SOLDI, 2004). Solvents of log $P_{oct} <2$ are called hydrophilic and are not considered suitable for biocatalysis because they strongly disturb the interaction water/biocatalyst, with consequent enzyme inactivation or denaturation. Solvents of log $P_{oct} >4$ are called hydrophobic and do not disturb the water layer, maintaining the biocatalyst in the native state.

The way solvents affect the enzymatic activity and the enantioselectivity is still not well understood and the hypothesis suggested explaining the phenomenon is not conclusive (COSTA; PERALTA, 1999). Researchers emphasize that each result found is restrict to each specific system, and generalizations must not be done. Thereby, due to the fact that enzymes behave differently after treatments in different pressurized solvents, results obtained for one enzymatic system must not be applied to other enzymatic systems.

Temperature is another factor that substantially affects the enzyme activity. The temperature increase can denature the enzyme, characterizing the loss of the native conformation and modification of the tertiary and quaternary structure. Thus, the enzyme has no longer activity. Each enzyme presents a melting temperature (T_m), which corresponds to the temperature where the protein is 50% unfolded, under heating conditions. Meanwhile, heat denaturation is dependent on the relation time/temperature, i. e., the intensity and the duration of the thermal treatment are crucial. A slight modification of the active site conformation can lead to the complete loss of catalytic activity of some enzymes (SCRIBAN, 1985; BELITZ; GROSCH, 1997).

One of the main properties of enzymes solubilized in non-aqueous solvents is the enhancement of their thermal stability compared to the aqueous medium. There is an enhancement in the mobility of protein molecules in water in high temperatures, and that can increase the denaturation effect (ZALE; KLIBANOV, 1986). Thus, it is natural that enzymes show greater thermostability in a non-aqueous medium.

Opposite to thermal treatments, when both covalent and non-covalent bonds are affected, during high pressure exposure under room temperature the covalent bonds are only slightly affected and, consequently, the primary structure is preserved during the treatment

(CHEFTEL, 1995). However, relatively weak hydrophobic interactions or hydrogen bonds, or even some ionic bonds can be broken (HENDRICKX et al., 1998).

Depending on the magnitude of the pressure applied, the extent of the changes in the protein structure can vary from one enzyme to another. Then, it is possible that no changes in the enzyme structure would occur even when it is exposed to high pressure. To carry out enzymatic reactions under high pressure it is very important to study the enzyme behavior in the pressurized fluid, because some enzymes show an apparent activation under pressure while others show deactivation, as it will be discussed in the following section.

2.6 ENZYMATIC ACTIVITY IN PRESSURIZED FLUIDS

KASCHE; SCHLOTHAUER; BRUNNER (1998) affirm that, prior to the enzymatic reaction in pressurized fluids, it is of fundamental importance to evaluate the enzyme behavior in these fluids, once the loss of activity can lead to low reaction rates and formation of secondary products.

When a biocatalyst or an enzymatic preparation is selected for a specific reaction, the solvent, the water content, the solubility of substrates and products must be evaluated and optimized (DALLA-VECHIA; NASCIMENTO; SOLDI, 2004). Thus, before carrying out an enzymatic reaction under high pressure, it is necessary to check which variables affect the enzymatic catalysis in pressurized fluids, and evaluate their effect on the enzyme activity and stability. Usually, the combined effect of variables is verified.

Table 3 shows a summary of studies performed with commercial and homemade free enzymes submitted to pressurized or supercritical fluid treatment. The catalytic activities were measured before and after treatment. This table was taken from our review paper, published in June of 2017, entitled "X-Ray Crystallography as a Tool to Determine Three-Dimensional Structures of Commercial Enzymes Subjected to Treatment in Pressurized Fluids" (FEITEN et al., 2017).

It is possible to observe in Table 3 that the enzyme activity changes significantly after exposure to SCF, depending on the enzyme source, water content, type of pressurized fluid and the treatment experimental conditions (temperature, pressure, exposure time).

Table 3. Summary of free enzymes submitted to treatment in pressurized fluids.

Enzyme Source	Fluid	Pressure (bar)	Temperature (°C)	Time (h)	Residual Activity	Reference
Lipase from *Candida rugosa* Type VII, powder, obtained from Sigma	CO_2	83	50	16-50	85% (83 bar, 50 °C, 50 h)	KAO; EKHORUTOMWEN; SAWAN, 1997
	SF_6	41-415	20-60	16-50	96% (415 bar, 50 °C, 50 h)	
Lipase AY30 from *Candida rugosa*, purchased from Amano (Nagoya)		51-150	20-65	11	96% (150 bar, 65 °C, 11 h)	
Lipase PS from *Burkholderia cepacia*, powder, provided by Amano (Nagoya)		150	25-105	1	110% (150 bar, 45 °C, 1h)	
Lipase from *Aspergillus niger*, powder, purchased from Fluka	CO_2	150	75	24	108%	GIEßAUF et al., 1999
Crude esterase from porcine liver, powder, provided by Sigma		150	75	24	91%	
Lipase from *Candida cylindracea*, powder, purchased from Sigma		150	75	24	110%	

Description	Solvent	Pressure	Temp	Time	Result	Reference
Lipase from hog pancreas, solid, supplied by Fluka		150	75	1-50	602% (150 bar, 75 °C, 24 h)	
Lipase from porcine pancreas, solid, from Serva (Heidelberg)	CO_2	150	75	1.5-24	860% (150 bar, 75 °C, 24 h)	GIEßAUF; GAMSE, 2000
Esterase EP10 from *Burkholderia gladioli*, crude extract and purified, lyophilized, donated by Department of Biotechnology, University of Technology, Graz, Austria		150	35-75	24	EP10 crude: 104% (150 bar, 35 °C, 24 h) EP10 purified: 99% (150 bar, 35 °C, 24 h)	
Esterase from porcine liver, purchased from Sigma Aldrich	CO_2	200	20-100	1	100% (200 bar, 50 °C, 1 h)	BAUER et al., 2000
Lipase AY30 from *Candida rugose* supplied by Amano (Nagoya, Japan)		150-300	40	22	104% (300 bar, 40 °C, 22 h)	
Lipase from porcine pancreas (PPL), powder, given by the supplier	CO_2	150	75	24	751% 945% (100 µl water added)	BAUER et al., 2001
Lipase from *Pseudomonas fluorescens* (L056P)						
Lipase from *Rhizopus javanicus* (L036P)	CO_2 Propane	300	40	24	100%	

Lipase from *Rhizopus javanicus* (L036P)						
Lipase from *Rhizopus niveus* (L060P)						HABULIN; KNEZ, 2001
Lipase from porcine pancreas (L115P)						
Lipase from *Candida rugosa* (L034P); all purchased from Biocatalysts (Wales, UK)						
L-amino acid oxidase from *Crotalus adamanteus*, purchased from Kemika (Croatia)	CO_2	110	40	24	115%	FINDRIK et al., 2005
Radish (*Raphanus sativus* L.) peroxidase (POD) in aqueous solution and lyophilized, extracted at Department of Food Engineering, URI, Brazil	CO_2	70-255	30-50	1-6	POD in solution: 212% (70 bar, 30 ºC, 1 h) POD lyophilized for 12 h: 41.5% (70 bar, 30 ºC, 1 h) POD lyophilized for 24 h: 15% (70 bar, 30 ºC, 1 h)	FRICKS et al., 2006
Peroxidase (POD) and polyphenoloxidase (PPO) from crude extract of mate tea leaves (*Ilex paraguariensis* St. Hill), extracted at Department of Food Engineering, URI, Brazil	CO_2	70-255	30-50	1-6	POD: 125% (70 bar, 30 ºC, 1 h) PPO: 64% (93 bar, 40 ºC, 3.5 h)	PRIMO et al., 2007

D-Hydantoinase purchased from Sigma–Aldrich (Cat number H4028) lyophilized and in aqueous solution	CO_2 Propane	80-230	20-40	0.5-2	Lyophilized in CO_2 (230 bar, 20 ℃, 0.5 h): 110% Lyophilized in propane (230 bar, 20 ℃, 2 h): 108% Aqueous solution in CO_2 (80 bar, 30 ℃, 2 h): 55%	
D-Hydantoinase from adzuki bean (*Vigna angularis*) lyophilized and in aqueous solution, extracted at Department of Food Engineering, URI, Brazil	CO_2 Propane	80-230	20-40	0.5-2	Lyophilized extract in CO_2 (80 bar, 20 ℃, 0.5 h): 105% Lyophilized extract in propane (80 bar, 40 ℃, 2 h): 105% Aqueous solution, in CO_2 (80 bar, 30 ℃, 2 h): 65% Aqueous solution, in propane (150 bar, 40 ℃, 2 h): 100%	ANDRADE et al., 2008
Hen egg-white lysozyme, powder, purchased from Sigma (St. Louis, MO, USA)	CO_2	138-207	40-60	2	106% (138 bar, 40 ℃, 2 h)	WANG et al., 2009
Orange pectin methylesterase PME (Product No. P5400), purchased from Sigma-Aldrich Co. (Beijing, China), in solution	CO_2	80-300	55	0.17	85% (80 bar, 55 ℃, 0.17 h)	ZHOU et al., 2009

Lipoxygenase LOX (Fluka No.62340) from *Glycine max* (soybean), powder	CO_2	100-500	30-55	0.5	26% (100 bar, 30 ℃, 0.5 h)	LIAO et al., 2009
Horseradish (*Armoracia rusticana*) peroxidase (HRP) isoenzyme C purchased from Fluka (RZ = 3.0) in aqueous solution	CO_2	70-255	30-50	1-2	90% (70 bar, 30 ℃, 2 h)	
	Propane	50-200	30-50	1-2	100% (50 bar, 30 ℃, 2 h)	
						FRICKS et al., 2009
Horseradish (*Armoracia rusticana*) peroxidase (HRP) isoenzyme C purchased from Fluka (RZ = 3.0) powder	CO_2	70	30	2	100%	
	Propane	50	30	2	100%	
Lipase from *Penicillium simplicissimum* lyophilized, produced at Department of Food Engineering, URI, Brazil					427% (30 bar, 35 ℃, 1 h)	
	Propane	30-70	35	1-6		KUHN et al., 2010
Lipase from *Aspergillus parasiticus* lyophilized, produced at Department of Food Engineering, URI, Brazil					121.6% (70 bar, 35 ℃, 1 h)	
β-amylase, purchased from Sigma (USA)					90% (86 bar, 40 ℃, 1 h, 250 rpm)	
	CO_2	10-172	40	0.08-2		WANG et al., 2010

Crude isoamylase, from *Pseudomonas amyloderamosa* WU7211-2 from JD210 by UV and NTG mutagenesis, provided by BCRC (Biosource Collection and Research Center, Hsinchu, Taiwan)					100% (110 bar, 40 ºC, 40 min, 250 rpm)	
Lipase Amano AY30 (*Candida rugosa*) lyophilized and resuspended					Lyophilized: 170% (115 bar, 45 ºC, 1.45 h) Resuspended: 84% (30 bar, 35 ºC, 0.5 h)	
Lipase Amano PS (*Burkholderia cepacia*) lyophilized and resuspended	Propane	30-200	35-55	0.5-3	Lyophilized: 347% (200 bar, 35 ºC, 0.5 h) Resuspended: 127% (200 bar, 35 ºC, 1 h)	FRANKEN et al., 2010
Non-commercial lipase from *Yarrowia lipolytica* (produced at Department of Food Engineering, URI, Brazil), lyophilized and resuspended					Lyophilized: 125% (200 bar, 35 ºC, 1 h) Resuspended: 85% (30 bar, 35 ºC, 0.5 h)	
α-amylase from *Aspergillus oryzea*, supplied in its free form from ORBA Biochemistry Co. Istanbul, Turkey	CO_2	50-300	28-80	1-3	168% (240 bar, 41 ºC, 1.5 h)	SENYAY-ONCEL; YESIL-CELIKTAS, 2011
β-galactosidase from *Kluyveromyces marxianus* CCT 7082 lyophilized at Department of Food Engineering, URI, Brazil	CO_2	74-311	37	1-6	177% (74 bar, 37 ºC, 1 h)	MANERA et al., 2011
	Propane	30-250	37	1-6	211% (30 bar, 37 ºC, 1 h)	

		10-250	37	1-6	162% (10 bar, 37 ℃, 1 h)	
	n-butane	10-250	37	1-6	162% (10 bar, 37 ℃, 1 h)	
Mushroom tyrosinase (T-3824), purchased from Sigma-Aldrich Co. (Beijing, China), in solution	CO_2	50-150	35-55	0.33	85% (80 bar, 35 ℃, 0.33 h)	HU et al., 2011
β-galactosidase from *Kluyveromyces marxianus* CCT 7082 lyophilized at Department of Food Engineering, URI, Brazil	CO_2	75	37	1	72%	
	Propane	30	37	1	103%	
	n-butane	10	37	1	109%	BRAGA et al., 2012
	LPG	30-270	37	1-6	94% (270 bar, 37 ℃, 1 h)	
Candida rugosa lipase (CRL type VII) purchased from Sigma Co. Ltd (St, Louis, MO)					122% (70 bar, 45 ℃, 10 min)	
Pseudomonas fluorescens lipase (PFL) purchased from Sigma Co. Ltd (St, Louis, MO)	CO_2	50-200	35-45	0.17-0.67	163% (200 bar, 45 ℃, 40 min)	CHEN et al., 2013a

Rhizopus oryzae lipase (ROL) purchased from Sigma Co. Ltd (St, Louis, MO)					209% (150 bar, 40 ℃, 25 min)	
Cellulase from *Trichoderma reesei* (NS50013) provided by Novozymes Latin American (Brazil)	LPG	30-270	40-55	1-6	220% (30 bar, 40 ℃, 1 h)	SILVA et al., 2013d
	LPG + US (123 W)	30-270	40-55	1-6	384% (123W, 150 bar, 47.5 ℃, 1 h)	
Candida rugosa Lip7 (CRL7), powder, purchased from Sigma Co. (St. Louis, MO, USA)	CO_2	60-100	35-40	0.5-2.5	188% (100 bar, 40 ℃, 0.5 h)	LIU et al., 2012
CALB from *Candida antarctica*, in solution, purchased from Nov Norvisk (Denmark)					105% (100 bar, 40 ℃, 0.5 h)	LIU et al., 2013a
Lipase PS from *Burkholderia cepacia*, in solution, obtained from Amano Pharmaceutical Co., Ltd. (Nagoya, Japan)	CO_2	60-100	35-40	0.33-2.5	116% (100 bar, 40 ℃, 0.5 h)	
Candida rugosa lipase (CRL), powder, purchased from Sigma Co. (St, Louis, MO, USA)	CO_2	60-150	40	0.33	133% (150 bar, 40 ℃, 0.33 h)	LIU et al., 2013b
Pseudomonas cepacia lipase, powder, purchased from Amano Pharmaceutical Co. Ltd. (Nagoya, Japan)	CO_2	50-200	35-45	0.17-0.67	130% (150 bar, 40 ℃, 25 min)	CHEN et al., 2013b

Palatase 20000 L (lipase from *Rhizomucor miehei* in an aqueous solution) purchased from Sigma Aldrich					135% (150 bar, 50 ℃, 1 h)	
Lipozyme CALB L (lipase from *Candida antarctica* in an aqueous solution), provided by Novozymes (Denmark)	CO_2	100-250	35-75	1-6	112% (150 bar, 35 ℃, 3 h)	MELGOSA et al., 2015

2.7 PROTEIN CHARACTERIZATION TECHNIQUES

The main disadvantage of enzyme catalysts in comparison to chemical ones is the relatively low stability in the native state and its high cost. There is an increasing interest in the development of biocatalysts for industrial application that exhibit high activity, stability and reuse ability, and these improvements have been obtained through chemical, physical or genetic modifications. As seen in a careful literature review, such improvements have been reached by submission of enzymes to high pressure treatment in pressurized fluids, but just a few studies have been carried aiming to deeply analyze the structural changes of these enzymes after such treatments. The scarce literature is summarized by application of molecular dynamic (MD) models to simulate the three-dimensional structure of enzymes treated in pressurized fluids (MONHEMI et al., 2012; MONHEMI; HOUSAINDOKHT, 2012; HOUSAINDOKHT; BOZORGMEHR; MONHEMI, 2012; HOUSAINDOKHT; MONHEMI, 2013).

There are several techniques documented in the literature to determine the secondary and tertiary structures of enzymes, each one with its own peculiarities. To determine the three-dimensional structure of proteins, meaning locate the position of amino acid residues in space, X-ray crystallography, nuclear magnetic resonance (NMR) and cryo-electron microscopy (cryo-EM) are the methods of choice (STRYER, 1995; LEHNINGER; NELSON; COX, 1995).

Regardless of the technique chosen, enzyme samples should be highly pure and homogeneous, which is usually not observed for commercial enzymes. Therefore, some techniques commonly used for protein purification, characterization and structural determination are summarized in this section, as they were applied to the enzyme studied in the course of this research.

2.7.1 Size-exclusion chromatography

Size-exclusion chromatography (SEC) separates molecules on the basis of the hydrodynamic radius, not molar mass (Figure 5). When an aqueous solution is used to transport the sample through the column, SEC is also called gel filtration. A column is filled with a stationary phase, composed of a porous material such as sepharose or sephadex, that will admit ions and small molecules (purple) into their pores but not large ones (shown in red). When a mixture of molecules and ions

dissolved in a solvent is applied at the top of the column, the smaller molecules (and ions) are distributed through a larger volume of solvent than is available to the large molecules. Consequently, the large molecules move more rapidly through the column, and in this way the mixture can be separated (fractionated) into its components. The porosity of the gel can be adjusted to exclude all molecules above a certain size.

Figure 5. Scheme of size exclusion chromatography (SEC). Source: Adapted from GE HEALTHCARE, 2010.
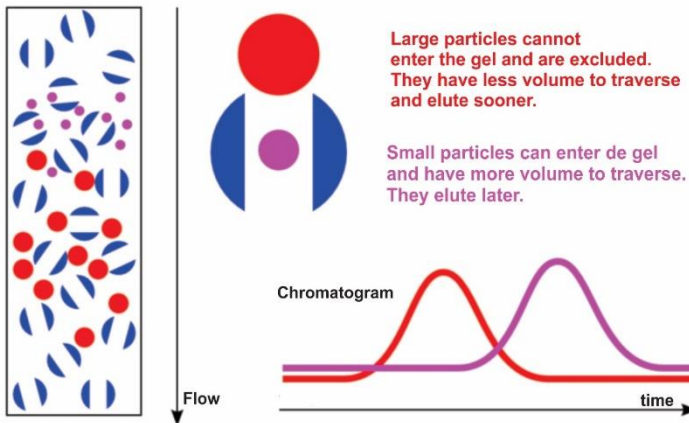
Gel filtrations are able to isolate multimeric forms or aggregates from the monomeric target protein. As relatively stable interactions are preserved during gel filtration, it can also be used to separate complexes of proteins or RNA-protein complexes, for example.

2.7.2 Ion-exchange chromatography

Ion-exchange chromatography enables to separate a mixture of proteins on the basis of their different isoelectric points (pI). Negatively or positively charged functional groups are coupled to a matrix (stationary phase) to bind positively or negatively charged molecules, respectively. Above its pI, a protein is negatively charged and can be bound to an anion exchanger. Otherwise, below its pI, a protein is positively charged and then can be bound to a cation exchanger. After

the sample is bound to the stationary phase equilibrated with buffer of low ionic strength, elution is carried out by changing the mobile phase gradually to a buffer of high ionic strength or different pH. Components exhibiting equal electrostatic interactions with the stationary phase elute at the same retention volume.

2.7.3 Differential Scanning Fluorimetry

Identifying conditions in which protein samples are stable over long periods of time and that prevent aggregation or denaturation is extremely helpful for experiments involving analytical and biophysical techniques that require high protein concentrations. Many factors can influence protein stability, such as buffers (chemical composition as well as pH); salts; detergents, whose interactions with the protein are non-specific; and ligands, which bind proteins at specific sites.

Buffer choice is of extreme importance for purification since it should promote protein stability. Normally, for crystallization assays, low salt buffers with low molarity of the buffer compound are required. Low salt buffers avoid salt crystal formation and low buffer molarity allows pH variability when the protein buffer encounters the mother liquor. Also, certain salts such as phosphate derivatives are avoided because they crystallize very easily in combination with a variety of salts in the mother liquor.

The stability of a protein is characterized by the Gibbs free energy of unfolding (ΔG_U), which is temperature-dependent. The stability of most proteins decreases as the temperature increases, meaning that ΔG_U decreases and reaches zero at the equilibrium point where the concentrations of folded and unfolded protein are equal. At this equilibrium point, the temperature is called melting temperature (T_m) (BECKTEL; SCHELLMAN, 1987; EDSALL, 1995).

Differential Scanning Fluorimetry (DSF) or Thermofluor is a useful technique to choose the proper buffer (pH, buffer type and concentration, salt type and concentration) for protein purification and crystallization. DSF monitors the thermal unfolding of proteins in the presence of a fluorescent dye that is highly fluorescent in a non-polar environment compared to aqueous solution where the fluorescence is quenched. To date, SYPRO orange is the dye possessing the most favorable properties for DSF owing to its signal to noise ratio. Additionally, the relatively long wavelength of excitation of SYPRO

orange (near 500 nm) decreases the likelihood that buffer components would interfere with the optical properties of the dye.

Practically, DSF is performed using a real-time PCR instrument and monitors the fluorescence intensity of the dye as a function of the temperature. Upon protein unfolding by thermal denaturation, the aromatic moieties of the dye preferentially binds to the now exposed hydrophobic patches of the protein and the fluorescence intensity increases. This generates a sigmoidal curve that can be described as a two-state transition and the T_m, which corresponds to the temperature where the protein is 50% unfolded, can be extracted from the curve by determining the first derivative via fitting the data points with a Boltzmann equation (NIESEN; BERGLUND; VEDADI, 2007).

DSF is an excellent method to screen for conditions/compounds that stabilize proteins due to the small amounts and low protein concentrations required as well as for providing an easy readout for identification of such stabilizing conditions. Basically, the T_m value of the protein under each condition of the screen needs to be compared with the reference T_m, which is generally provided by protein in purification buffer. The best buffer would be the one in which the protein presents the highest melting temperature, i.e., that one in which the protein is more stable upon heating.

2.7.4 Circular Dichroism

Plane polarized light consists of two circularly polarized components of equal magnitude, one rotating counter-clockwise (left handed) and the other clockwise (right handed). The circular dichroism technique (CD) measures the differential absorption of these two components by a solution. This effect will occur when a molecule is chiral (optically active) (for example, a carbon atom with four different substituents or a disulphide bond which is chiral because of the dihedral angles of the C-S-S-C atoms), or when it is covalently linked to a chiral center or placed in an asymmetric environment by virtue of the three-dimensional structure adopted by the molecule (KELLY; PRICE, 1997; 2000). In practice, the plane polarized light is split into its two circularly polarized components by passage through a modulator. If one of the components is absorbed by the sample to a greater extent than the other after passage through the sample, the resultant light would be elliptically polarized. The CD spectropolarimeter does not recombine the two components but rather detects them separately. The dichroism at a given

wavelength is then expressed as either the difference in absorbance of the two components or as the ellipticity in degrees (θ). A CD spectrum is obtained when the dichroism is measured as a function of the wavelength.

CD spectra of proteins between 260 and 190 nm can be analyzed for different secondary structural types like α-helix, parallel and anti-parallel β-sheet, turn, and others. When a folded protein is heated, the equilibrium between the native (N) and unfolded (U) states is shifted towards the denatured form. This transition can be followed by monitoring the change in ellipticity of an, e.g., α-helical protein that becomes a random coil peptide chain during denaturation. Using such "melting analysis", it is possible to obtain certain thermodynamic parameters that describe the folding reaction, like the apparent melting temperature T_m, for example. The melting temperature is defined as the temperature where the unfolded species and the folded species coexist in equal amounts and can be determined graphically (KELLY; PRICE, 1997; 2000).

2.7.5 Multi-Angle Light Scattering

Light scattering is one of the few absolute methods available for determination of molecular mass and certainly is applicable over the broadest range of molecular weights of any method (WYATT, 1993).

Recently, size exclusion chromatography (SEC) is used in combination with the multi-angle light scattering (MALS) method to determine the absolute molecular mass, the distribution and the average size of particles in solution, by separating molecules according to their size (and shape to some extent) as they pass through a gel filtration medium packed in a column and detecting how they scatter light at several angles (WITTGREN; WAHLUND, 1997; ASTEFANEI et al., 2015; VEZOCNIK et al., 2015). The combined SEC-MALS method has many applications, such as the assessment of the oligomeric state of a protein, quantification of protein aggregation and determination of protein conjugate stoichiometry.

SEC alone is a relative method. Molecular weight measurements with light scattering are an absolute method. Combining SEC with MALS will result in the measurement of absolute molecular weight, independent from column calibration.

It is possible to control the conditions to retrieve detailed information about the light scattering. The wavelength (λ), polarization,

and intensity (I_i) of the incident light can be chosen and adjusted. The size of the laser beam and the field of view of the detector define a scattering volume. The scattered light (I_s) from this volume can be detected as a function of angle (θ) and polarization.

By controlling the above mentioned parameters, it is possible to determine the molar mass (M), size (r_g), second virial coefficient (A_2), and translational diffusion coefficient (D_t) of a solute in solution. One of the tremendous advantages of MALS over almost any other method is that these properties can be measured *in solution* in a non-invasive manner.

2.7.6 Crystallization

The main goal in X-ray crystallography is to derive the three dimensional structure of a given protein or protein complex based on a set of X-ray scattered intensities measured in different directions in space. This process can be divided in three basic steps (RUPP, 2010): protein crystal formation; diffraction pattern collection; and structural model determination.

The three basic steps, the basic theory and practical methods of X-ray crystallography, as well as sample preparation are discussed in details in our review paper, published in June of 2017, entitled "X-Ray Crystallography as a Tool to Determine Three-Dimensional Structures of Commercial Enzymes Subjected to Treatment in Pressurized Fluids" (FEITEN et al., 2017).

2.7.7 Mass spectrometry

Mass spectrometry is a powerful physical tool to characterize the molecules by measuring the mass/charge of their ions. The coupled mass spectrometry (MS/MS) is an important analytical technique used to quantify known materials, to identify unknown compounds within a sample and to elucidate the composition and chemical properties of different organic molecules (KANG, 2012). The complete process involves the conversion of the sample into gaseous ions, with or without fragmentation, which are then characterized by their mass to charge ratios (m/z) and relative abundances.

The first step in the mass spectrometric analysis of compounds is the production of a gas phase ions of the compound, basically by electron ionization. This molecular ion undergoes fragmentation. Each

primary produced ion derived from the molecular ion, in turn, also undergoes fragmentation, and on the process continues. The ions are separated in the mass spectrometer according to their mass-to-charge ratio and are detected in proportion to their abundance. A mass spectrum of the molecule is thus produced. Ions provide information concerning the nature and the molecular structure of their precursor molecule. In the spectrum of a pure compound, the molecular ion, if present, appears at the highest value of m/z (followed by ions containing heavier isotopes) and gives the molecular mass of the compound.

Liquid Chromatography coupled to tandem Mass Spectrometry (LC-MS/MS) is a powerful analytical tool for the analysis of polar, semi-volatile and thermally labile organic compounds of a wide molecular weight range (SCHREIBER; BORTON, 2010). Similar to HPLC, LC-MS/MS utilizes a compound's intrinsic affinity for both a "mobile phase" (typically a buffered solvent) and a "stationary phase" porous solid support with specialized coating). Essentially, a pump is used to provide a continuous flow of a solvent into which a dissolved sample is introduced. Once the sample is in the solvent flow, it travels through an analytical column. The compounds present in the sample mixture are then separated depending on their affinity to the coated particles in the column. After the components in the sample are separated, they pass through a mass detector. The mass detector response and the "retention time" (time it takes for a compound to pass from the injector to the detector) of the compound(s) of interest may then be compared to a reference material.

2.7.8 Deglycosylation

Protein glycosylation, that is, the attachment of a saccharide moiety to a protein, is a modification that occurs either co-translationally or post-translationally. The two major types of glycosylation consist of the addition of glycans to an asparagine (*N*-linked) or to a serine or threonine (*O*-linked), and are both involved in the maintenance of protein conformation, activity, mobility and stability, in protein protection from proteolytic degradation, and in protein intracellular trafficking and secretion (ROTH; YEHEZKEL; KHALAILA, 2012; GOETTIG, 2016). Figure 6 shows the basic core and most relevant structures of *N*-glycans and *O*-glycans.

Figure 6. Basic core structures of *N*-glycans (**A**) and *O*-glycans (**B**). Source: GOETTIG, 2016.
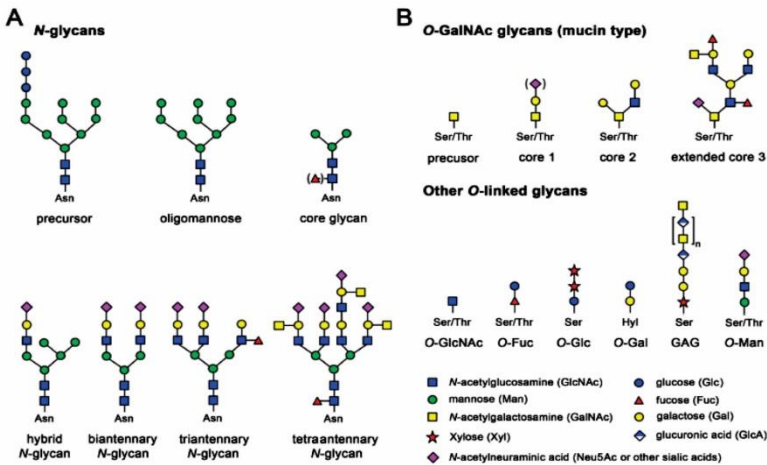
In proteins, the *N*-linked oligosaccharide is attached to the amide group of an asparagine residue within the consensus peptide sequence NXS/T (asparagine-X-serine/threonine), where X is any amino acid except proline. The most efficient cleaving enzyme for *N*-glycan moiety would be a glycoamidase, particularly glycoamidase F (PNGase F), which cleaves the bond between N-acetyl glucosamine (GlcNAc) and an asparagine residue, thereby converting asparagine to aspartic acid (Figure 7).

Figure 7. *N-* and *O-* glycosylation. Source: New England BioLabs Inc.
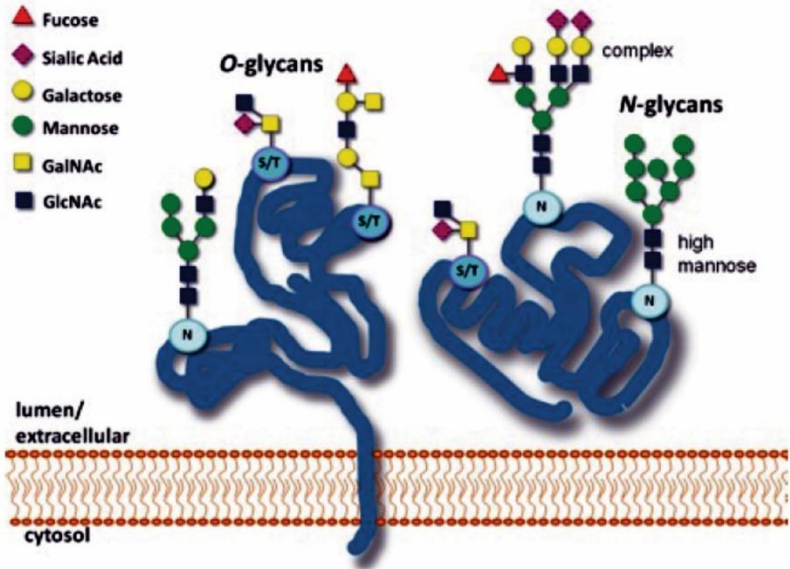
PNGase F cleaves most types of *N*-linked oligosaccharides, including complex structures (e.g., high mannose, hybrid, and multi-sialylated structure), up to tetraantennary trees and oligosaccharides containing sulfate-substituted residues, as shown in Figure 8. However, for cleavage under native conditions high concentrations of PNGase F may be required (ROTH; YEHEZKEL; KHALAILA, 2012).

Figure 8. Schematic representation of glycoprotein treated with PNGase F. Source: New England BioLabs Inc.
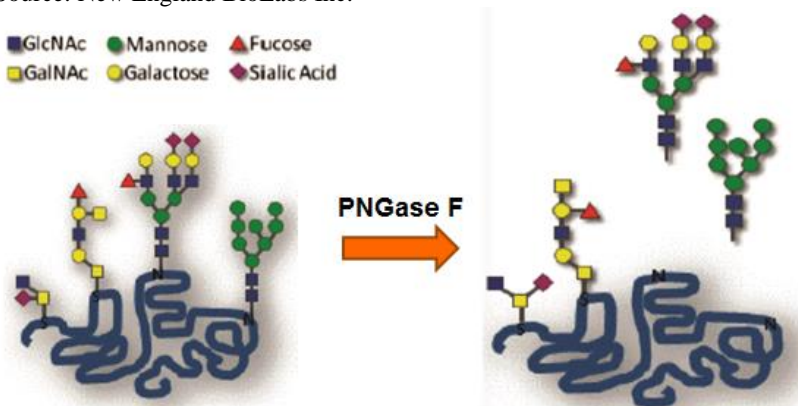
2.8 FINAL CONSIDERATIONS

This literature review section presented the state of art related to enzyme application, especially lipases, in pressurized fluids - the biocatalyst and solvent features - and the variables that affect the process and the enzymatic activity under high pressure.

A detailed search in the specialized literature pointed out a lack of studies concerning structural modifications of enzymes caused by the treatment under high pressure in supercritical fluids. With that in mind, it is important to investigate the behavior of lipase B from *Candida antarctica* in pressurized fluids, which is a lipase widely used in food, chemical and pharmaceutical industries. In this context, this research project investigated the influence of process variables on the CalB activity and storage stability under low temperatures after treatment. Additionally, CD, MALS and MS were adopted to characterize CalB. Finally, the three-dimensional structure of the treated and untreated CalB was determined.

3 MATERIAL AND METHODS

In this section, all the material and methods used in the course of this research are detailed. This thesis was partially developed at Laboratory of Thermodynamics and Supercritical Technology of the Department of Chemical and Food Engineering from the Federal University of Santa Catarina (UFSC), and partially at the Structural Biochemistry Laboratory of the Department of Biology, Chemistry and Pharmacy from the Freie Universität Berlin (FUB).

3.1. MATERIALS

3.1.1. Enzyme

Lipase B from *Candida antarctica* (CALB L®), recombinant, in an aqueous solution, used in all experiments carried out at UFSC, was kindly donated by Novozymes Brazil (Araucária-PR). For all experiments carried out at FUB, CalB from *Candida antarctica*, produced by Novozymes, was purchased from Sigma-Aldrich, recombinant, expressed in *Aspergillus niger*, in aqueous solution.

N-Glycosidase F (PNGase F) from *Flavobacterium meningosepticum* (theoretical molecular weight of 36 kDa) was purchased from New England BioLabs Inc., supplied in a buffer containing 50 mM NaCl, 20 mM Tris-HCl pH 7.5, 5 mM Na_2EDTA and 50% glycerol. PNGase F activity, given by the supplier, was 15,000 units, and one unit was defined as the amount of enzyme required to remove more than 95% of the carbohydrate from 10 µg of denatured RNase B in 1 hour at 37 °C in a total reaction volume of 10 µL (65 NEB units = 1 IUB milliunit).

3.1.2. Solvent

For the experiments carried out at UFSC, carbon dioxide (CO_2) (99.9% purity) was purchased from White Martins. Liquefied petroleum gas (LPG), purchased from Liquigás S.A (Brazil), was constituted by a mixture of propane (50.3 wt%), n-butane (28.4 wt%), isobutane (13.7 wt%), ethane (4.8 wt%), other minor constituents (methane, pentane, isopentane, etc.) and 140 ppm of sulfur (COMIN et al., 2015).

Carbon dioxide used for experiments carried out at FUB was purchased from Linde (99.5% purity).

3.1.3. Chemicals

All chemicals used in this study and their suppliers are listed in Table 4.

Table 4. List of chemicals.

Chemical	Supplier
4-nitrophenol	Sigma-Aldrich, Brazil
4-nitrophenyl palmitate (*p*-NPP)	Sigma-Aldrich, Brazil
1,4-Dithiothreitol (DTT)	Roth, Germany
2-methyl-2,4-pentanediol (MPD)	Fluka, Germany
Acetic acid	Roth, Germany
Acrylamide solution Rotiphorese Gel 30 (29.2% acrylamide, 0.8% N,N'-methylene-bis-acrylamide)	Roth, Germany
Ammonium peroxodisulfate (APS), 10%	Merck, Germany
Bovine Serum Albumin (BSA), 99%	Sigma-Aldrich, Brazil
Citric acid monohydrate	Vetec, Brazil
Coomassie® Brilliant Blue G-250 solution	Bio-Rad, Germany
Glycerol	Merck, Germany
NP-40 (10% nonyl phenoxypolyethoxylethanol)	New England BioLabs Inc.
Potassium phosphate	Roth, Germany
Polyethylene glycol (PEG) 400	Sigma-Aldrich, Germany
Polyethylene glycol (PEG) 3350	Sigma-Aldrich, Germany
Sodium bicarbonate	Vetec, Brazil/ Roth, Germany
Sodium carbonate	Vetec, Brazil/ Roth, Germany
Sodium chloride (NaCl)	Roth, Germany
Sodium dihydrogen phosphate	Vetec, Brazil/ Roth, Germany
Sodium dodecylsulfate (SDS)	Serva, Germany
Sodium hydrogen phosphate	Vetec, Brazil/ Roth, Germany
Sodium hydroxide (NaOH)	Merck, Germany
Trisodium citrate dehydrate	Vetec, Brazil
1,2-Bis(dimethylamino)ethane (TEMED)	Roth, Germany
Tris-(hydroxymethyl)-aminomethane (Tris)	Roth, Germany

3.1.4. Buffers and solutions

Solutions listed in Table 5 were prepared with Milli-Q water and filter-sterilized (0.22 µm). The pH of buffers was adjusted by addition of buffered stock solutions or by titration with 32 % HCl or 10 M NaOH.

Table 5. List of buffers and solutions.

Buffer/Solution	Composition
10×Glycoprotein Denaturing Buffer	5% sodium dodecyl sulfate (SDS); 400 mM 1,4-dithiothreitol (DTT)
10×GlycoBuffer 2	500 mM sodium phosphate pH 7.5
10×SDS Running Buffer	250 mM Tris pH 6.8, 2 mM Glycine, 1% (w/v) SDS
5×SDS Loading Buffer	250 mM Tris pH 6.8, 8% (w/v) SDS, 10% (v/v) β-ME, 30% (v/v) glycerol, 0.02% (w/v) bromophenol blue
Circular Dichroism Buffer	50 mM potassium phosphate pH 7.4
Coomassie Staining Solution	0.025% (w/v) Coomassie (R250); 0.025% (w/v) Coomassie (G250); 30% (v/v) isopropanol; 7.5% (v/v) acetic acid
Destaining Solution I	40% (v/v) ethanol, 20% (v/v) acetic acid
Destaining Solution II	10% (v/v) acetic acid
Gel Filtration Buffer	20 mM sodium phosphate pH 7.5 @ 4ºC, 100 mM NaCl
High Salt Buffer	20 mM Tris pH 8 @ 4ºC, 1.5 M NaCl
Low Salt Buffer	20 mM Tris pH 8 @ 4ºC, 50 mM NaCl
SEC-MALS Buffer	20 mM Tris pH 7.5 @ 4ºC, 100 mM NaCl, 0.02% (v/v) sodium azide

3.1.5. Consumables and instruments

Items and devices that were routinely used in this work are listed in Table 6 and Table 7, respectively.

Table 6. List of consumables.

Item	Supplier
Ultrafiltration membrane filters (Amicon Ultra, 10 kDa)	Millipore, USA
Crystallization plates MRC, 96 well, sitting drop	Molecular Dimensions, UK
Dialysis membranes	Spectra/Por, USA
Eppendorf safe-lock micro test tubes	Eppendorf, Brazil / Germany
Sterile filters 0.22 μm	Sarstedt, Germany
Syringes	Braun, Germany
Tubes (5 mL, 10 mL, 15 mL and 50 mL)	Greiner-Bio-One, Germany

Table 7. List of instruments.

Device	Manufacturer
Äkta Purifier	GE Healthcare, Germany
Beamline 14.2	Bessy II, Helmholtz-Zentrum Berlin, Germany
Crystallization robot	Zinsser, Germany
Digital camera Camedia C-5050 Zoom	Olympus, Japan
Electrophoresis power supply	Bio-Rad, Germany
Gel electrophoresis equipment	Bio-Rad, Germany
Heating blocks	Eppendorf, Germany
Ice machine	Ziegra, UK
Magnetic stirrer RH basic 2	IKA, Germany
Microscope SZ-PT	Olympus, Japan
Milli-Q synthesis Advantage A10	Millipore, USA
Mounted CryoLoop	Hampton Research, USA
NanoDrop 2000 Spectrometer	Thermo Fisher Scientific, USA
pHmeter, Professional Meter PP-20	Sartorius, Germany
Pipetboy	Brand, Germany
Pipettes	Gilson, USA

70

Scales XS205 DualRangeR	Mettler Toledo, Germany
Scales XS4002S DeltaRangeR	Mettler Toledo, Germany
Scanner	Epson, Germany
UV-Visible Spectrophotometer Ultrospec 3100 *pro*	Amersham Biosciences, Germany
Speed vac concentrator 5301	Eppendorf, Germany
Centrifuge	Quimis, Brazil
Microcentrifuge Micro Star 17	VWR, UK
Vortex Genie 2	Scientific Industries, USA

3.2 METHODS

3.2.1   Purification

3.2.1.1 Size-exclusion chromatography

CalB from *Candida antarctica* (theoretical molar mass of 33022 Da), purchased from Sigma-Aldrich, was purified *via* size exclusion chromatography (SEC) column (Superdex® 75, 26/60) using 0.02 M sodium phosphate buffer pH 7.5 and 0.1 M sodium chloride. The column characteristics were internal diameter of 26 mm, length of 60 cm, matrix composed of dextran and cross-linked agarose, particle size of 34 µm, maximum flow rate of 2.6 mL/min (maximum pressure of 0.3 MPa), molar mass range between $3x10^3$ and $7x10^5$ Da and bed volume of 320 mL (GE Healthcare, 28-9893-34). For each single purification, 5 mL of CalB were loaded in the column at a flow rate of 2 mL/min at 4 °C using an Äkta purifier system. Aliquots of 2 mL were collected and fractions were analyzed by SDS-PAGE and then concentrated.

3.2.1.2 Ion-exchange chromatography

Aiming at increasing the purity of CalB (theoretical isoelectric point of 5.8) purified by SEC, the protein was further loaded into an anion exchange column (Mono Q® 10/100 GL) and into a cation exchange column (Mono S® 10/100 GL) which were equilibrated in 20 mM Tris pH 8.0 and 50 mM NaCl. The elution step was carried out with a linear gradient from 50 to 1500 mM NaCl in both columns. Mono Q® characteristics were internal diameter of 10 mm, length of 106 mm, matrix composed of monodisperse porous polystyrene/divinyl benzene beads (quaternary ammonium strong anion), particle size of 10 µm, maximum flow rate of 6 mL/min (maximum pressure of 4 MPa) and bed volume of 8 mL (GE Healthcare, 17-5167-01). Mono S® characteristics were internal diameter of 10 mm, length of 106 mm, matrix composed

of monodisperse porous polystyrene/divinyl benzene beads (methyl sulfonate strong cation), particle size of 10 μm, maximum flow rate of 6 mL/min (maximum pressure of 4 MPa) and bed volume of 8 mL (GE Healthcare, 17-5169-01). 2 mL of CalB at 10 mg/mL were loaded into the columns at a flow rate of 0.5 mL/min at 4 °C using an Äkta purifier system. Aliquots of 2 mL were collected and fractions were analyzed by SDS-PAGE.

3.2.2 Sodium dodecyl sulfate polyacrylamide gel electrophoresis

Sodium dodecyl sulfate polyacrylamide gel electrophoresis (SDS-PAGE) was used to analyze the collected fractions of each peak obtained from gel filtration and from the ion-exchange purifications (GALLAGHER, 2006). The percentage of the separating gel was aligned to the size of the analyzed protein (12.5%). The gel composition is shown in Table 8.

Table 8. SDS-polyacrylamide gel composition.

Component	Separating gel 12.5% (v/v)	Stacking gel (v/v)
Separating gel buffer	25%	-
Stacking gel buffer	-	25%
Acrylamide 30%, Bisacrylamide (37.5:1)	42%	13%
APS 10%	0.5%	0.5%
TEMED	0.05%	0.05%

Protein samples were denatured in SDS loading buffer and heated to 95 °C for 5 minutes. All gels were ran at 250 V in running buffer until the bromophenol blue front reached the bottom of the gel or just went out of the gel (around 35 minutes). Coomassie® staining solution was applied for 7-15 minutes, then distaining was carried out using distaining solution I (5 minutes) and distaining solution II (1 hour - over-night).

3.2.3 Protein quantification

Fractions of the peak identified in SDS-PAGE as CalB (33-35 kDa) were pooled and concentrated to 10 mg/mL. Protein concentrations were determined with the NanoDrop® 2000

Spectrophotometer (Peqlab). The absorption at a wavelength of 280 nm was divided by the CalB extinction coefficient ε_{280} assuming all cysteine residues are reduced, i. e., all the cysteine residues are bound by the sulfur atoms forming cystine dimers. Extinction coefficient ε_{280} was calculated using the ExPASy ProtParam tool (1.25). To test potential contamination with nucleic acids, the ratio of 280 and 260 nm was measured; indicating absorption of protein and nucleic acids, respectively.

3.2.4 Protein concentration

The Bio-Rad Protein Assay is a dye-binding assay in which a differential color change of the dye occurs in response to various concentrations of protein (BRADFORD, 1976). The absorbance maximum for an acidic solution of Coomassie® Brilliant Blue G-250 dye shifts from 465 nm to 595 nm when binding to protein occurs (FAZEKAS DE St. GROTH; WEBSTER; DATYNER, 1963; REISNER; NEMES; BUCHOLTZ, 1975; SEDMAK; GROSSBERG, 1977).

Protein Assay Dye Reagent Concentrate is a solution containing dye, phosphoric acid, and methanol. Dye reagent was prepared by diluting 1 part Dye Reagent Concentrate with 4 parts Milli-Q® water. The reagent was then filtered to remove particulates.

A solution of bovine serum albumin (BSA) was prepared at 1 mg/mL in Milli-Q® water and the standard curve was obtained with the assays presented in Table 9. Then, 5 mL of the diluted dye reagent were added in each test tube and mixed. Tubes were incubated at room temperature for at least 5 minutes and the absorbance of the samples was measured at 595 nm. For CalB protein content determination, 100 μL of the sample were diluted in 2.5 mL of the dye reagent and, after 5 minutes, the absorbance was measured in 595 nm.

Table 9. BSA standard curve.

Assay	Volume of BSA solution at 1 mg/mL (mL)	Volume Milli-Q® water (mL)	Protein mass (μg)
1	0	0.1	0
2	0.02	0.08	20
3	0.04	0.06	40
4	0.06	0.04	60
5	0.08	0.02	80
6	0.1	0	100

3.2.5 Hydrolysis activity

3.2.5.1 Standard assay

CalB activity was measured by hydrolysis of the synthetic substrate 4-nitrophenyl palmitate (*p*-NPP) (CHIOU; WU, 2004). The method is based on the reaction schematized in Figure 9, where the substrate *p*-NPP is hydrolyzed by the lipase releasing *p*-nitrophenol and palmitic acid. The lipase activity is determined by estimation of *p*-nitrophenol released, which is a yellow chromogen with maximum emission at 410 nm. The method of *p*-NPP hydrolysis presents advantages of being fast and practical to use and requires small volumes of sample (WINKLER; STUCKMANN, 1979; JAEGER et al., 1994; JAEGER; EGGERT, 2002; SAXENA et al., 2003a; 2003b; GUPTA; GUPTA; RATHI, 2004).

Typically, an aliquot of 0.1 mL of lipase solution was added to 1 mL of 0.05 M sodium phosphate buffer pH 7, and then to 1 mL of substrate alcoholic solution (*p*-NPP 0.5% dissolved in absolute ethanol). The reaction mixture was incubated in a water bath at 30 ºC for 5 minutes. Then the reaction was stopped by adding 2 mL of sodium carbonate 0.5 N, following by centrifugation at 3500 rpm (maximum 2800 xg) for 10 minutes. Afterwards, an aliquot of 0.1 mL of the supernatant was diluted in 9 mL of sodium phosphate buffer and the absorbance enhancement induced by the release of *p*-nitrophenol from the *p*-NPP hydrolysis was measured with a spectrophotometer (Ultrospec[TM] 3100 *pro*, Amersham Biosciences) at 410 nm wavelength. The standard protocol to measure the hydrolysis of *p*-NPP described above was used for all the experiments carried out at UFSC.

One unit (U) of enzymatic activity was defined as the amount of enzyme which catalyzes the release of 1 μmol of *p*-nitrophenol per minute in the specified experimental conditions. Specific activity (U/mg) was calculated by the ratio between the hydrolysis activity (U/mL) and the total protein content (mg/mL) determined by Bradford.

Figure 9. Hydrolysis reaction of 4-nitrophenyl palmitate with release of the phenolate chromogen.

p-nitrophenyl palmitate (colorless)   *p*-nitrophenol (yellow)   palmitic acid (colorless)
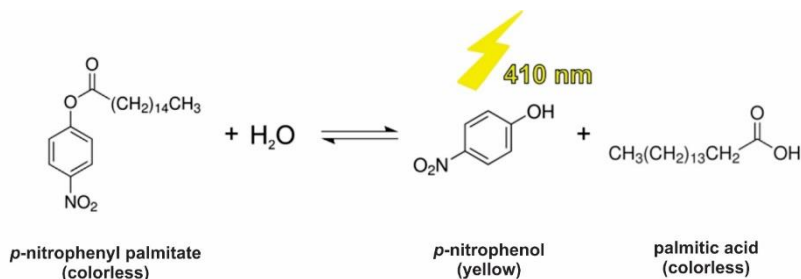
3.2.5.2 Downscaling

Aiming to reduce the amount of enzyme required for the activity assay, we modified the activity tests carried out at FUB. 5, 10, 15 and 20 µg of purified CalB were mixed with 0.5% *p*-NPP alcoholic solution (volume ratio CalB:*p*-NPP of 1:10) and 0.2 M sodium phosphate buffer pH 7 diluted in Milli-Q water to obtain a final molarity of 0.05 M in a total volume reaction of 50 µL. Reactions were performed at 30 ºC for 10 min, and stopped by adding the same volume (50 µL) of sodium carbonate 0.5 N. The reaction mixtures were centrifuged at 17000 g for 15 minutes. 50 µL of each supernatant were diluted to 800 µL with 0.05 M sodium phosphate buffer pH 7 and the sample absorbance was read at 410 nm.

After defining the best protein concentration to measure the hydrolysis activity, a kinetic study was carried out to define the best time of reaction. Hydrolysis activity data was expressed in U/µg.

3.5.5.3 Inhibition assays

The activity of CalB (purified at 10 mg/mL) against two inhibitors was also evaluated. Phenylmethanesulfonyl fluoride (PMSF) and ethylenediaminetetraacetic acid (EDTA) are known for being effective inhibitors of lipases with serine hydrolase activity (KANWAR et al., 2005). PMSF was tested in concentrations of 5, 10, 15 and 20 mM in a CalB:*p*-NPP molar ratio of 1:5. EDTA (pH 8) was also tested in a

CalB:*p*-NPP molar ratio of 1:5 in concentrations of 25, 50, 100 and 200 mM. Each assay was mixed to sodium phosphate buffer 0.2 M pH 7 (which was diluted in Milli-Q water to obtain a final molarity of 0.05 M in a total volume reaction of 50 µL). Reactions were performed at 30 ºC for 5 min, and stopped by adding the same reaction volume (50 µL) of sodium carbonate 0.5 N. The reaction mixtures were centrifuged at 17000 g for 15 minutes. 50 µL of each supernatant were diluted to 800 µL with sodium phosphate buffer and the sample absorbance was read at 410 nm.

3.2.5.4 Temperature and pH influence on activity

In order to investigate the CalB activity behavior in different pH and temperatures from those used for the standard hydrolysis activity assay, we performed several tests in pH 4.8, 7.5 and 9.2, and 30 and 60 ºC. 0.05 M buffers were prepared: citric acid/trisodium citrate buffer pH 4.8, sodium phosphate buffer pH 7.5 and sodium carbonate/sodium bicarbonate buffer pH 9.2.

CalB activity was measured as described in section 3.2.5.1, varying the enzyme temperature of incubation, buffer and temperature of activity assay incubation, as shown in Table 10.

Table 10. pH and temperature conditions tested for the CalB hydrolysis activity.

Assay	Incubation	Temperature of measurement (ºC)	pH buffer
1			4.8
2		30	7.5
3	Stored at 4 ºC in the fridge		9.2
4			4.8
5		60	7.5
6			9.2
7			4.8
8		30	7.5
9	1 h at 65 ºC in a water bath		9.2
10			4.8
11		60	7.5
12			9.2

3.2.6   Differential Scanning Fluorimetry

DSF experiments were carried out in a 96-well plate in a plate reader combined with a thermocycler (Stratagene Mx3005P, Agilent Technologies). Gel filtration purified CalB was diluted to 0.15 mg/mL in the final purification buffer supplemented with 10×SYPRO orange (1:500 dilution of the stock) in a total volume of 10 µL and pipetted into each well of a 96-well plate. The temperature was increased from 25 °C to 95 °C and the fluorescence emission was monitored in steps of 1 °C/min with hold steps of 30 seconds between reads. The fluorescence intensity was then plotted as a function of temperature. Different buffer compositions and compounds were tested for their stabilizing effect on the protein. All 96 conditions (compounds and compositions) tested are listed in Table 11.   The sigmoidal curve from each condition was normalized and corrected for the background signal of the fluorophore in the buffer. The inflection points of the curves, representing the thermal melting temperature of the protein in the respective conditions, were compared.

Table 11. Buffer compounds and compositions of the 96-well screening plate.

	1	2	3	4	5	6	7	8	9	10	11	12
A	50 mM NaAcetate pH 4.0	50 mM NaAcetate pH 4.4	50 mM NaCitrate pH 5.0	50 mM NaCitrate pH 5.4	50 mM NaCacodylate pH 6.0	50 mM NaCacodylate pH 6.4	50 mM NaPhosphate pH 7.0	50 mM NaHEPES pH 7.5	50 mM TrisHCl pH 8.0	50 mM TrisHCl pH 8.4	50 mM BORAX pH 9.0	50 mM BORAX pH 9.4
B	50 mM NaAcetate pH 4.0; 100 mM NaCl	50 mM NaAcetate pH 4.4; 100 mM NaCl	50 mM NaCitrate pH 5.0; 100 mM NaCl	50 mM NaCitrate pH 5.4; 100 mM NaCl	50 mM NaCacodylate pH 6.0; 100 mM NaCl	50 mM NaCacodylate pH 6.4; 100 mM NaCl	50 mM NaPhosphate pH 7.0; 100 mM NaCl	50 mM NaHEPES pH 7.5; 100 mM NaCl	50 mM TrisHCl pH 8.0; 100 mM NaCl	50 mM TrisHCl pH 8.4; 100 mM NaCl	50 mM BORAX pH 9.0; 100 mM NaCl	50 mM BORAX pH 9.4; 100 mM NaCl
C	50 mM NaAcetate pH 4.0; 200 mM NaCl	50 mM NaAcetate pH 4.4; 200 mM NaCl	50 mM NaCitrate pH 5.0; 200 mM NaCl	50 mM NaCitrate pH 5.4; 200 mM NaCl	50 mM NaCacodylate pH 6.0; 200 mM NaCl	50 mM NaCacodylate pH 6.4; 200 mM NaCl	50 mM NaPhosphate pH 7.0; 200 mM NaCl	50 mM NaHEPES pH 7.5; 200 mM NaCl	50 mM TrisHCl pH 8.0; 200 mM NaCl	50 mM TrisHCl pH 8.4; 200 mM NaCl	50 mM BORAX pH 9.0; 200 mM NaCl	50 mM BORAX pH 9.4; 200 mM NaCl
D	50 mM NaAcetate pH 4.0; 500 mM NaCl	50 mM NaAcetate pH 4.4; 500 mM NaCl	50 mM NaCitrate pH 5.0; 500 mM NaCl	50 mM NaCitrate pH 5.4; 500 mM NaCl	50 mM NaCacodylate pH 6.0; 500 mM NaCl	50 mM NaCacodylate pH 6.4; 500 mM NaCl	50 mM NaPhosphate pH 7.0; 500 mM NaCl	50 mM NaHEPES pH 7.5; 500 mM NaCl	50 mM TrisHCl pH 8.0; 500 mM NaCl	50 mM TrisHCl pH 8.4; 500 mM NaCl	50 mM BORAX pH 9.0; 500 mM NaCl	50 mM BORAX pH 9.4; 500 mM NaCl
E	20 mM NaHEPES pH 7.5, 100 mM NaCl, 1 mM $MgCl_2$	20 mM NaHEPES pH 7.5, 100 mM NaCl, 5 mM $MgCl_2$	20 mM NaHEPES pH 7.5, 100 mM NaCl, 10 mM $MgCl_2$	20 mM NaHEPES pH 7.5, 100 mM NaCl, 1 mM $CaCl_2$	20 mM NaHEPES pH 7.5, 100 mM NaCl, 5 mM $CaCl_2$	20 mM NaHEPES pH 7.5, 100 mM NaCl, 10 mM $CaCl_2$	20 mM NaHEPES pH 7.5, 100 mM NaCl, 1 mM $MnCl_2$	20 mM NaHEPES pH 7.5, 100 mM NaCl, 5 mM $MnCl_2$	20 mM NaHEPES pH 7.5, 100 mM NaCl, 10 mM $MnCl_2$	20 mM NaHEPES pH 7.5, 100 mM NaCl, 1 mM $ZiCl_2$	20 mM NaHEPES pH 7.5, 100 mM NaCl, 5 mM $ZiCl_2$	20 mM NaHEPES pH 7.5, 100 mM NaCl, 10 mM $ZiCl_2$

F	20 mM NaHEPES pH 7.5, 100 mM NaCl, 1 mMFeCl$_3$	20 mM NaHEPES pH 7.5, 100 mM NaCl, 5 mM FeCl$_3$	20 mM NaHEPES pH 7.5, 100 mM NaCl, 10 mM FeCl$_3$	20 mM NaHEPES pH 7.5, 100 mM NaCl, 50 mM KCl	20 mM NaHEPES pH 7.5, 100 mM NaCl, 100 mM KCl	20 mM NaHEPES pH 7.5, 100 mM NaCl, 200 mM KCl	20 mM NaHEPES pH 7.5, 100 mM NaCl, 50 mM LiCl	20 mM NaHEPES pH 7.5, 100 mM NaCl, 100 mM LiCl	20 mM NaHEPES pH 7.5, 100 mM NaCl, 200 mM LiCl	20 mM NaHEPES pH 7.5, 100 mM NaCl, 50 mM NH$_4$Cl	20 mM NaHEPES pH 7.5, 100 mM NaCl, 100 mM NH$_4$Cl	20 mM NaHEPES pH 7.5, 100 mM NaCl, 200 mM NH$_4$Cl
G	20 mM NaHEPES pH 7.5, 100 mM NaCl, 1 mM MgSO$_4$	20 mM NaHEPES pH 7.5, 100 mM NaCl, 5 mM MgSO$_4$	20 mM NaHEPES pH 7.5, 100 mM NaCl, 10 mM MgSO$_4$	20 mM NaHEPES pH 7.5, 100 mM NaCl, 50 mM Li$_2$SO$_4$	20 mM NaHEPES pH 7.5, 100 mM NaCl, 100 mM Li$_2$SO$_4$	20 mM NaHEPES pH 7.5, 100 mM NaCl, 200 mM Li$_2$SO$_4$	20 mM NaHEPES pH 7.5, 100 mM NaCl, 50 mM (NH$_4$)$_2$SO$_4$	20 mM NaHEPES pH 7.5, 100 mM NaCl, 100 mM (NH$_4$)$_2$SO$_4$	20 mM NaHEPES pH 7.5, 100 mM NaCl, 200 mM (NH$_4$)$_2$SO$_4$	20 mM NaHEPES pH 7.5, 100 mM NaCl, 1 mM Glycerol	20 mM NaHEPES pH 7.5, 100 mM NaCl, 5 mM Glycerol	20 mM NaHEPES pH 7.5, 100 mM NaCl, 10 mM Glycerol
H	20 mM NaHEPES pH 7.5, 100 mM NaCl, 50 mM AmAcetate	20 mM NaHEPES pH 7.5, 100 mM NaCl, 100 mM AmAcetate	20 mM NaHEPES pH 7.5, 100 mM NaCl, 200 mM AmAcetate	20 mM NaHEPES pH 7.5, 100 mM NaCl, 1 mM MgAcetate	20 mM NaHEPES pH 7.5, 100 mM NaCl, 5 mM MgAcetate	20 mM NaHEPES pH 7.5, 100 mM NaCl, 10 mM MgAcetate	20 mM NaHEPES pH 7.5, 100 mM NaCl, 50 mM NaFormiate	20 mM NaHEPES pH 7.5, 100 mM NaCl, 100 mM NaFormiate	20 mM NaHEPES pH 7.5, 100 mM NaCl, 200 mM NaFormiate	H$_2$O	Protein in its buffer + Sypro orange (Reference)	H$_2$O

3.2.7   Circular Dichroism

CD measurements were carried out on a J-810 spectropolarimeter (Jasco Analytical Instruments) in a quartz cuvette of 0.1 cm path length. Far-UV spectra (190–260 nm) were recorded with CalB at 0.1 mg/mL in 0.05 M potassium phosphate pH 7.4, at 20 °C and at 95 °C with a scan rate of 50 nm/min and a data pitch of 0.1 nm. In order to investigate the CalB thermal resistance, the enzyme (0.25 mg/mL) was previously denatured at 95 °C for 5 min and then the CD spectra was recorded at 20 °C in the same running conditions above. Three consecutive scans were accumulated and averaged for each sample. Data were baseline corrected and secondary structure contents were calculated using CDNN software (BÖHM; MUHR; JAENICKE, 1992). Melting profiles were recorded between 20 and 95 °C with the proteins at 0.1 mg/mL in the same buffer by monitoring the CD signal at 220 nm. The temperature was ramped at 2 °C/min with data sampling at every 0.1 °C. After the denatured curve was measured, we recorded a folding curve in order to investigate the CalB ability for refolding, running from 95 to 20 °C, at 2 °C/min and data sampling at every 0.1 °C.

3.2.8   Multi-Angle Light Scattering

CalB from *Candida antarctica* (theoretical molar mass of 33022 Da), purchased from Sigma Aldrich (Germany), was previously purified in a size exclusion chromatography (SEC) column (Superdex® 75 26/60, GE Healthcare, 28-9893-34) in 0.02 M sodium phosphate buffer pH 7.5 and 0.1 M sodium chloride and concentrated to 10 mg/mL. The 10 mg/mL purified CalB was then dissolved in buffer, composed of 0.02 M Tris pH 7.5 and 0.1 M sodium chloride with 0.02% (v/v) sodium azide added to prevent bacterial growth, to a concentration of 6.66 mg/mL, and a new separation was performed on a Superdex® 75 10/300 SEC column connected to a MALS device at a flow rate of 0.6 mL/min. The column characteristics were internal diameter of 10 mm, length of 300 mm, matrix composed of cross-linked agarose and dextran, particle size of 13 μm, maximum flow rate of 1 mL/min (maximum pressure of 1.8 MPa), molar mass range between $3x10^3$ and $7x10^4$ Da and bed volume of 24 mL (GE Healthcare, 17-5174-01). Same settings and column were used to perform SEC-MALS for CalB treated in CO_2 (35

ºC, 160 bar and 1 h) and LPG (65 ºC, 30 bar, 1 h), in order to check the oligomeric state of the lipase after treatment.

In order to investigate the oligomeric state of the enzyme in solution, SEC-MALS measurements were also carried out with the gel filtration purified CalB at 10 mg/mL incubated with the substrate 4-nitrophenyl palmitate (*p*-NPP) (dissolved in ethanol at 13 mM) in the molar ratio enzyme:substrate of 1:5 and with the enzyme previously inhibited by 10 mM of phenylmethylsulfonyl fluoride (PMSF) incubated with *p*-NPP (molar ratio CalB: substrate of 1:5). For all these experiments we applied the same column, buffer and running settings as used to analyze the purified CalB.

The detection was performed using a miniDAWN TREOS three-angle light scattering detector with a laser wavelength of 660 nm (Wyatt Technology), equipped with RefractoMax520 refractive index detector (ERC Inc.). The temperature was kept constant at 18 °C during all measurements. For data collection and analysis, Astra 6.1.4 software (Wyatt Technology) was used. Detectors were aligned, corrected for band broadening and photodiodes were normalized with BSA as a reference. For calculation of the molecular mass, the protein concentration was determined from the differential refractive index with a specific refractive index increment (dn/dc) of 0.185 mL/g.

3.2.9   Crystallization

To identify initial crystallization conditions, different commercially available crystallization reagents were screened in 96-well MRC plates (Qiagen; Hamptom Research) by sitting drop vapor diffusion technique. Drops of 200 nL (100 nL protein solution + 100 nL reservoir) were dispensed using a Cartesian liquid dispensing robot with 8 channels (Zinsser, Germany).

Initial hits were usually refined by manual setups in 24-well plates. Commercial additive screens (Hamptom Research) were routinely tested to improve crystallization conditions.

Crystallization of purified untreated CalB was carried out at 18 ºC. Diffraction data were collected at beamline 14.2 at BESSY II (HZB, Berlin, Germany) and beamline P14 of PETRA III (DESY, Hamburg, Germany) and processed with XDS (KABSCH, 2010). The structure of untreated CalB was solved by molecular replacement using the 1TCA coordinates (1.55 Å resolution) as a model. Initial phases were calculated using *Phaser* (McCOY et al., 2007). Model building was

performed using COOT (EMSLEY; COWTAN, 2004) and refinement using REFMAC5 (VAGIN et al., 2004) and Phenix (ADAMS et al., 2010).

3.2.10 Deglycosylation assay

The most efficient cleaving enzyme for *N*-glycan moiety is glycoamidase, particularly glycoamidase F (PNGase F), which cleaves the bond between N-acetyl glucosamine (GlcNAc) and an asparagine residue, thereby converting asparagine to aspartic acid. PNGase F cleaves most types of *N*-linked oligosaccharides, including complex structures (e.g., high mannose, hybrid and multisialylated structure), up to tetra antennary trees and oligosaccharides containing sulfate-substituted residues. However, for cleavage under native conditions, high concentrations of PNGase F may be required (ROTH; YEHEZKEL; KHALAILA, 2012).

Deglycosylation reactions with PNGase-F were performed following the standard protocol given by the supplier (https://www.neb.com/protocols/2014/07/31/pngase-f-protocol) with some modifications. Briefly, for deglycosylation under denaturing conditions, 2 µL (20 µg) of CalB purified by gel filtration were mixed with 1 µL of 10xGlycoprotein Denaturing Buffer and H_2O to make a 10 µL total reaction volume. The reaction mixture was heated at 100 °C for 10 minutes, followed by chilling on ice and centrifuged for 10 seconds. Then, 2 µL of 10xGlycoBuffer 2 were added to the reaction followed by 2 µL of 10% NP-40 and 6 µL of H_2O to make a total reaction volume of 20 µL. Finally, 10 µL of PNGase F were added, gently mixed and the reaction was incubated at 37 °C for 24 hours.

For deglycosylation under non-denaturing conditions, 2 µL (20 µg) of CalB purified by gel filtration were mixed with 2 µL of 10xGlycoBuffer 2 and H_2O to make a 20 µL total reaction volume. Then, 10 µL of PNGase F were added, gently mixed and the reaction was incubated at 37 °C for 24 hours.

A control reaction was performed replacing the PNGase F volume by H_2O under non-denaturing conditions.

All three reactions were sampled and analyzed on SDS-PAGE gels. Hydrolysis activity measurements were also conducted for all samples.

A kinetics study was performed following the non-denaturing reaction and the volumes were scaled up to allow aliquots to be taken every day during 5 days.

3.2.11 Mass Spectrometry

LC-MS/MS was used to determine the molecular weight of CalB and try to identify other compounds which come from the original commercial buffer and remain in the solution even after size exclusion chromatography.

Samples of purified CalB (control) and CalB enzymatically deglycosylated in a native reaction with PNGase F were sent to Dr. Christof Lenz, who performed the mass spectrometric analysis of the CalB samples (Group of Dr. Henning Urlaub; Bioanalytical Mass Spectroscopy, Max Planck Institute of Biophysical Chemistry, Göttingen, Germany).

CalB was first digested with trypsin and the fragments were analyzed in a coupled TripleTOF™ 5600 LC-MS/MS C18 mass spectrometer under standard conditions. Proteins were identified by searching fragment spectra against the NCBI non-redundant database using Mascot as a search engine.

3.2.12. High pressure treatment

3.2.12.1 Equipment assembling

The experimental apparatus for high-pressure treatment of CalB at UFSC consisted basically of a reservoir of solvent; two thermostatic baths (Nova Ética, 521/2D) for temperature control; a syringe pump (ISCO, 260D); one variable volume jacketed cell made of stainless steel, with a maximum volume of 28 mL and working volume of about 12 mL, with two coupled sapphire windows for visual observation; one absolute pressure transducer (Smar, LD301) equipped with a portable gauge (Smar, HT201) with an accuracy of ±0.4 bar (0.04 MPa). The schematic diagram of the apparatus is shown in Figure 10. The device enabled me to conduct the experiments up to 350 bar (35 MPa) and 80 °C (FRICKS et al, 2006; FRANKEN et al., 2010). All experimental assembly lines employed tubes made of stainless steel with external diameter (OD) of 1/16" (HIP), and included a "check valve" between the pump and the solvent reservoir (HIP, 15-41AF1-T 316SS) to prevent

backflow of the pressurized solvent. Two other micrometer valves (HIP, 15-11AF2 316SS) completed the experimental apparatus, one located after the syringe pump, in the cell inlet, to allow solvent loading, and another one to allow the pressurization of the piston by the cell background. A general view of the experimental apparatus and the cell used in the experiments at UFSC can be seen in Figures 11 and 12.

Figure 10. Schematic diagram of the experimental apparatus for CalB treatment in pressurized fluids. A - solvent reservoir; B/J - thermostatic baths; C - syringe pump; D - transducer and gauge of pressure; E - jacketed cell made of stainless steel; F - sapphire windows; G/H - micrometric valves for feeding and pressurization, respectively; I - piston.
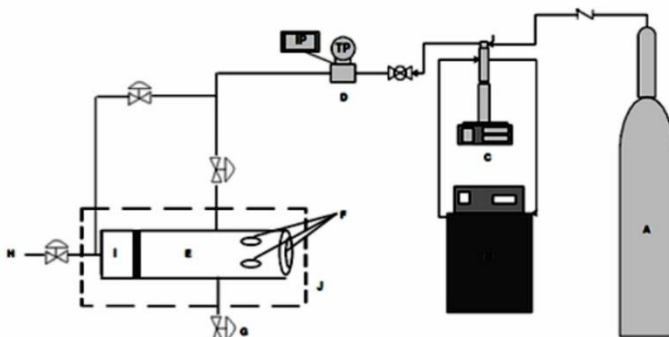
Figure 11. Overview of the experimental apparatus for CALB L® treatment in pressurized fluids at UFSC. A - solvent reservoir; B/H - thermostatic baths; C - syringe pump; D - transducer and gauge of pressure; E - jacketed cell made of stainless steel; F/G - micrometric valves for feeding and pressurization, respectively; I – temperature gauge.

Figure 12. Detail of the jacketed cell made of stainless steel.

A similar apparatus was assembled at FUB with some modifications. The syringe pump was replaced by a high performance liquid chromatography (HPLC) pump (Waters® 515) and the solvent was cooled using a glycerin bath added to dry ice. Figure 13 shows the experimental setup at FUB.

Figure 13. Overview of the experimental apparatus for CalB treatment in pressurized fluid at FUB. A - solvent reservoir; B - thermostatic bath; C – glycerin/dry ice bath; D - HPLC pump; E/F - manometers; G - jacketed cell made of stainless steel; H/I – micrometric valves for feeding and pressurization, respectively; J - temperature gauge.
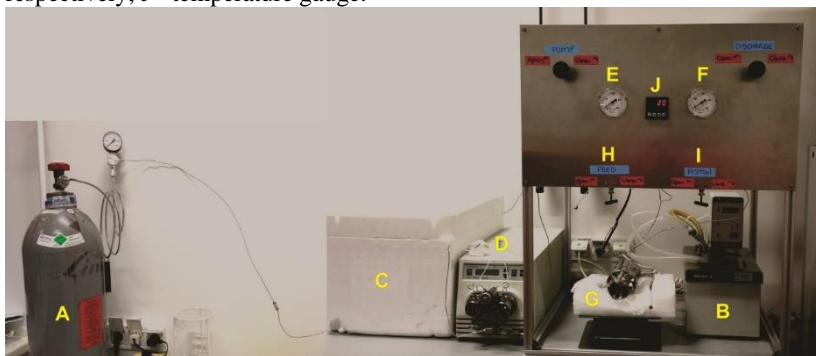
3.2.12.2 CalB treatment

The experimental procedure for CalB (donated by Novozymes Brazil) treatment in pressurized fluids at UFSC consisted, firstly, in the adjustment of the thermostatic bath at 7 ºC for cooling the fluid in the pump piston; and the other thermostatic bath at the set temperature for the experiment (35-65 °C for CO_2 and 25-65 ºC for LPG treatment). Then, the enzyme solution was fed into the cell (6.2 and 4.5 grams of CalB, for CO_2 and LPG treatment, respectively), followed by feeding the solvent at a known pressure and in the defined mass ratio (1:1). After that, the system was subjected to pressurization (75-275 bar for CO_2 and 30-90 bar for LPG) under different exposure times (1-6 hours), keeping the rate of pressurization and depressurization fixed at 10 bar/min (KUHN et al., 2010; SILVA et al., 2013b; 2013c). The system was depressurized by programming a displacement in the syringe pump piston and then opening the micrometric valve, used in the low-pressure region, near the saturation pressure of CO_2.

Tables 12 and 13 show the 2^3 full factorial experimental design used for the experiments carried out at UFSC. The minimum temperature and pressure variables were defined according to the critical temperature and pressure of CO_2 (31 °C and 73.8 bar, respectively) and exposure time according to the available literature (OLIVEIRA et al., 2006a; 2006b; FRICKS et al., 2006; PRIMO et al., 2007; KUHN et al., 2010; 2011; 2013; MANERA et al., 2011; SILVA et al., 2012; 2013a). As the supercritical temperature of LPG is not practicable for enzymes (T_c = 112 ºC, P_c = 39.5 bar), the gas was used in the liquid compressed state and the variables were defined according to the literature (KUHN et al., 2011; 2013; SILVA et al., 2013a; 2013c; 2013d).

Some experiments (12-16, Table 12) were performed to evaluate only the temperature influence on the lipase activity, without the influence of pressure, in which the enzyme was exposed to a steady stream of CO_2 at a flow rate of 0.08 mL/min per 5 minutes, followed by closure of the feeding valve, allowing the enzyme to be incubated with the fluid in a sort of "modified atmosphere", in a defined temperature and for a defined time, without pressurizing the system.

Enzymatic activity was determined before (initial activity) and after (final activity) the high-pressure treatment. The effect of the treatment was measured by means of the residual specific activity,

which is the ratio between the specific activity after and before exposure, expressed as a percentage.

Table 12. 2^3 full factorial experimental design for the CalB treatment in supercritical CO_2. Experiments 12-16 were carried out without pressurization of the system.

Assay	Temperature (ºC)	Pressure (bar)	Time (h)
1	- 1 (35)	- 1 (75)	- 1 (1)
2	+1 (65)	- 1 (75)	- 1 (1)
3	- 1 (35)	+1 (275)	- 1 (1)
4	+1 (65)	+1 (275)	- 1 (1)
5	- 1 (35)	- 1 (75)	+1 (6)
6	+1 (65)	- 1 (75)	+1 (6)
7	- 1 (35)	+1 (275)	+1 (6)
8	+1 (65)	+1 (275)	+1 (6)
9	0 (50)	0 (175)	0 (3.5)
10	0 (50)	0 (175)	0 (3.5)
11	0 (50)	0 (175)	0 (3.5)
12	- 1 (35)	-	- 1 (1)
13	+1 (65)	-	- 1 (1)
14	- 1 (35)	-	+1 (6)
15	+1 (65)	-	+1 (6)
16	0 (50)	-	0 (3.5)

Table 13. 2^3 full factorial experimental design for the CalB treatment in pressurized LPG.

Assay	Temperature (ºC)	Pressure (bar)	Time (h)
1	- 1 (25)	- 1 (30)	- 1 (1)
2	+1 (65)	- 1 (30)	- 1 (1)
3	- 1 (25)	+1 (90)	- 1 (1)
4	+1 (65)	+1 (90)	- 1 (1)
5	- 1 (25)	- 1 (30)	+1 (6)
6	+1 (65)	- 1 (30)	+1 (6)
7	- 1 (25)	+1 (90)	+1 (6)
8	+1 (65)	+1 (90)	+1 (6)
9	0 (45)	0 (60)	0 (3.5)
10	0 (45)	0 (60)	0 (3.5)
11	0 (45)	0 (60)	0 (3.5)

After both experimental designs were carried out, CalB was submitted to the best conditions without solvent loading into the cell (1 h at 35 ºC and 75 bar; and 1 h at 65 ºC and 30 bar), in order to check the isolated influence of the pressure and temperature on the activity.

At FUB, due to equipment restrictions, the maximum pressure evaluated was 160 bar. The experimental conditions studied for unpurified CalB (Sigma-Aldrich) and for CalB purified by gel filtration, both treated in supercritical CO_2 at FUB, are shown in Table 14.

Table 14. Experimental conditions used for CalB (Sigma-Aldrich) and for CalB purified by gel filtration treatment in supercritical CO_2 at FUB.

	Temperature (ºC)	Pressure (bar)	Time (h)
	65	160	1
	65	160	6
CalB from Sigma	35	80	0.5
	35	80	1
	35	160	1
	35	160	1
	35	160	3.5
CalB purified	35	80	1
	35	80	3.5
	35	80	6

3.2.12.3 Stability after treatment

As we aimed at structural investigation of the treated enzyme via X-ray crystallography and crystal growth may take from a few hours to several weeks, it was important to test how long the effects of the pressurized fluid treatment persist on the enzymatic activity. Moreover, the longer the effect lasts, the more advantageous it is from an industrial point of view.

With that in mind, CalB treated in the best condition with SC-CO_2 (experiment 1) was stored at 4 ºC (fridge), -10 ºC (freezer) and flash frozen in liquid nitrogen (-196 ºC) and stored at -10 ºC. Stability of CalB treated in the best condition with LPG (experiment 2) was monitored for samples stored at 25 ºC (bench), 4 ºC (fridge), and flash frozen in liquid nitrogen (-196 ºC) and stored at -80 ºC. Residual activity was periodically monitored for 60 days.

88

4.   RESULTS AND DISCUSSION

4.1.   CALB HYDROLYSIS ACTIVITY

Lipase B from *Candida antarctica* (CALB L®), kindly donated by Novozymes Brazil in an aqueous solution, was used in all experiments carried out at UFSC. Total protein concentration of that solution, measured by Bio-Rad Protein Assay, was 8.2 mg/mL.

CalB hydrolysis activity, measured as described in section 3.2.5.1, was about 3.5 U/mL.

From the values found for the initial hydrolysis activity and total protein content of CalB solution (3.5 U/mL and 8.2 mg/mL, respectively), the specific activity of the lipase was calculate at 0.43 U/mg.

4.2.   HIGH PRESSURE TREATMENT

4.2.1.   SC-CO_2 treatment

Results in terms of CalB residual specific activity (ratio of the specific activity after treatment with supercritical CO_2 and the specific activity of untreated lipase, %) from experiments that evaluated the effect of temperature, pressure and exposure time on the enzyme activity, as well as experiments without pressurization ("modified atmosphere") are compiled in Table 15. Values of residual specific activity are averages of two repetitions. Mass ratio enzyme:CO_2 was fixed to 1:1, and the rates of pressurization and depressurization to 10 bar/min. CalB hydrolysis activity was measured as described in section 3.2.5.1.

Table 15. Residual specific activity (%) of CalB submitted to supercritical CO_2 treatment at UFSC. Experiments 12-16 were carried out without pressurization of the system ("modified atmosphere").

Assay	Temperature (°C)	Pressure (bar)	Time (h)	Residual specific activity (%) ± standard error
1	- 1 (35)	- 1 (75)	- 1 (1)	132.3 ± 3.8
2	+1 (65)	- 1 (75)	- 1 (1)	101.6 ± 5.1
3	- 1 (35)	+1 (275)	- 1 (1)	95.3 ± 3.0
4	+1 (65)	+1 (275)	- 1 (1)	103.5 ± 5.2
5	- 1 (35)	- 1 (75)	+1 (6)	102.8 ± 8.7
6	+1 (65)	- 1 (75)	+1 (6)	80.2 ± 6.2
7	- 1 (35)	+1 (275)	+1 (6)	89.6 ± 1.9
8	+1 (65)	+1 (275)	+1 (6)	90.1 ± 2.5
9	0 (50)	0 (175)	0 (3.5)	93.9 ± 3.7
10	0 (50)	0 (175)	0 (3.5)	91.2 ± 5.4
11	0 (50)	0 (175)	0 (3.5)	95.4 ± 4.4
12	- 1 (35)	-	- 1 (1)	101.9 ± 6.8
13	+1 (65)	-	- 1 (1)	109.9 ± 10.5
14	- 1 (35)	-	+1 (6)	102.9 ± 2.1
15	+1 (65)	-	+1 (6)	117.8 ± 6.5
16	0 (50)	-	0 (3.5)	110.9 ± 9.8

Analyzing the experiments 12-16 of Table 15, we conclude that the "modified atmosphere" of CO_2 in the unpressurized system did not influence the CalB residual specific activity. The slight increase of the CalB hydrolysis activity under some conditions can be explained by its activation at high temperatures (see section 4.3.9). Moreover, we observed different behavior of CalB under different experimental conditions. In experiment 1, a considerable increase in CalB residual specific activity was observed (132.3%) while in other conditions the residual specific activity remained unaltered or was decreased, as in experiment 6 (80.2%), in which the largest loss of activity was observed. In general, long exposure times to mild or high pressures led to a decrease on the CalB specific hydrolysis activity.

4.2.1.1. *Effect of high pressure*

The effects of pressure on protein structure and function can vary dramatically depending on the magnitude of the pressure, the reaction mechanism, and the overall balance of forces responsible for maintaining the protein's structure.

Electrostatic interactions of the protein (salt bridges or ionic bonds) usually are strongly destabilized with the increasing pressure, while the hydrogen bonds are strongly stabilized at high

pressures. According to KUNUGI (1992), the hydrogen bonds can be intensified by increasing pressure because of the reduction of the interatomic distances, leading to smaller molecular size. The shortening of hydrogen bonds, in addition to the collapse of internal cavities, can contribute to the compression of proteins under pressure. Therefore, the protein stability is negligibly influenced by the hydrogen bonds when it is submitted to pressurized fluids (HEI; CLARK, 1994; MICHELS; HEI; CLARK, 1996). Additionally, covalent bonds compression or breaking, and/or aggregation of unfolded protein are effects not expected to occur under high pressure (MOZHAEV et al., 1996a).

On the other hand, hydrophobic interactions are responsible for directing non-polar side chains to cluster inside proteins and are major driving forces for proper folding (BOONYARATANAKORNKIT; PARK; CLARK, 2002). Although hydrostatic pressure is an important tool for investigating the role of hydrophobic residues in the stability of proteins, the actual behavior of hydrophobic residues within proteins under pressure remains unclear.

Pressure-induced hydration can also reduce the number of intramolecular hydrogen bonds, due to the formation of intermolecular hydrogen bonds with water, resulting in increased conformational fluctuations of peripheral protein segments that are generally more mobile. This increase of the polypeptide hydration leads to a mobility enhancement by dragging of the polar groups by the solvent, allowing conformational changes, either favoring the exposure of the active site hydrophobic residues to catalysis or leading to the unfolding and subsequent denaturation of the protein (MOZHAEV et al., 1996a; 1996b; MICHELS; HEI; CLARK, 1996; BOONYARATANAKORNKIT; PARK; CLARK, 2002).

Ion pairs in proteins are short-range interactions that occur between negatively and positively charged amino-acid side chains over a distance of 4 Å or less. The role of ion pairs in proteins is to stabilize the tertiary and quaternary structure. Dissociation of ion pairs leads to electrostriction, which is the contraction of solvents such as water and alcohols due to alignment of dipolar solvent molecules in the electric field of an exposed charge. Because contraction of solvents leads to a volume decrease, pressure is expected to favor ion-pair disruption. When a protein unfolds,

normally sheltered hydrophobic residues in the protein interior are exposed to water as are ionized residues near the surface of the folded protein. Several model studies have indicated that interactions between exposed ionic groups and the surrounding solvent give rise to negative volume changes (ΔV, which is the volume difference between the reversibly denatured protein and the native protein, including solvation volumes) because of a phenomenon called electrostriction. Studies suggest that volume changes for the solvation of non-polar side chains are positive. If the ΔV for solvation of hydrophobic groups is indeed positive, then the volume change accompanying unfolding of a very hydrophobic protein will be positive, and pressure may stabilize the native structure by inhibiting unfolding (HEI; CLARK, 1994; BOONYARATANAKORNKIT; PARK; CLARK, 2002).

4.2.1.2. Effect of SC-CO$_2$

Several studies in the current theme-related literature refer to the use of CO$_2$ as solvent (GIEßAUF et al., 1999; GIEßAUF; GAMSE, 2000; BAUER; GAMS; MARR, 2001; FINDRIK et al., 2005; OLIVEIRA et al., 2006a; 2006b; FRICKS et al., 2006; PRIMO et al., 2007; ANDRADE et al., 2008; EISENMENGER; REYES-DE-CORCUERA, 2009; WANG et al., 2009; FRANKEN et al, 2010; KUHN et al., 2010; 2011; 2013; MANERA at al., 2011; SENYAY-ONCEL; YESIL-CELIKTAS, 2011; BRAGA et al., 2012; LIU et al., 2012; 2013a; 2013b; SILVA et al., 2012; 2013a; 2013b; 2013c; CHEN et al., 2013a; 2013b) and we can observe that there is no linear trend as different enzymes can show loss or gain in activity under CO$_2$, depending on the enzyme source, enzyme buffer and experimental conditions employed.

It is assumed that the use of CO$_2$ leads to loss of enzymatic activity mainly due to its hydrophilic features (log P$_{oct}$<2). According to several authors, CO$_2$ could strip off the intrinsic water from the enzyme, which is essential to the maintenance of its activity (OLIVEIRA et al., 2006a; 2006b; FRICKS et al., 2006; PRIMO et al., 2007).

HOUSAINDOKHT et al. (2012) used molecular dynamics (MD) to investigate the effect of SC-CO$_2$, in comparison to the water, on the structural properties of a new variant of *Candida antarctica* lipase B, cp283Δ7. The analysis of root mean square

deviation showed that in SC-CO$_2$, the structural variations of the enzyme are more pronounced than those of in the aqueous solution and therefore dissolving enzyme in SC-CO$_2$ impose an undesirable instability on its structure. Moreover, the radius of gyration showed that in SC-CO$_2$ the compactness of the enzyme structure is reduced, which leads to decreased stability. The secondary structure analysis revealed that in SC-CO$_2$ the amounts of α-helix and β-sheet contents of enzyme are reduced and the amount of random coil is increased.

According to NAKAYA et al. (2001), CO$_2$ has the solubility in water reduced with decreasing pressure and less irreversible damage is caused to the tertiary structure of the enzyme in mild pressure. Such effect can be observed in our results, as a higher activity increase (residual activity of 132%) was obtained when CalB was exposed to mild pressure for short time (75 bar for 1 hour in experiment 1). When high pressures were applied for long exposure times (275 bar for 6 hours) or the enzyme was exposed for long time to mild pressure, like in experiment 6 (75 bar for 6 hours), we observed considerable loss of activity (residual activity of 90% in experiments 7 and 8, and 80% in experiment 6).

KAMAT et al. (1995) and later, CELEBI et al. (2007) suggested that CO$_2$ could dissolve itself in the enzyme hydration layer, thereby altering the local pH and, consequently, affecting the enzyme activity. In non-aqueous media, enzymes change their activity if the pH of the micro-aqueous environment around them is altered. The effects on activity would naturally be the result of changes in the ionization state of either residue side chains or the ionization states of bound enzyme-substrate complexes.

With that in mind, we have measured the pH of the CalB solution before and after treatment in several experimental conditions with CO$_2$ as well as with LPG, and we did not observe changes on the pH values. The pH for all samples, treated or untreated, was in a range of 3.9 - 4.1.

CO$_2$ may also form covalent complexes with free amino groups on the surface of the enzyme. These complexes, called carbamates, would result in charge removal of lysine residues, and could potentially affect enzyme activity (KAMAT et al., 1995; CELEBI et al., 2007). Figure 14 shows a scheme of the reaction. Carbamylation reactions are capable of altering the structure and

functional properties of proteins and have been implicated in the mechanisms of several disease conditions.

Figure 14. Reaction of amine and carbon dioxide.

$$2R\text{-}NH_2 + CO_2 \leftrightarrow RNHCOO^-.RNH_3^+ \quad (\text{excess } NH_2)$$

or

(excess CO_2)
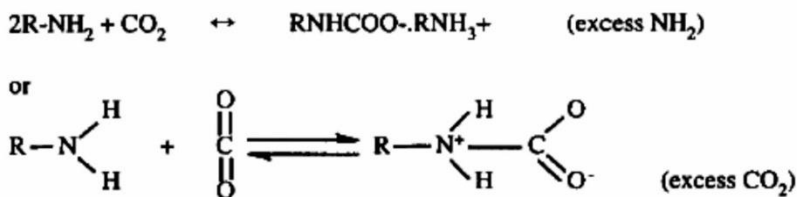
DIAF; BECKMAN (1995) and KAMAT et al. (1995) showed that under temperatures below 60 °C, significant fractions of proteins are covalently modified in SC-CO_2. They highlight that just because a protein has been modified does not mean, a priori, that its function will be altered. However, in the case of lipase-catalyzed acrylate transesterifications in SC-CO_2, they believe that the low activity of the enzyme can be accounted for a mechanism of inhibition via solvent-induced carbamate formation.

This unstable or reduced activity enzyme complex is formed at low temperatures, but it is dissociated at higher temperatures. Above 60 ºC, the protein would be unmodified. Such modification might have happened to CalB in experiments 3 and 7, in which the enzyme was exposed to 275 bar at 35 ºC.

4.2.1.3. Combined effect of pressure and temperature

Several phenomena have been observed when exposing enzymes to pressurized fluids, and the effects seem to depend on the protein, protein buffer and temperature and pressure conditions used. Some enzymes have shown increased activity when exposed to supercritical carbon dioxide under mild conditions of temperature and pressure, for short exposure times (MELGOSA et al., 2015; CHEN et al., 2013a; 2013b; LIU et al., 2012; MANERA et al., 2011; GIEβAUF; GAMSE, 2000). On the other hand, according to LIN et al. (2006), enzymes exposed for long periods to high temperatures combined with pressurized fluid may suffer loss of their catalytic power.

MELGOSA et al. (2015) investigated the behavior of two commercial enzymes in solution (Palatase 20000 L® and Lipozyme CALB L®) in SC-CO$_2$, varying temperature (35-70 ºC), pressure (100-250 bar), time of exposure (1-6 hours) and pressurization/depressurization cycles (1-3). They verified an increase on the relative activities for both enzymes treated under moderate conditions, while in high temperatures, pressures and long exposure times there were losses of activity (residual activity of 80%). The highest residual activity of CalB was 112%, verified in 150 bar, 35 ºC, 3 hours of exposure and 1 pressurization/depressurization cycle. We could reach an activity of 132.3% in experiment 1, which is considerably greater than the result obtained by these authors.

MANERA et al. (2011) submitted β-galactosidase from *Kluyveromyces marxianus* CCT 7082, lyophilized, to pressurized CO$_2$ and the residual activity increased up to 177% (37 ºC, 70 bar, depressurization rate of 10 kg/m^3.min and 1 hour exposure).

LIU et al. (2012), treated a lipase from *Candida rugosa* Lip7 (CRL 7), in solution, with sub and supercritical CO$_2$, and observed residual activity of 188% when they applied 100 bar at 40 ºC during 30 minutes.

MICHELS; HEI; CLARK (1996) affirm that the volume reduction associated with electrostriction should be counteracted by high temperature due to disruption of the highly ordered structure of electrostricted water. Because pressure favors electrostriction, it can promote disruption of protein salt bridges and induce protein denaturation. On the other hand, pressure may bring about protein stabilization if there are weak interdomain ion pair interactions not exposed to solvent, which may be strengthened by pressure.

Pressure-induced stabilization has been discussed from the viewpoint of resisting thermal unfolding at elevated temperatures, but this phenomena is not applicable to all proteins, in part because pressure can increase and not decrease fluctuations, as observed for proteins such as apomyoglobin, RNase T1, and phosphoglycerate kinase (TANAKA et al., 2000). Still, there are temperatures at which each protein is stabilized by pressure, and a distinct pressure at which the concentration of folded protein is at a maximum. HEI and CLARK (1994) found that increased thermostability correlated

with increased hydrophobicity and postulated that pressure stabilization was also related to increased hydrophobicity at interdomain interfaces. Several proteins have been shown to be stabilized against thermal inactivation by pressure, including α-chymotrypsin (MOZHAEV, 1996b), protease from *Methanococcus jannaschii* (HEI; CLARK, 1994), and glutamate dehydrogenases from *Pyrococcus furiosus* and *Thermococcus litoralis* (SUN et al, 1999; 2001).

MOZHAEV et al. (1996b) investigated α-chymotrypsin (CT) at 50 °C under a pressure of 3600 bar and the enzyme showed 30 times higher activity than the activity at normal conditions (20 °C, 1 atm). At pressures higher than 3600 bar, the enzymatic activity is decreased due to a pressure-induced denaturation. Elevated hydrostatic pressure is also efficient for increasing stability of CT against thermal denaturation. For example, at 55 ºC, CT is almost instantaneously inactivated at atmospheric pressure, whereas under a pressure of 1800 bar CT retains its anilide-hydrolyzing activity during several dozen of minutes.

At 65 ºC and even when 275 bar were applied to CalB, its activity was maintained. According to MOZHAEV et al. (1996a; 1996b), a possible explanation for the enzymes stability to thermal inactivation by high pressure would be due to the antagonist effects of pressure and temperature on the ability of some functional groups of the protein to interact with the water. The hydration of charged groups by water molecules is intensified by pressure and weakened by high temperatures (EISENMENGER; REYES-DE-CORCUERA, 2009). In an initial step of thermal inactivation, the protein loses certain amount of essential water molecules, and this loss can generate a structural rearrangement in the protein. High pressure has an opposite effect, favoring the hydration of charged groups. In other words, high hydrostatic pressure application enforces the protein hydration layer, preventing the thermal inactivation.

BOONYARATANAKORNKIT; PARK; CLARK (2002) claim that pressure-induced thermostabilization is due to the fact that temperature and pressure are opposing forces in terms of entropy. Increasing temperature leads to disorder, while increasing pressure leads to order. This is not always true, however, as increasing pressures may lead to hydration of protein interiors, as

seen in section 4.2.1.1., resulting in increased conformational fluctuations and disorder.

4.2.2. LPG treatment

Table 16 shows the results, in terms of residual specific activity of CalB, of experiments that evaluated the effect of temperature, pressure and exposure time on the enzyme activity after treatment with LPG. Values of residual specific activity are averages of two repetitions. Mass ratio enzyme:LPG was fixed to 1:1, and the rates of pressurization and depressurization to 10 bar/min.

CalB shows different behavior under different experimental conditions when exposed to LPG (Table 16). We observed an increase of its hydrolysis activity in experiment 2 (142.4%) and the largest loss of activity was observed in experiment 8 (83.7%).

SILVA et al. (2013d) investigated the influence of pressurized LPG and pressurized LPG combined with ultrasound treatment on the activity of a commercial cellulase (from *Trichoderma reesei* (NS50013)). They observed residual activity of 220% when the enzyme was treated with LPG in 30 bar, 40 ºC during 1 hour, and 384% when it was submitted to 150 bar, 47.5 ºC, during 1 hour in LPG combined with ultrasound (123 W).

Table 16. Residual specific activity (%) of CalB submitted to liquefied petroleum gas treatment at UFSC.

Assay	Temperature (ºC)	Pressure (bar)	Time (h)	Residual specific activity (%) ± standard error
1	- 1 (25)	- 1 (30)	- 1 (1)	96.2 ± 6.2
2	+1 (65)	- 1 (30)	- 1 (1)	142.4 ± 2.3
3	- 1 (25)	+1 (90)	- 1 (1)	101.6 ± 3.8
4	+1 (65)	+1 (90)	- 1 (1)	94.7 ± 2.9
5	- 1 (25)	- 1 (30)	+1 (6)	86.3 ± 7.2
6	+1 (65)	- 1 (30)	+1 (6)	108.2 ± 5.1
7	- 1 (25)	+1 (90)	+1 (6)	105.2 ± 3.0
8	+1 (65)	+1 (90)	+1 (6)	83.7 ± 6.3
9	0 (45)	0 (60)	0 (3.5)	101.4 ± 4.2
10	0 (45)	0 (60)	0 (3.5)	100.8 ± 3.1
11	0 (45)	0 (60)	0 (3.5)	101.9 ± 3.9

It is noteworthy to point out that CalB submitted to the best conditions without solvent loading into the cell (1 h at 35 ºC and

75 bar; and 1 h at 65 ºC and 30 bar), did not show significant changes on the hydrolysis activity, meaning that there is no influence of the pressure and temperature on the CalB activity when there is no solvent contact.

Although several enzymes are not stable in harsh conditions of SC-CO$_2$, recent findings have shown that the enzymes are active and stable in propane under same pressure and temperature conditions. There are, however, no clear reasons for such behavior. Trying to find out an explanation for the stability and high activity of enzymes in propane, MONHEMI; HOUSAINDOKHT (2012) investigated the *Candida antarctica* lipase B (CalB) microenvironment in near-critical propane using molecular dynamic simulation (MD). For comparison with other solvent models the enzyme was also simulated in water, hexane and SC-CO$_2$. They found that the enzyme in SC-CO$_2$ shows high structural deviations from the native form while, when in near-critical propane, CalB displays small structural deviations and its three dimensional architecture are very close to those of the enzyme in the mild aqueous solution. CalB structural deviations in near-critical propane are also lower than those of in hexane. α-helix and β-sheet contents of the enzyme remain intact in near-critical propane. Front of the enzyme, which includes α5 and α10 at the active site entrance, is mostly exposed to the propane environment. The hydrophobic nature of α5 and α10 makes their environment to be free of waters. Instead, propane molecules are accumulated on these regions. Exposing the active site entrance (including α5 as a short lid) to the hydrophobic media is a famous mechanism namely "interfacial activation" in which most of lipases can function well.

Thereby, the interaction of hydrophobic substrates such as lipids or fatty acids to the catalytic triad is easier. Due to the hydrophilic nature of CO$_2$ molecules, they cannot stabilize the hydrophobic side chains. Moreover, it was found that the activity of the enzyme in near-critical propane can be related to the water distribution on the surface of the enzyme. CO$_2$ molecules disperse most of waters about the catalytic triad but propane molecules cannot disperse these crystallographic waters, required to catalysis. Existence of water molecules around the catalytic triad of the enzyme in near-critical propane may be another factor which determines more activity of the enzyme in this compressed gas.

HOUSAINDOKHT; MONHEMI (2013) also showed via MD a similar behavior of *Burkholderia cepacia* lipase in compressed propane: the lid of the lipase was opened, which enables the substrate entrance to the active site and so the enzyme presented an active conformation. Moreover, it was found that in the compressed propane, similar to the aqueous solution, the enzyme has a native conformation.

Although the mechanisms of protein stabilization by high pressure have still not been clarified, it is supposed that the intra and intermolecular interactions, the charged groups' hydration, the essential water disruption and the stabilization of hydrogen bonds, play an important role on the phenomena explanation (EISENMENGER e REYES-DE-CORCUERA, 2009).

With that in mind, we set up a collaboration project with Markus Wahl Group at the Freie Universität Berlin, who features a cutting-edge Structural Biochemistry Laboratory, aiming to try to visualize structural changes in CalB when treated with CO_2 and LPG, which would be responsible for the changes on its catalytic activity.

For crystallization trials, it is mandatory that the enzyme remains active for the period of time the crystals take to grow. For this reason, we performed an evaluation of the stability of CalB stored at low temperatures after treatment under conditions of experiment 1 with CO_2 and experiment 2 with LPG, in which we observed the highest hydrolysis activity increments.

4.2.3.   Stability of CalB at low temperatures after treatment in pressurized fluids

Treated enzymes were monitored during 60 days. CalB treated in condition 1 with CO_2, was stored in the refrigerator (4 °C), freezer (-10 °C) and flash-frozen in liquid nitrogen (-196 °C) followed by storage in the freezer (-10 °C). CalB treated in condition 2 with LPG, was stored at 25 ℃ (bench), 4 ℃ (fridge), and frozen in liquid nitrogen (-196 ℃) and stored at -80 ℃. The residual specific activity of the enzymes was monitored periodically in these different systems, and the results of the stability study, in relative specific activity (%) are shown in Figure 15.

Figure 15. Stability of CalB, (**A**) treated in SC-CO$_2$ under 35 °C, 75 bar, 1 hour, lipase:CO$_2$ ratio 1:1 (m/m), pressurization and depressurization rates of 10 bar/min, stored for 60 days at 4 °C, -10 °C and flash-frozen in liquid N$_2$ (-196 °C) followed by storage at 10 °C, and (**B**) treated in LPG under 65 °C, 30 bar, 1 hour, lipase:LPG ratio 1:1 (m/m), pressurization and depressurization rates of 10 bar/min, stored for 60 days at 25 ℃ (bench), 4 ℃ (fridge), and frozen in liquid nitrogen (-196 ℃) and stored at -80 ℃.
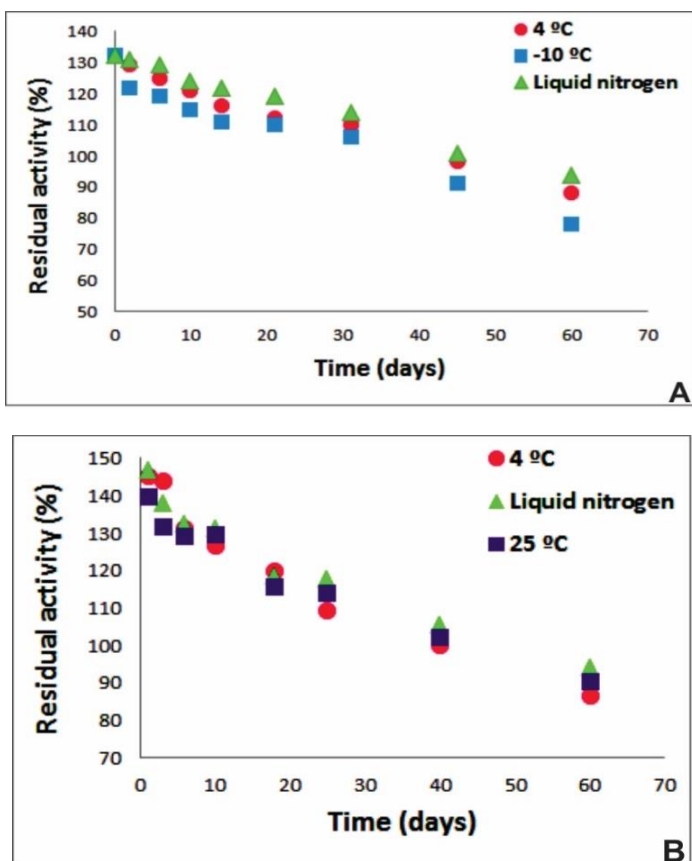
It can be seen in Figure 15 (a) and (b) that CalB treated with SC-CO$_2$ and LPG gradually loses activity over time at low

temperatures in all three systems studied. However, it can be clearly seen that the residual activity of the enzyme treated at high pressure was still above 100% until the 20th day of storage, which enabled crystallization trials with treated CalB.

There was no difference on the residual activity loss of CalB treated with LPG and stored at different temperatures. Greater difference was observed between CalB treated with CO_2 and flash-frozen in liquid nitrogen (-196 °C) followed by storage in freezer (-10 °C) and CalB stored in freezer at -10 ºC.

The protein denaturation level induced by freezing is a complex function of the freezing rate as well as the final absolute temperature (WANG, 2000). The effects related to the freezing rates on protein stability are variable. Since solubility of non-polar groups in water increases with decreasing temperature due to increased hydration of the non-polar groups, solvophobic interaction in proteins weakens with decreasing temperature. The decreasing solvophobic interaction in proteins can reach a point where protein stability reaches zero, causing cold denaturation.

Tattini Jr. et al. (2006) observed, analyzing the physicochemical and structural behavior of bovine serum albumin (BSA) under two freezing rates (2.5 ºC/min (slow-freezing) and 30 ºC/min (quick-freezing)), via Raman spectroscopy, more structural modifications on the slowly frozen BSA. This supports the idea that SC-CO_2 treated CalB stored at 4 and 10 degrees, and therefore partially denatured, shows lower activity compared to the treated enzyme flash frozen in liquid nitrogen. We cannot explain, however, the reason why slow freezing rates did not affect the LPG treated enzyme.

4.3.   PURIFICATION

4.3.1.   Size-exclusion chromatography

Lipase B from *Candida antarctica* (CalB) expressed in *Aspergillus niger* purchased from Sigma-Aldrich was purified in a size-exclusion chromatography (SEC) column (Superdex® 75, 26/60) using 0.02 M sodium phosphate buffer pH 7.5 and 0.1 M sodium chloride. For each single purification, 5 mL of CalB were

loaded into the column at a flow rate of 2 mL/min at 4 °C using an Äkta purifier system. Aliquots of 2 mL were collected and fractions were analyzed by SDS-PAGE and the fractions of the peak corresponding to CalB (theoretical molar mass of 33022 Da) were concentrated to 10 mg/mL. Figures 16 and 17 show the gel filtration chromatogram and the SDS-PAGE for the CalB purified by gel filtration, respectively.

Figure 16. Chromatogram showing the profile of the CalB migration on a Superdex 75 26/60.
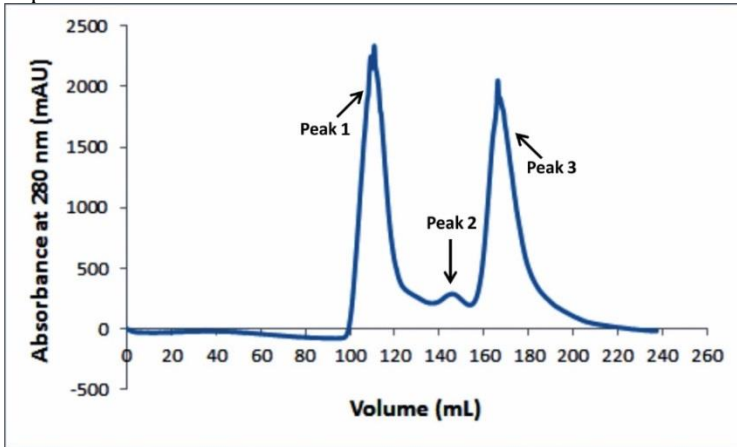
Figure 17. SDS-PAGE for fractions of CalB purified by gel filtration.
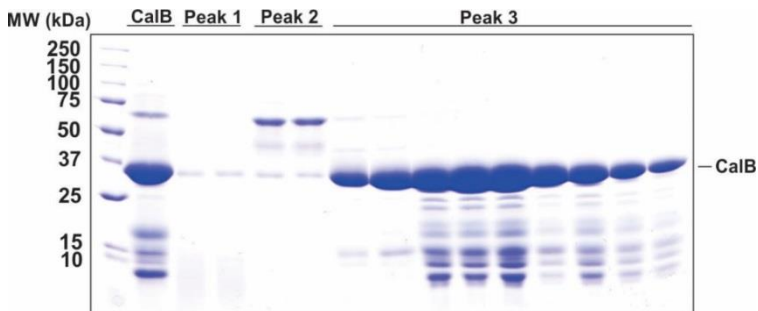
In the SDS-PAGE, we can clearly see that CalB corresponds to the third peak of the chromatogram, as observed by

the band in the region of the molecular weight slightly below the marker band of 37 kDa. We can also see that there are still some impurities of low molecular weight co-migrating with CalB. In order to improve purity, fractions of peak three from gel filtration were pooled, diluted in low salt buffer (20 mM Tris pH 8.0 and 50 mM NaCl) and run in ion-exchange columns.

4.3.2. Ion-exchange chromatography

CalB (theoretical isoelectric point of 5.8) purified by SEC and concentrated to 10 mg/mL was loaded into an anion exchange column (Mono Q® 10/100 GL) which was equilibrated in low salt buffer. 2 mL of CalB (10 mg/mL) were loaded into the column at a flow rate of 0.5 mL/min at 4 °C using an Äkta purifier system. Elution was carried out with a linear gradient from 50 to 1500 mM NaCl. Aliquots of 2 mL were collected and fractions were analyzed by SDS-PAGE. Figures 18 and 19 show the anion exchange chromatogram and the SDS-PAGE for the CalB purified by anion exchange chromatography, respectively.

In the chromatogram, we can see that CalB did not bind to the column and is present in the flow through (FT). In order to check CalB binding to the cation exchange column, we also performed CalB purification in a Mono S® 10/100 GL, employing all the same parameters as used for the Mono Q® purification. CalB also did not bind to the Mono S® column as observed for the Mono Q®. Since 5.8 is the theoretical pI of CalB, we suggest that the actual pI of the protein differs from the calculated one. Additionally, the CalB present in the FT from both ion exchange columns was slightly more pure than the protein after GF, most likely due to the fact that contaminants bound to the ion exchange columns while the protein passed through. In any case, we decided to keep the GF column as the only purification step.

Figure 18. Chromatogram showing the profile of the CalB migration on a Mono Q® 10/100 GL. Red line indicates the salt gradient.
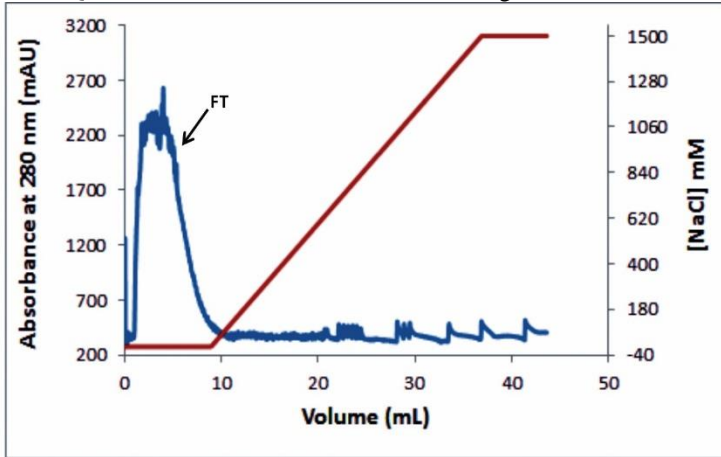
Figure 19. SDS-PAGE with fractions of CalB purified by anion exchange chromatography.
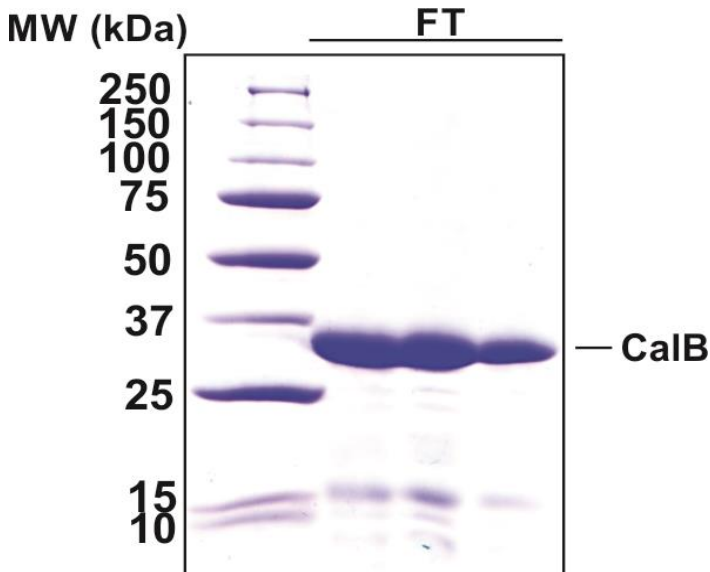
4.3.3. CalB hydrolysis activity

For all experiments carried out at FUB, CalB purchased from Sigma-Aldrich was used. Total protein concentration of that solution, measured by Bio-Rad Protein Assay, was 6.8 mg/mL. CalB hydrolysis activity was about 1.4 U/mL, measured as described in the section 3.2.5.2.

CalB purified by gel filtration and concentrated to 10 mg/mL presented a hydrolysis activity of 1.7 U/mL, very similar to the value before GF. We therefore conclude that the enzyme did not suffer any activity loss during purification, buffer exchange and concentration.

4.3.3.1. Downscaling

To reduce the amount of enzyme required to perform the activity assay, activity tests carried out at FUB were adapted to use low protein concentrations, as described in section 3.2.5.2. Table 17 shows the hydrolysis activity for different amounts of purified CalB, measured in triplicate.

Table 17. Hydrolysis activity for different amounts of CalB.

Mass of CalB (µg)	Activity (U/mg)
5	0.22± 0.02
10	0.18± 0.01
15	0.13± 0.03
20	0.1± 0.02

As we can see in Table 16, less amount of protein leads to higher hydrolysis activity. We can possibly justify this behavior to the fact that a huge amount of enzyme added to the reaction would impede the proper contact enzyme-substrate, which would lead to the chromogenic *p*-nitrophenol release. Thus, we decided to use 5 µg of CalB in the following hydrolysis activity assays.

4.3.3.2. Kinetics of hydrolysis of p-NPP

After defining the best protein concentration to measure the hydrolysis activity, a kinetic study was carried out to define the

best time of reaction. Figure 20 presents the kinetics curve for the hydrolysis of *p*-NPP by 5 µg of purified CalB.

We can see in Figure 20 that the *p*-NPP hydrolysis to *p*-nitrophenol by CalB is very fast and the maximum production of *p*-nitrophenol is reached in 10 minutes of reaction. From 5 to 10 minutes the increment in activity is so low that we decided to fix the time for all activity measurements to 5 minutes.

Figure 20. Kinetics of *p*-NPP hydrolysis by 5 µg of purified CalB.
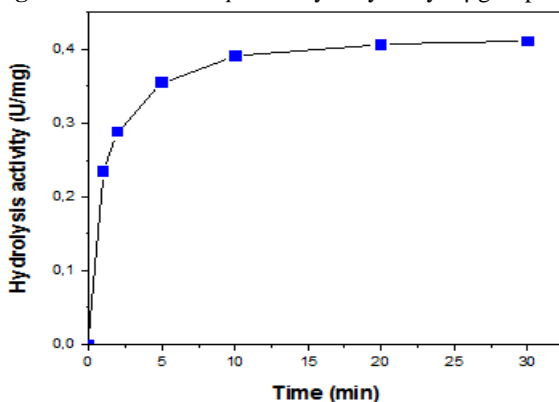
4.3.3.3. Inhibitors

CalB activity in the presence of the inhibitors phenylmethanesulfonyl fluoride (PMSF) and ethylenediaminetetraacetic acid (EDTA) was also investigated. PMSF (5, 10, 15 and 20 mM) and EDTA (25, 50, 100 and 200 mM) were tested in a CalB:*p*-NPP molar ratio of 1:5 assays. Figure 21 shows the residual hydrolysis activity (%) for CalB inhibited by different concentrations of (a) PMSF and (b) EDTA. Hydrolysis activity of CalB without inhibitor was defined as 100% residual activity.

We can see in Figure 21 (a) that PMSF inhibits up to 80% of the CalB hydrolysis activity at 10 mM concentration. Higher concentration of PMSF did not inhibit Calb any further. In Figure 21 (b) we observe that EDTA also inhibits CalB hydrolysis activity, however, less effectively. The maximum inhibition found was 63% in 200 mM EDTA.

Figure 21. Residual hydrolysis activity of CalB inhibited by (**A**) PMSF and (**B**) EDTA.
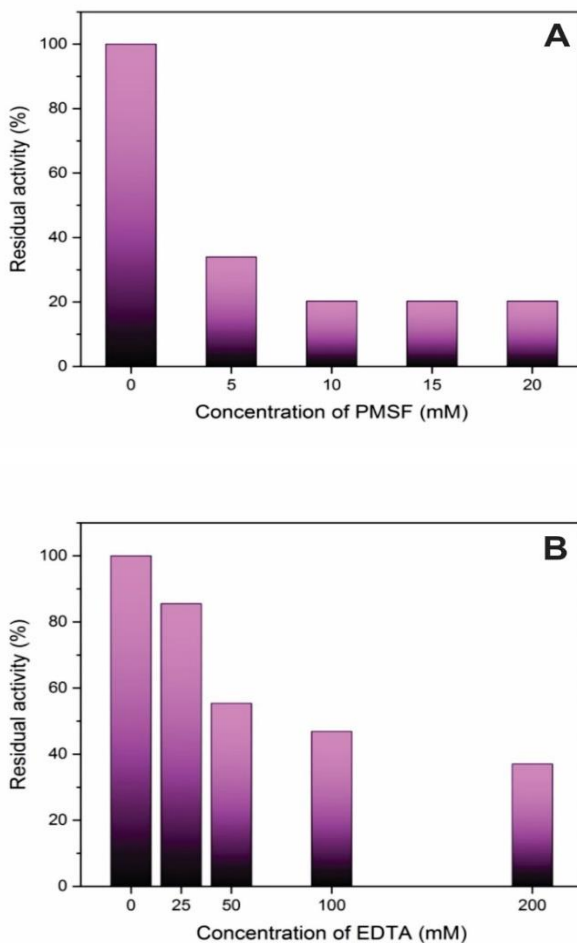
KANWAR et al. (2005) investigated various treatments for inhibition of hydrolysis activity of several lipases (lipases from *Bacillus coagulans* MTCC-6375, *Pseudomonas aeruginosa* MTCC-4713 and *Pseudomonas cepacia*, and commercial grade

lipolytic preparations such as lipozyme, lipolase and porcine pancreatic lipase) via a colorimetric method using *p*-NPP as substrate. Addition of a serine protease inhibitor, PMSF (15 mM) or EDTA (200 mM), inhibited *B. coagulans* lipase activity by 99.5% and 100%, respectively. EDTA was also effective in inhibiting completely the activity of lipases from *P. aeruginosa* MTCC-4713 and *P. cepacia*, lipozyme, lipolase and porcine pancreatic pancreas. PMSF (15 mM) completely inhibited the activity of *P. aeruginosa* MTCC-4713 lipase, and partially inhibited the activity of *P. cepacia* lipase, lipozyme, lipolase and porcine pancreatic lipase by 34.7, 60, 15.2 and 20.2, respectively.

Inhibition by PMSF indicates that the enzymes are regulated by a serine residue at their catalytic site (JAEGER; REETZ, 1998). CalB inhibition by PMSF indicates it is a typical lipase with serine hydrolase activity at the catalytic site.

4.3.4. Differential Scanning Fluorimetry

In DSF, SYPRO Orange interacts with exposed hydrophobic regions generated by partial or full unfolding of proteins. The dye is quenched in aqueous solutions, but when the aromatic moieties of the dye intercalates into a hydrophobic pocket, it regains its fluorescence. The sudden unfolding of the proteins in the sample will lead to a sharp increase of the fluorescent signal over a short temperature range. A sharp sigmoidal curve allows for the calculation of a melting temperature (T_m), which corresponds to the temperature where the protein is 50% unfolded. The best buffer would be the one in which the protein presents the highest melting temperature, i.e., the one in which the protein is more stable upon heating.

Ninety-six different buffer compositions and compounds were tested for their stabilizing effect on the CalB upon heating from 25 to 95 ºC. CalB melting temperatures (T_m, ºC) in the 96 different buffers are shown in Figure 22.

Figure 22. T_m (ºC) for CalB in 96 different buffer conditions.
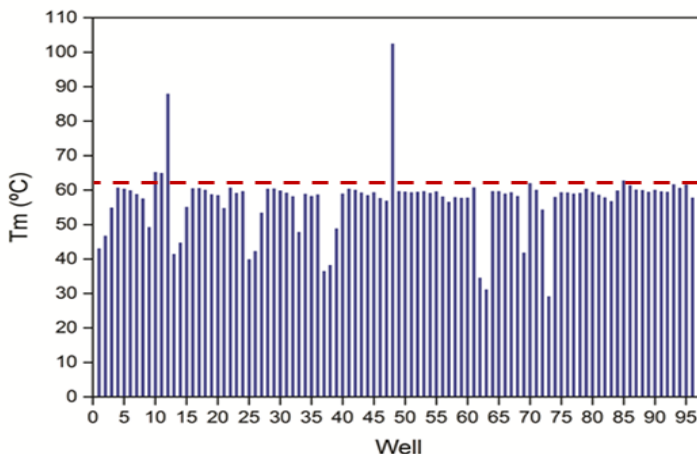
Conditions A10, A11, A12, D12 and H1 (wells 10, 11, 12, 48, and 85, respectively) showed CalB melting temperatures (Tm) greater than the control condition H11 (well 95) of 61.5 ºC (Table 18). We believe that the well 48 is not reliable because a melting temperature of 102.3 ºC is not realistic for any protein. From these results, we conclude that CalB is more stable in high pH buffers (around 9).

We can observe that the SYPRO Orange has low affinity to the protein in temperatures below 65 ºC, indicating that just a few hydrophobic regions are exposed in the native structure. When temperature was increased above 65 ºC, increase in the SYPRO Orange CalB interaction was observed, indicating that the hydrophobic regions of the protein were exposed, which was followed by aggregation and protein denaturation.

Table 18. T_m (ºC) for CalB in the best buffer conditions.

Well	Condition	T_m (ºC)
10	A10 50 mM TrisHCl pH 8.4	65.1
11	A11 50 mM BORAX pH 9.0	64.9
12	A12 50 mM BORAX pH 9.4	87.8
48	D12 50 mM BORAX pH 9.4; 500 mM NaCl	102.3
85	H1 20 mM NaHEPES pH 7.5, 100 mM NaCl, 50 mM AmAcetate	62.6
95	H11 Protein in its buffer + SYPRO orange (Reference)	61.5

Normally, for crystallization assays, low salt buffers with low molarity of the buffer compound are required, to avoid salt crystal formation during screening and to allow pH variability when the protein buffer encounters the crystallization solution (mother liquor), respectively. For this reason, we decided to keep CalB in the gel filtration buffer, sodium phosphate 0.02 M pH 7.5, for all crystallization trials.

4.3.5. Circular Dichroism

Far-UV spectra (190–260 nm) were recorded with CalB at 0.1 mg/mL in 0.05 M potassium phosphate pH 7.4, at 20 °C and at 95 ºC. In order to investigate the CalB thermal resistance, the enzyme (0.25 mg/mL) was previously denatured at 95 ºC for 5 min and then the CD spectra was recorded at 20 ºC. These spectra are shown in Figure 23. In table 19, we can see the distribution of the secondary structure elements for the three data sets collected for CalB shown in Figure 23.

Figure 23. Far-UV spectra (190–260 nm) for CalB collected at 20 °C (**A**), 95 ℃ (**B**) and for CalB previously denatured at 95 ℃ for 5 min and collected at 20 ℃ (**C**).
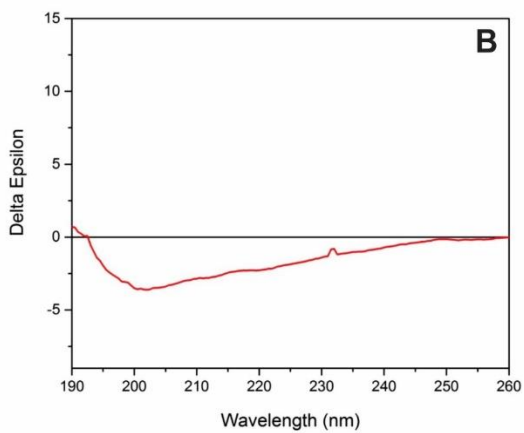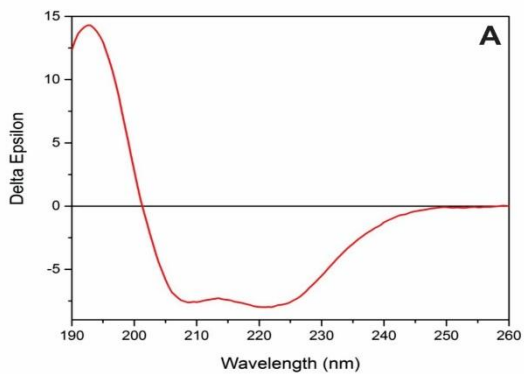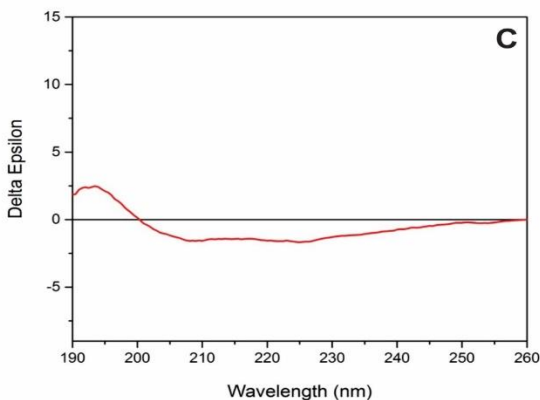
Table 19. Secondary structure element distribution obtained from curves of native CalB collected between 190-260 nm at 20 ºC and 95 ºC, and from CalB denatured at 95 ºC for 5 min and collected at 20 ºC.

Secondary Structure Element	CalB, at 20 ºC (%)	CalB, at 95 ºC (%)	CalB denatured, at 20 ºC (%)
Helix	29.1	18.1	17.6
Antiparallel	12.4	21.8	24.7
Parallel	9.4	11.9	12.8
Beta-turn	17.7	20.9	20.6
Random Coil	34.9	38.8	42.8
Total Sum	103.5	111.5	118.5

Analyzing Figure 23 and Table 19 it is possible to see that CalB is denatured when heated to 95 ºC. Such behavior can be seen both when the far-UV spectra for the native CalB was collected at 95 ºC and when CalB was previously denatured at 95 ºC for 5 min and the spectra was collected at 20 ºC. Both data sets collected after exposing CalB at 95 ºC generated low α-helix contents (about 40% reduction), indicating protein unfolding, which is characterized by α-helix content reduction and random coil content increase.

The far-UV spectra collected at 20 ºC shows a typical curve of a folded protein and the secondary structure element distribution shows that CalB, in fact, is an α/β hydrolase (50.9% of the elements are composed by α-helix and β-sheet parallel and antiparallel).

Melting profiles were recorded between 20 and 95 °C with CalB at 0.1 mg/mL in the same buffer by monitoring the CD signal at 220 nm. In order to investigate the CalB ability to unfold/refold, another curve was recorded from 95 to 20 ºC after the first curve (20 to 95 ºC) had been measured. These melting curves are shown in Figure 24.

Figure 24. Melting curves of CalB collected at 220 nm between (**A**) 20 and 95 °C and (**B**) 95 and 20 ºC.
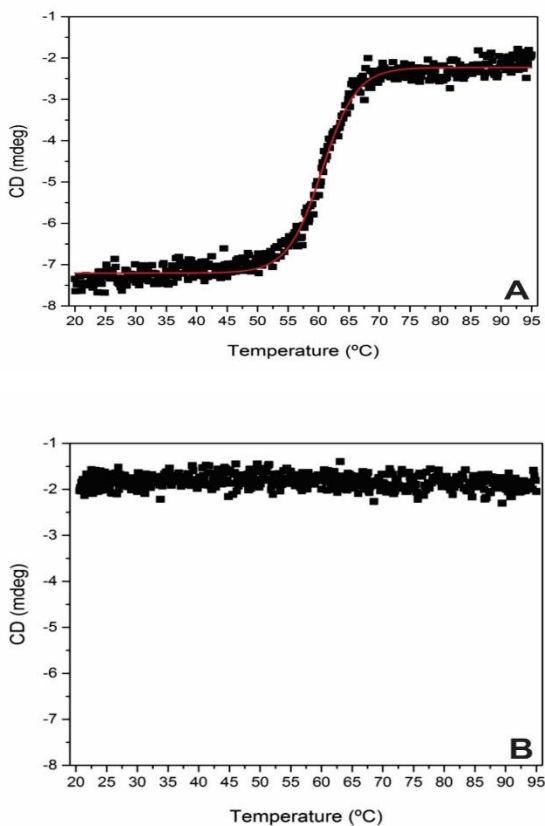
Clearly, we can see in Figure 24 that CalB is denatured after being exposed to temperatures above 65 ºC. It is also not possible

to refold the protein going from 95 ºC to 20 ºC. Analysis of the melting curve of CalB collected at 220 nm between 20 and 95 °C resulted in a melting temperature of 60.6 ºC, which is in agreement with the T_m obtained by DSF measurements (61.5 ºC).

4.3.6. Crystallization

To compare the structure of untreated CalB with the CalB treated in SC-CO$_2$ and compressed LPG, we first performed a screening with different commercially available crystallization reagents in 96-well MRC plates by sitting drop vapor diffusion technique to identify initial crystallization conditions of unpurified CalB. Drops of 200 nL (100 nL protein solution + 100 nL reservoir) were dispensed using a Cartesian liquid dispensing robot with 8 channels (Zinsser, Germany).

We did not manage to get crystals of the unpurified CalB, most likely due to its complex buffer of undefined composition. Crystallization of purified untreated CalB was then carried out at 18 ºC and initial hits were usually refined by manual setups in 24-well plates using the sitting drop vapor diffusion technique as well. Commercial additive screens were routinely tested to improve crystallization conditions.

CalB crystals were obtained by mixing 1 µL of protein solution at 10 mg/mL with 1 µL of reservoir solution (0.1 M tris(hydroxymethyl)aminomethane (Tris) pH 7, 0.2 M sodium chloride (NaCl), 29% (v/v) polyethylene glycol (PEG 3350)) and addition of 2-methyl-2,4-pentanediol (MPD) as additive. The crystals appeared between 3 and 5 days (Figure 25). The crystals were cryo-protected by transfer into a solution containing mother liquor (0.1 M Tris pH 7, 0.2 M NaCl, 29% (v/v) PEG 3350) and 20% (v/v) PEG 400, and then flash-cooled in liquid nitrogen. These crystals diffracted to 1.7 Å.

Figure 25. CalB crystals obtained in 0.1 M Tris pH 7, 0.2 M NaCl, 29% (v/v) PEG 3350.
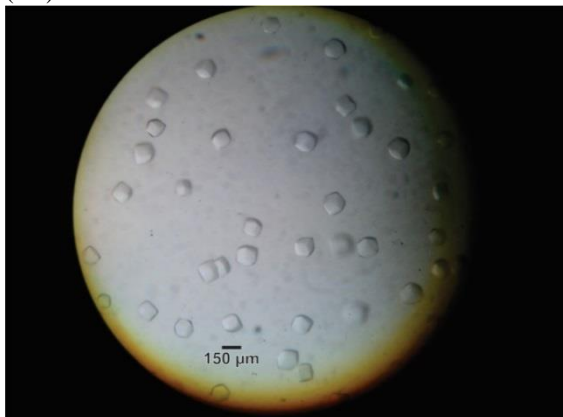
Diffraction data (Figure 26) were collected at beamline 14.2 of BESSY II (HZB, Berlin, Germany) and beamline P14 of PETRA III (DESY, Hamburg, Germany) and processed with XDS. Table 20 and 21 show the data collection parameters and the data processing statistics, respectively.

Figure 26. X-ray diffraction from a CalB crystal.
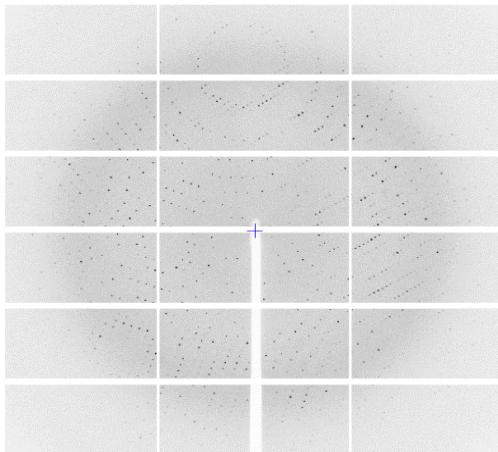
Table 20. Data collection parameters for untreated CalB.

No. of crystals	1
Beamline	P14
Wavelength [Å]	0.9763
Rotation range per image (ºC)	0.1
Total rotation range (ºC)	180
Exposure time per image (s)	0.3

Table 21. Data processing statistics for untreated CalB. Values in parenthesis are for the high resolution shell.

Space group	P 21 3
Wavelength [Å]	0.9763
Unit cell a, b, c [Å]	130.32; 130.32; 130.32
α, β, γ [°]	90; 90; 90
Resolution [Å]	75.24 - 1.703 (1.764 – 1.703)
Unique reflections	155193 (24210)
Completeness [%]	99.2 (95.5)
I/σ	9.38 (1.04)
R-meas [%]	10.4 (174.2)
CC(1/2)	99.7 (25.1)
Redundancy	4.28 (4.18)

The structure of untreated CalB was solved by molecular replacement using the coordinates of 1TCA CalB, as a model (see section 2.3). Initial phases of CalB were calculated using *Phaser*. Model building was performed using COOT and refinement with REFMAC5 and *Phenix* (Figure 27).

Figure 27. X-ray structure of CalB, purchased from Sigma-Aldrich, solved at 1.7 Å resolution. CalB (pink) superimposed to 1TCA (red) (**A**), lid (purple) (**B**), active site (Ser105, Asp187 and His224) (**C**) and (**D**), N-glycosylation (NAG and MAN) (**E**).

C

D

E
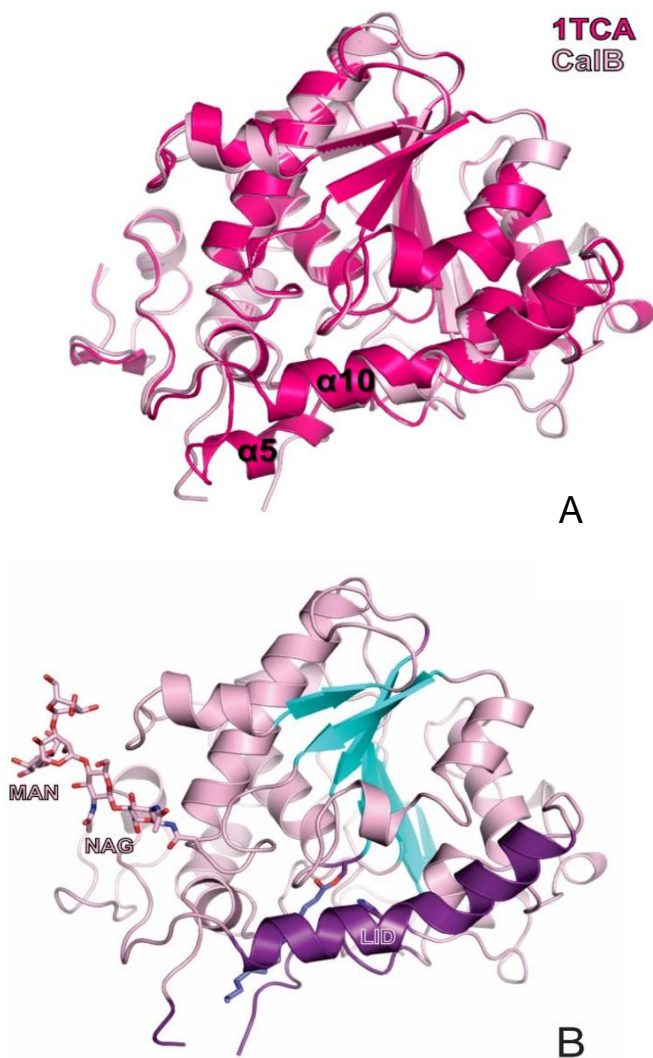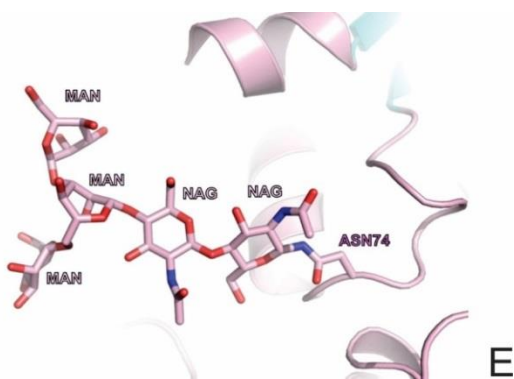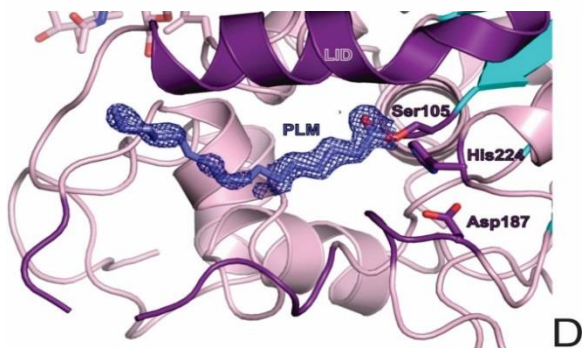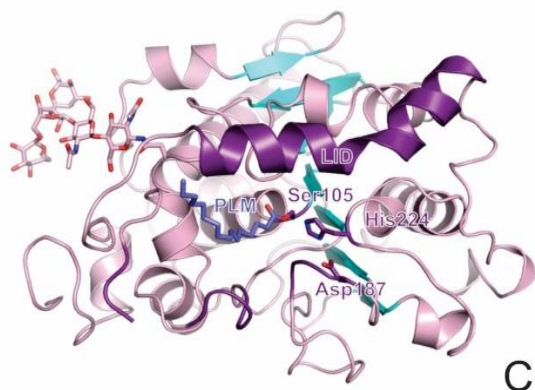
In Figure 27, by superimposing CalB structure with 1TCA, we notice that α5 is not present in our CalB structure (b). α5 is part of the lid (which is composed by the elements in purple in Figure 3 (a)). We believe that α5 is not present in our structure due to the presence of a ligand at the active site of CalB (Figure 27 (c) and (d)). We assume that binding of the ligand at the active site destabilizes α5, which is of high mobility, making it invisible in our electronic density.

UPPENBERG et al. (1994) suggested that α5 and α10 act as a lid and α5 plays the most important role to control the entrance to the active site of CalB. It is suggested that enzyme conformation is closed in aqueous environments; thus, the access to the catalytic triad would be blocked by the lid (ZHU et al., 2000; GONÇALVES et al., 2014; STAUCH; FISHER; CIANCI; 2015).

ZHU et al. (2000) showed that when *Thermomyces lanuginosus* lipase (TLL) is bound to substrate analogs, the helix forming the lid is displaced and the active site becomes exposed.

We tentatively modeled a fatty acid in a tetrahedral intermediate state of the reaction covalently bound to Ser105 (PLM). This state is represented by the acyl-enzyme intermediate E* in Figure 4 (see section 2.3). Why such intermediate is trapped in the enzyme active site is still not clear. Although there are many structures of CalB deposited in the Protein Data Bank (PDB), this is the first structure showing an intermediate bound-state enzyme.

We also can see in CalB structure not only the N-acetylglucosamine (NAG), as in 1TCA, but three more mannoses (MAN) attached to asparagine 74 (Figure 27 (e)), which can indicate higher order of branching hexoses.

Table 22 shows the statistics of the refinement step and Table 23 the secondary structure element distribution calculated from the X-ray structure of CalB.

Table 22. Refinement statistics.

Non-hydrogen atoms	5155
R $_{work}$	0.1706 (0.287)
R $_{free}$	0.213 (0.326)
N° of protein chains	2
Average B-factor [Å]	32.4
Rmsd Bond length [Å]	0.019
Bond angles [°]	2.034
Ramachandran outliers [%]	0
Ramachandran favored [%]	95.8

Table 23. Secondary structure element distribution for native CalB calculated from the X-ray structure compared to CD measurements.

Secondary Structure Element	Calculated from X-ray structure (%)	Measured by CD (%)
α-helices	32.8	29.1
β-sheets	9.7	21.8
Random Coil	57.5	49.1
Total Sum	100	100

α-helix content is very similar and in agreement with the CD data collected for native CalB at 20 ºC. The β-sheet content assigned by the CD measurements (sum of parallel and antiparallel) is, however, very far from the β-sheet content observed in the crystal structure (21.8% against 9.7%).

4.3.7.   Deglycosylation

CalB, purified by gel filtration (10 mg/mL), was submitted to deglycosylation with PNGase F under denaturing and non-denaturing conditions in order to assess the effect of glycosylation on the activity of the protein. A control reaction was performed replacing the PNGase F by H_2O under non-denaturing conditions.

Activity assays were carried out for the three samples: control, CalB deglycosylated under denaturing conditions and CalB deglycosylated under native conditions, in duplicate. Results are presented in Table 24.

Table 24. Hydrolysis activity for control, CalB deglycosylated under denaturing conditions and CalB deglycosylated under native conditions.

Reaction	Activity (U/mg) (%) ± standard error	Residual Activity (%)
Control	0.21±0.01	100
Native	0.24±0.03	114
Denaturing	0.16±0.01	76

The activity results shown in Table 23 for glycosylated and deglycosylated CalB are not conclusive. Although CalB deglycosylated under native conditions had a 14% increment on the hydrolysis activity, the standard error does not allow us to convincingly state that CalB activity is influenced by glycosylation. Activity measurements of the enzyme deglycosylated under denaturing conditions show lower values compared to the control. CalB loses activity most likely due to the harsh denaturing buffer and not due to deglycosylation.

Blank et al. (2006) expressed and purified CalB in the periplasm of *Eschericha coli a*nd compared the molecular weight of this enzyme to the glycosylated and deglycosylated CalB expressed in *Aspergillus oryzae.* They also determined the specific activities of the enzymes for three different substrates: *p*-nitrophenol butyrate (*p*-NPB), *p*-nitrophenol laurate (*p*-NPL) and carboxyfluorescein diacetate (CFDA). For CalB from *A. oryzae,* the glycosylated enzyme was used while CalB produced in *E. coli* lacked glycosylation. The authors observed no difference in the enzymatic activity of CalB from *A. oryzae* and *E. coli* for all substrates. Based on these results, no conclusion can be drawn from the function of the glycosylation on the activity of the protein.

The three samples, control, CalB deglycosylated under denaturing conditions and CalB deglycosylated under native conditions, were run on SDS-PAGE gel (Figure 28).

Figure 28. SDS-PAGE gel for control, CalB deglycosylated under denaturing conditions and CalB deglycosylated under native conditions.
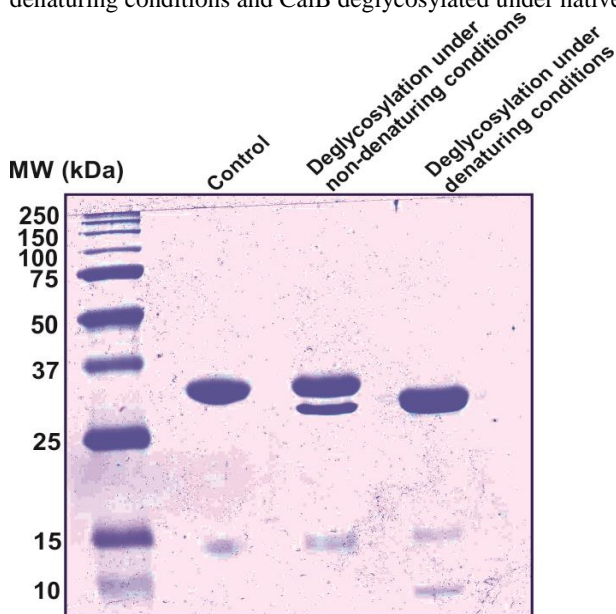
In the SDS-PAGE, there are two bands above 30 kDa present in the sample of CalB deglycosylated under native conditions. The lower band could represent either minor amounts of deglycosylated enzyme or PNGase F, as its molecular weight observed by MS (MORAIS et al., 2017) is 34775 Da. This lower band is the only species found in the sample of CalB deglycosylated under denaturing conditions, suggesting that the deglycosylation reaction is very efficient under denaturing conditions.

We also can see that a new tiny band appeared in the very low molecular weight range, below 10 kDa, when CalB was deglycosylated under denaturing conditions, indicating a new product formation (Figure 28). This lower band was not assigned though.

We also performed a kinetic study for CalB deglycosylation under native conditions to evaluate if the hydrolysis activity would increase after 5 days compared to the control kinetic reaction.

Samples were taken every day for hydrolysis activity measurements, and the results are shown in Figure 29.

Figure 29. Kinetics for CalB deglycosylation under native conditions compared to the control.
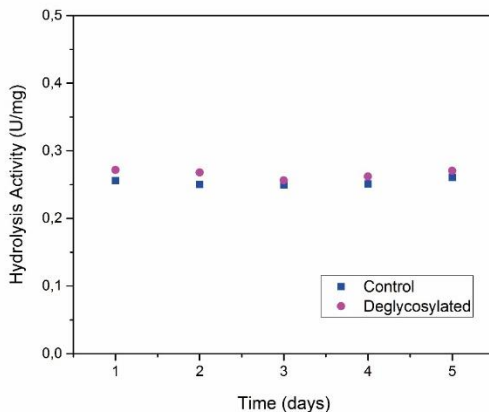
In Figure 29 is shown that the hydrolysis activity for the control and for CalB deglycosylated under native conditions does not change after 5 days of incubation. However, we cannot conclude either that there is any degree of deglycosylation happening during this period or that deglycosylation would promote some change on the hydrolysis activity of CalB. Probably the best alternative would be to increase the amount of PNGase F added to address any influence, but due to the high costs of the enzyme we did not perform these tests. Hydrolysis activity for CalB deglycosylated under non-denaturing conditions was slightly higher than for the control during all the monitored time. Since we did not have enough samples to send all aliquots to MS analysis, we cannot confirm that the slight increase in activity is due to deglycosylation.

In order to address the glycosylation state of CalB after PNGase F treatment under native conditions, we performed MS analysis.

124

4.3.8.   Mass Spectrometry

Gel filtration purified CalB (control) and CalB after deglycosylation under native conditions with PNGase F were first digested with trypsin and the fragments were analyzed in a coupled TripleTOF™ 5600 LC-MS/MS C18 mass spectrometer under standard conditions. Figure 30 (a) shows the LC-MS/MS profile obtained for purified CalB after trypsin digestion, and (b) mass distribution for peak 3, identified as the CalB peak.

As we can see in Figure 30 (a) and (b), CalB is still not completely pure after size exclusion chromatography purification, since there are remaining species of 18 kDa or less present in the solution (peaks 1 and 2). CalB is identified as the main population in peak 3 and 5. CalB molecular weight of 35044 Da was calculated with peak 3. The higher molecular weight observed via MS, compared to the theoretical molecular weight of 33022 Da, is probably due to the high level of mannose glycosylation in asparagine 74 and the lipid-like ligand covalently bound to serine 105. The 162 Da extensions observed in peak 3 (marked with ellipses) are most likely due to the glycosylation, which follows a glycan distribution with hexose spacing.

Figure 30. TripleTOF™ 5600 LC-MS/MS C18 spectrum for CalB purified by gel filtration (**a**) and detail of CalB peak (**b**).

Figure b — Peak 3
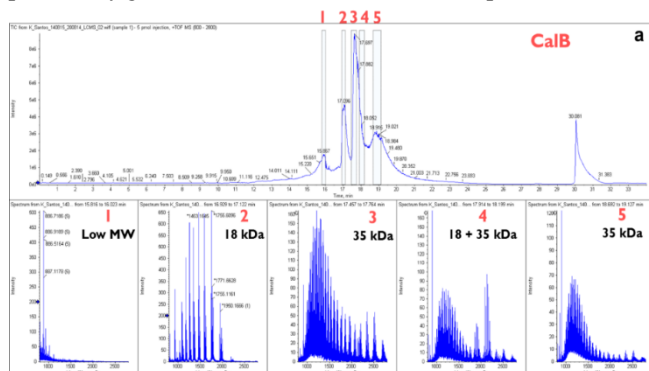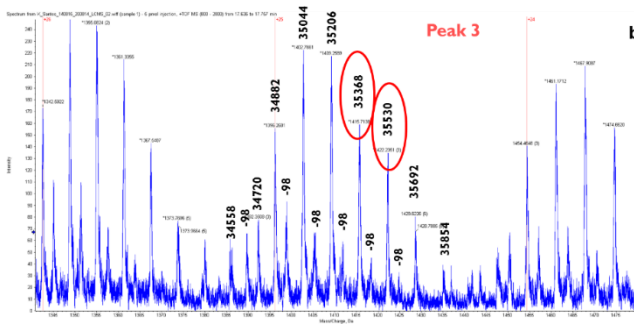
It is suggested that the loss of 98 Da can be due to phosphate adduct formation. Electron ionization of peptides and proteins often produces intense adduct ions resulting from the attachment of a moiety with mass of 98 Da. The formation of these adduct ions results in a substantial reduction in the mass spectrometric sensitivity and an undesirable increase in the complexity of the mass spectra. It was shown that when phosphate ions are removed from the samples by chemical means, adduct free ions are obtained from proteins yielding spectra with improved quality and sensitivity (CHOWDHURY et al., 1990).

Figure 31 (a) shows a comparison between the LC-MS/MS profiles of CalB and CalB deglycosylated by PNGase F under native conditions; (b) shows the mass distribution for both samples and (c) the LC-MS/MS profile obtained for CalB deglycosylated by PNGase F under native conditions after trypsin digestion.

Figure 31. LC-MS/MS profiles of CalB and CalB deglycosylated by PNGase F under native conditions (**a**) and mass distribution for both samples (**b**).
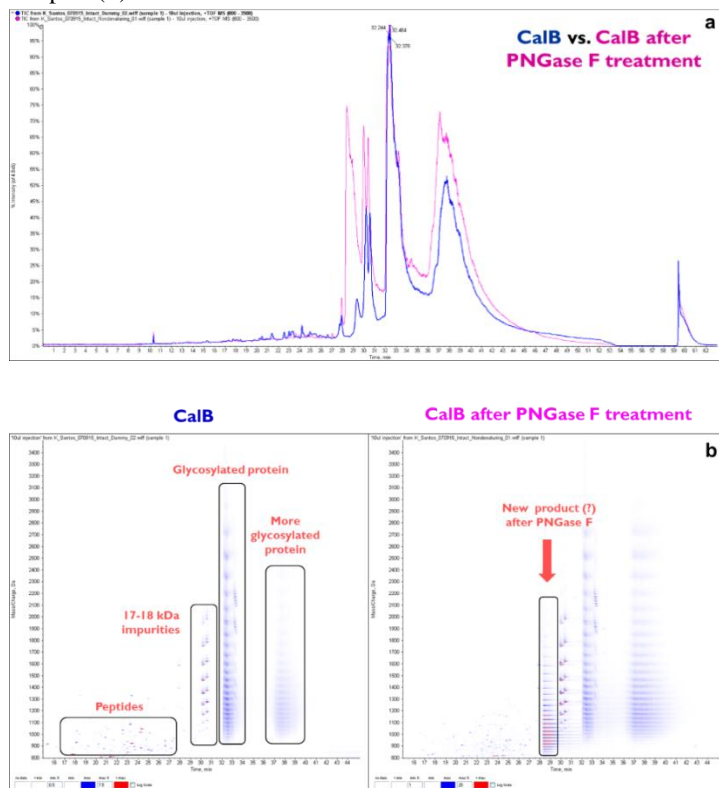
In Figure 31 (a) we can see clearly that both samples run with slightly different patterns in LC-MS/MS C18. In (b) we see a potential new product formation after CalB deglycosylation by PNGase F. After careful inspection of the mass of this new product, we found out that this is the exact mass of PNGase F, 34775 Da (MORAIS et al., 2017). This explains why the observed mass difference by deglycosylation of CalB was too small (expected molecular weight after deglycosylation 33 kDa).

Our MS results show that CalB is not deglycosylated under native conditions. These results suggests that the small differences observed in activity before and after PNGase treatment under

native conditions (Figure 31; Table 23) do not reflect deglycosylation but are rather small variations in the activity of the protein or in the technical measurements.

CalB deglycosylation under denaturing conditions, as recommended by the PNGase supplier, is efficient (Figure 28) and the harsh buffer conditions seem to only mildly reduce the enzyme activity. In order to assess the actual effect of the sugar on CalB activity and stability without side effects of harsh buffer conditions, we would need to express CalB using different expression hosts such as fungus or insect cells (that are capable of glycosylation) and *E. coli* (that is not able to glycosylate proteins).

4.3.9. Stability of CalB with temperature and pH variations

CalB activity was analyzed in pH 4.8, 7.5 and 9.2, and at 30 and 60 ºC, using 0.05 M citric acid/trisodium citrate buffer pH 4.8, 0.05 M sodium phosphate buffer pH 7.5 and 0.05 M sodium carbonate/sodium bicarbonate buffer pH 9.2. Table 25 presents the CalB hydrolysis activities under different temperatures of incubation, buffers and temperatures of the activity assay, measured in triplicates.

Table 25. CalB hydrolysis activity under different temperatures of incubation, buffers and temperatures of the activity assay.

Assay	Incubation	Temperature of measurement (ºC)	pH	Hydrolysis activity (U/mL) (%) ± standard error
1			4.8	-
2	Stored at 4 ºC in the fridge	30	7.5	3.4±1.5
3			9.2	6.1±1.8
4			4.8	-
5		60	7.5	12.1±1.9
6			9.2	21.4±2.1
7			4.8	-
8	1 h at 65 ºC in a water bath	30	7.5	4.2±2.2
9			9.2	8.3±1.6
10			4.8	-
11		60	7.5	16.9±3.0
12			9.2	23.7±2.1

By investigating CalB activity in different pHs, we verified that CalB is not active in acidic pH (citric acid/trisodium citrate buffer pH 4.8) at any temperature. We can clearly observe that

CalB is more active in basic pH (9.2) compared to neutral pH. These results can be correlated to the DSF experiments which showed that CalB is more stable to thermal denaturation in pH around 9 (Table 18). Moreover, when we compare the temperature of incubation, we notice that CalB is slightly more active when previously activated at 65 ºC for 1 hour.

Enzyme activity increased 4-fold in all cases when measurements were carried out at 60 ºC compared to 30 ºC at pH 7.5. A 3-fold increment was observed for all measurements performed at pH 9.2 when CalB was submitted to the hydrolysis assay at 60 ºC compared to 30 ºC. The highest hydrolysis activity was observed at 65 ºC for 1 hour and measured in pH 9.2 at 60 ºC.

4.3.10. High pressure treatment at FUB

The equipment shown in Figure 13 (section 3.2.12.1) was assembled for several months while researching at FUB during this Doctoral project. This equipment presented some restrictions and, for this reason, the maximum pressure evaluated in the experiments was 160 bar. Results in terms of residual specific activity of CalB in the supplied buffer and CalB purified by gel filtration (ratio of specific activity after treatment with supercritical CO_2 and the specific activity of untreated lipase, %) of experiments that evaluated the effect of temperature, pressure and exposure time on the enzyme activity are compiled in Table 26. Values of residual specific activity are averages of three repetitions. Mass ratio enzyme:CO_2 was fixed to 1:1 for all assays.

Analyzing the results obtained at FUB we can see it was not possible to reproduce the results obtained at UFSC. We may attribute this non-reproducibility to the newly assembled equipment, mainly to the HPLC pump, which is not the most appropriated to pump CO_2, since it is a pump for liquid solvents and does not have a cooling system on its piston. Such system is very important to keep the CO_2 in the liquid state (temperatures below -10 ºC on its saturation pressure of 58 bar) in the tubes, and to control the flow rate and, consequently, the mass of pumped fluid. This could have led to the formation of two phases in the HPLC pump piston, consequently causing errors in the volume/mass of CO_2 added to the cell.

Table 26. Residual specific activity (%) of CalB in the supplied buffer and CalB purified by gel filtration submitted to supercritical carbon dioxide treatment at FUB.

		CalB in the supplied buffer		
Assay	Pressure (bar)	Temperature (ºC)	Time (h)	Residual specific activity (%) ± standard error
1	160	65	1	89.0 ± 3.9
2	160	65	6	75.4 ± 3.8
3	80	35	0.5	86.7 ± 6.1
4	80	35	1	88.7 ± 5.0
5	160	35	1	89.5 ± 1.9
		CalB purified		
1	160	35	1	97.4 ± 4.1
2	160	35	3.5	102.2 ± 2.8
3	80	35	1	93.3 ± 1.7
4	80	35	3.5	113.8 ± 3.2
5	80	35	6	102.1 ± 1.9

It is noteworthy to mention that all the experiments with the purified CalB were conducted at 35 ºC. All trials of treatment at 65 ºC resulted in complete evaporation of the buffer together with the CO_2 during the depressurization step. After cell depressurization, the enzyme was found precipitated in the cell and it could not be resuspended in buffer.

4.3.11. X-ray Crystallography

The crystallization trials were performed with three SC-CO_2 treated enzymes from experiments 2 and 5, with CalB in supplied buffer which lost activity after treatment (75.4 and 89.5%, respectively), and from experiment 4 with purified CalB which showed an increased activity after treatment (113.8%) (Table 26). CalB treated under conditions 2 and 5 was purified via GF, concentrated to 9.2 and 8.7 mg/mL, respectively, and crystallization trays were set. CalB previously purified by gel filtration and concentrated to 5.6 mg/mL was treated under conditions of assay 4 and then crystallization trials were carried out.

We performed a screening with different commercially available crystallization reagents in 96-well MRC plates by sitting

drop vapor diffusion technique to identify initial crystallization conditions for the three samples of treated CalB. Drops of 200 nL (100 nL protein solution + 100 nL reservoir) were dispensed using a Cartesian liquid dispensing robot with 8 channels. Initial hits were usually refined by manual setups in 24-well plates using the sitting drop vapor diffusion technique as well. All plates were set at 18 degrees.

Purified CalB from experiment 4 did not crystallize. Crystals of protein treated under experiment 5 conditions were obtained within 5 days in 0.1 M Tris pH 7, 0.2 M sodium chloride and 30% (v/v) PEG 3000 and reproduced in 24 well format by mixing 1 μL of protein solution at 8.7 mg/mL (experiment 5 - 160 bar, 35 ºC, 1 h) with 1 μL of mother liquor (0.1 M Tris pH 7, 0.2 M sodium chloride and 30% (v/v) PEG 3000).

The crystals were cryo-protected by transfer into a solution containing mother liquor and 30% (v/v) of glycerol, and then flash-cooled in liquid nitrogen. These crystals diffracted to 2.3 Å. Diffraction data for CalB from experiment 5 were collected at beamline 14.2 of BESSY II (HZB, Berlin, Germany) and processed with XDS. Table 27 and 28 show the data collection parameters and the data processing statistics, respectively.

We also obtained some crystals of CalB from experiment 2, but they did not diffract well and we could not get a good data set.

Table 27. Data collection parameters for CalB treated in supercritical CO_2 at 35 ºC, 160 bar and 1 hour, followed by GF.

No. of crystals	1
Beamline	14.2
Wavelength [Å]	0.9184
Rotation range per image (ºC)	0.1
Total rotation range (ºC)	180
Exposure time per image (s)	0.3

Table 28. Data processing statistics for CalB treated in supercritical CO_2 at 35 ºC, 160 bar and 1 hour, followed by GF.

Space group	P 21 3
Wavelength [Å]	0.9184
Unit cell a, b, c [Å]	130.36; 130.36; 130.36
α, β, γ [º]	90; 90; 90
Resolution [Å]	43.454 - 2.299 (2.44 – 2.299)
Unique reflections	33064 (5285)
Completeness [%]	100 (100)
I/σ	13.18 (2.75)
R-meas [%]	27.6 (145)
CC(1/2)	99.7 (76.1)
Redundancy	27.88 (26.58)

Several rounds of refinement were performed in Phenix, Refmac and Coot to refine and build the structure properly. Figure 32 shows the asymmetric unit of untreated CalB (a) in order to compare to SC-CO_2 treated CalB asymmetric unit (b). Figure 33 shows the X-ray structure of CalB treated in supercritical CO_2 superimposed to the untreated CalB. The refinement statistics are shown in Table 29.

Table 29. Refinement statistics for CalB treated in supercritical CO_2 at 35 ºC, 160 bar and 1 hour, followed by GF.

Non-hydrogen atoms	5312
R$_{work}$	0.1491 (0.22)
R$_{free}$	0.206 (0.268)
N° of protein chains	2
Average B-factor [Å]	34.64
Rmsd Bond length [Å]	0.019
Bond angles [°]	1.885
Ramachandran outliers [%]	0
Ramachandran favored [%]	97

132

Figure 32. Asymmetric unit of untreated CalB (**A**) and SC-CO₂ treated (**B**).
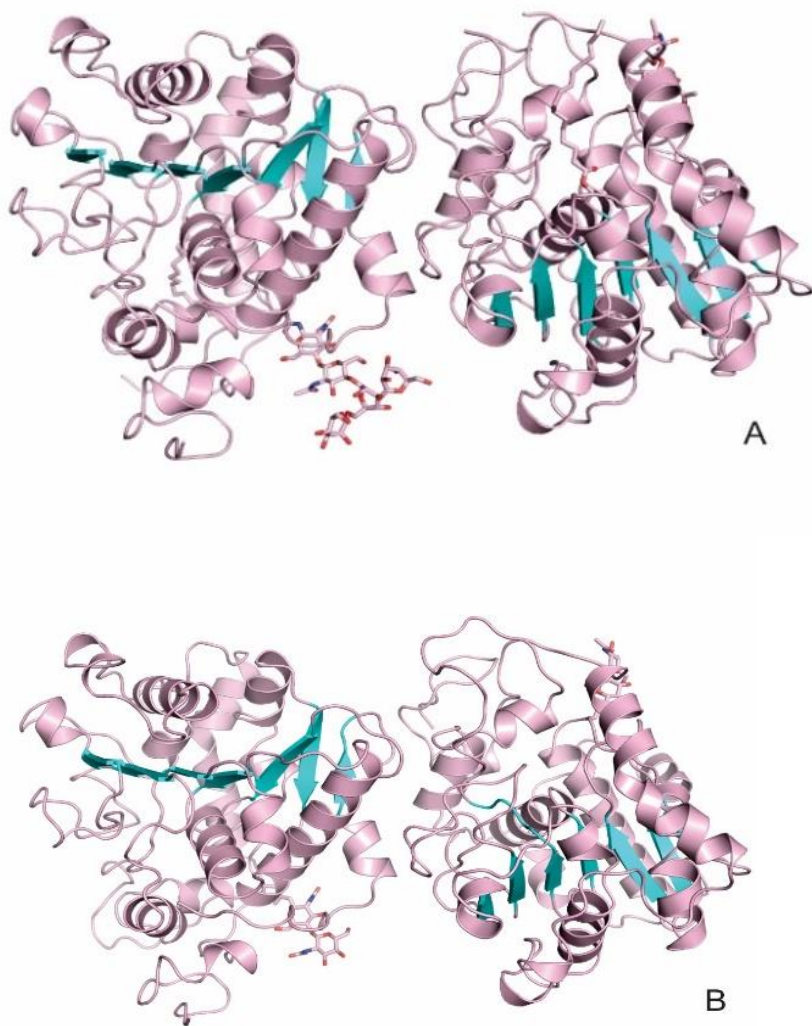
Figure 33. X-ray structure of CalB treated in supercritical CO_2 at 35 ºC, 160 bar and 1 hour, solved at 2.3 Å resolution, superimposed (light pink) to untreated CalB (magenta). *NAG* = N-acetylglucosamine. *PLM* = substrate bound.
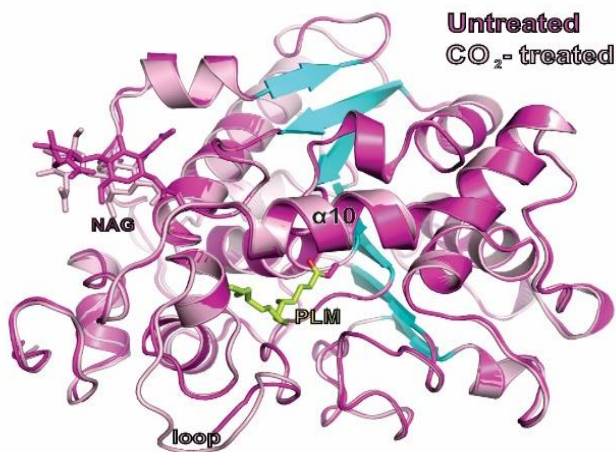
Untreated CalB was solved at 1.7 Å, two molecules were present in the asymmetric unit as seen in Figure 32 (a) and the crystal belonged to space group P 21 3. SC-CO_2 treated CalB structure also showed two molecules in the asymmetric unit (Figure 32 (b)) and the same asymmetric unit configuration (space group P 21 3), but was solved at 2.3 Å. The crystallization condition for untreated CalB was 0.1 M Tris pH 7, 0.2 M NaCl, 29% (v/v) PEG 3350 and MPD as additive; a similar condition was found for the SC-CO_2 treated CalB (0.1 M Tris pH 7, 0.2 M NaCl and 30% (v/v) PEG 3000).

We also performed a screening with different commercially available crystallization reagents in 96-well MRC plates by sitting drop vapor diffusion technique to identify initial crystallization conditions for CalB treated in LPG under conditions of experiment 2 (65 ºC, 30 bar, 1 hour), which showed residual activity of

142.4%. CalB was purified after LPG treatment *via* GF as described in section 3.2.1.1. Drops of 200 nL (100 nL protein solution + 100 nL reservoir) were dispensed using a Cartesian liquid dispensing robot with 8 channels. Initial hits were usually refined by manual setups in 24-well plates using the sitting drop vapor diffusion technique as well. All plates were set at 18 degrees.

Crystals of protein treated under experiment 2 conditions with LPG were obtained within 5 days in 16% PEG 3350 and 200 mM NaI, and reproduced in 24 well format by mixing 1 μL of protein solution at 10 mg/mL with 1 μL of mother liquor (16% PEG 3350 and 200 mM NaI).

The crystals were cryo-protected by transfer into a solution containing mother liquor and 12.5% (v/v) of 2-methyl-2,4-pentanediol (MPD), and then flash-cooled in liquid nitrogen. These crystals diffracted to 2.15 Å. Diffraction data for CalB from experiment 2 were collected at beamline 14.2 of BESSY II (HZB, Berlin, Germany) and processed with XDS. Table 30 and 31 show the data collection parameters and the data processing statistics, respectively.

Table 30. Data collection parameters for CalB treated in pressurized LPG at 65 ºC, 30 bar and 1 hour, followed by GF.

No. of crystals	1
Beamline	14.2
Wavelength [Å]	0.9184
Rotation range per image (ºC)	0.1
Total rotation range (ºC)	180
Exposure time per image (s)	0.3

Table 31. Data processing statistics for CalB treated in pressurized LPG at 65 ºC, 30 bar and 1 hour, followed by GF.

Space group	C 1 2 1
Wavelength [Å]	0.9184
Unit cell a, b, c [Å]	218.733; 126.019; 93.167
α, β, γ [°]	90; 104.916; 90
Resolution [Å]	46.19 - 2.15 (2.28 – 2.15)
Unique reflections	129095 (20186)
Completeness [%]	97.3 (94.5)
I/σ	7.26 (1.38)
R-meas [%]	19.9 (115.2)
CC(1/2)	99.1 (53.2)
Redundancy	4.88 (4.86)

Several rounds of refinement were performed in Phenix, Refmac and Coot to refine and build the structure properly. The refinement statistics are shown in Table 32.

Table 32. Refinement statistics for CalB treated in pressurized LPG at 65 ºC, 30 bar and 1 hour, followed by GF.

Non-hydrogen atoms	15983
R $_{work}$	0.1787 (0.369)
R $_{free}$	0.2111 (0.387)
N° of protein chains	6
Average B-factor [Å]	32.18
Rmsd Bond length [Å]	0.019
Bond angles [°]	1.843
Ramachandran outliers [%]	0
Ramachandran favored [%]	97.28

Figure 34 shows the asymmetric unit of LPG treated CalB. This structure was solved at 2.15 Å, presented six molecules in the asymmetric unit and the crystal belonged to a different space group compared to the previous two structures (C 1 2 1). The crystallization condition of LPG treated CalB consisted of 16% PEG 3350 and 200 mM NaI.

The asymmetric unit is composed by two trimmers bound back to back, interestingly, via the long lid alpha-helix, α10 (Figure 34 (c)). One trimmer has three molecules bound to PML at Ser105 (molecules A, B and C, Figure 34 (a)) and in the other one all molecules lack the ligand (molecules D, E and F, Figure 34 (b)).

Figure 34. Trimmer composed by molecules A, B and C (**A**); trimmer composed by molecules D, E and F (**B**); and asymmetric unit of LPG treated CalB formed by the two trimmers (**C**).
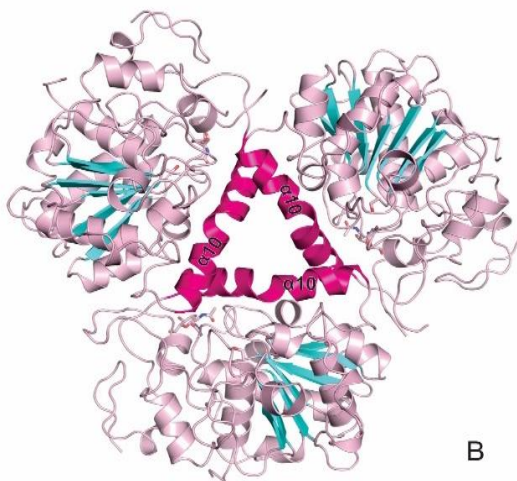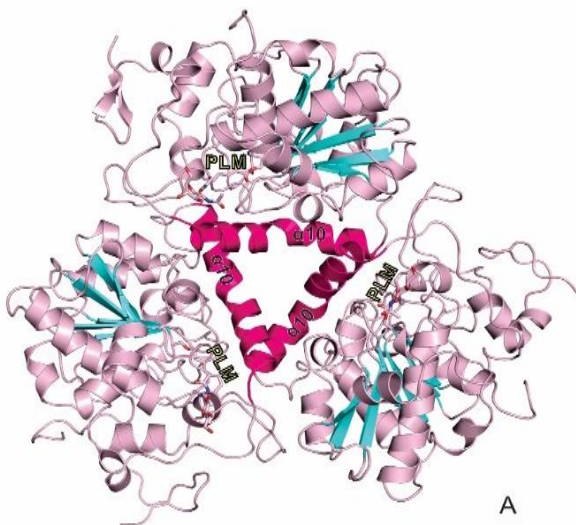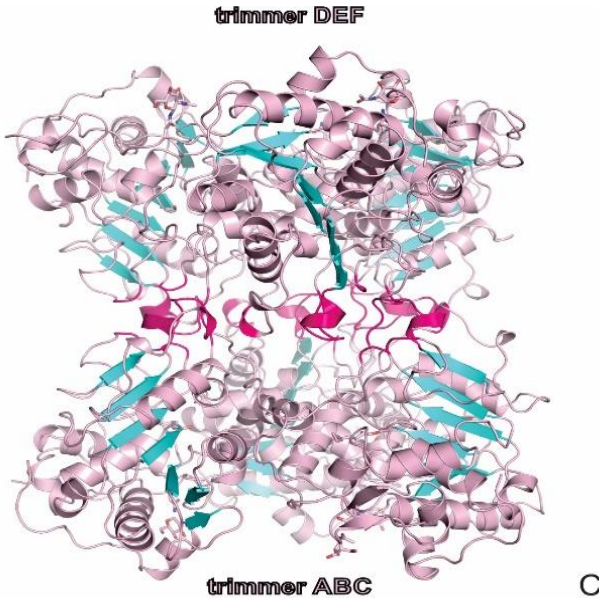
Figure 35 shows the X-ray structure of CalB treated in pressurized LPG superimposed to the untreated CalB. By comparing Figures 33 and 35, we can observe some changes in the CalB structure when exposed to $SC\text{-}CO_2$ and LPG, followed by GF. Interestingly, there is not enough density to place any substrate molecule in the active site of CalB treated in $SC\text{-}CO_2$ (Figure 33). This could be either due to the fact that CalB does not have the substrate molecule attached to Ser105 after CO_2 treatment or after gel filtration, or that the active site is not fully occupied, i.e., not all the molecules in the crystal are bound to the substrate, therefore yielding a poor density for the substrate in the active site. It is worth pointing out that this enzyme displayed residual activity of 89% after $SC\text{-}CO_2$ treatment.

Figure 35. X-ray structure of CalB treated in pressurized LPG at 65 ºC, 30 bar and 1 hour, solved at 2.15 Å resolution, superimposed (light pink) to untreated CalB (magenta). In (**A**) untreated CalB is superimposed to molecule A of LPG treated CalB, and in (**B**) it is superimposed to molecule D of LPG treated CalB. *NAG* = N-acetylglucosamine. *PLM* = substrate bound.
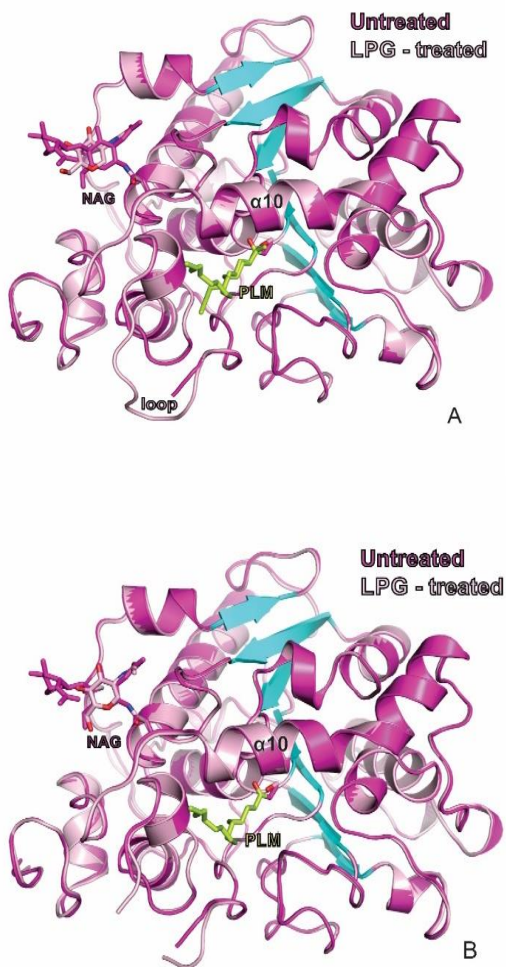
In Figure 35 (a) and (b) we see that it was possible to place a ligand bound to Ser105 in only three of the six molecules of the asymmetric unit of CalB treated with LPG (molecules A, B and C). The most suitable hypothesis to such behavior is that the active site is not fully occupied by the substrate in all the molecules of the crystal. Since no large conformational changes are observed when the ligand is bound, both populations of CalB (substrate-bound and apo) packed into the same crystal lattice. Residual activity of CalB after treatment in LPG was about 130%.

We can also observe that in SC-CO_2 treated CalB structure the region between residues 140 and 147, which correspond to α5 in 1TCA and is missing in our untreated CalB structure, consists of a loop region (Figure 33). Interestingly, the same loop is seen in the 4 molecules of the LPG treated CalB (molecules A, B, C and E), 3 of which have the substrate bound to Ser105 (molecules A, B and C) and is missing in the other 2 molecules (D, F), where PLM is not present (Figure 35 (a) and (b), respectively). We believe that the substrate presence at the active site is partially responsible for destabilization of α5 and, subsequently, 1, for the absence of density for the α5 in our untreated CalB structure or 2, the presence of a loop, that can be seen instead of α5 in the LPG-treated protein (molecules A, B and C). Both monomers of SC-CO_2 treated CalB and monomers A, B, C and E of LPG treated CalB are in the closed state, characterized by the unfolded loop between residues 140-147.

We can reason why we also observe a loop or a density gap in molecules D, E, and F from the LPG-treated and in molecules A and B from the CO_2-treated structures although the substrate is not modeled at their active sites. In this sense, these molecules should show an α5 like the apo 1TCA structure. One possibility is that the substrate is still partially bound in these molecules but in a very flexible fashion, which prevents it to be seen in the electron density. In such a situation of high flexibility in the neighborhood of the active site, we suggest that alpha-helix 5 cannot be formed and there is either no density for this region or a flexible (high B factor) loop is observed. Another hypothesis is that the substrate/product has detached from the active site and we are observing a molecule that is still in transition from the "loop" conformation to the alpha helix. It is possible that after release of

the substrate/product, the conformational rearrangements in this region were yet not triggered when the molecules still in the "loop" conformation were sequestered by nucleation and consequently crystal formation.

SKJØT et al. (2009) showed that, at pH 7, CALB in solution is likely to oscillate between the open and the closed conformation; hence, the reason for the lack of interfacial activation of CALB must be searched for elsewhere, rather than in the lack of a lid region in the structure. It is noteworthy that the removal of the Asp145 from the α5 region in the chimeras of CALB removed the activity pH dependence, clearly indicating a relationship between optimal activity pH and primary sequence of the lid region. The two variants, where the lid region was cloned from *Neurospora crassa* and from *Gibberella zeae*, on the other hand, yielded surprisingly low specific activities in the assay, with no clear pH dependency. In these two variants, the Asp145 is missing from the α5 sequence.

MOZHAEV et al. (1996b) observed that α-chymotrypsin (CT) was stabilized against pressure-induced conformational transition due to substrate binding (*N*-succinyl-*L*-phenylalanine-*p*-nitroanilide). Stabilization of CT towards inactivation by high pressure was also observed by TANIGUCHI and SUZUKI (1983) in the presence of another substrate, *p*-nitrophenyl acetate. At 20°C, CT-catalyzed hydrolysis of this substrate is accelerated by an increase in pressure up to 2500 bar. Stabilization against pressure-induced inactivation by binding of substrates was reported for other enzyme-substrate systems (BUCHET et al., 1990; COELHO-SAMPAIO et al., 1991; DEVILLE-BONNE and ELSE 1991; ERIJMAN et al., 1993; GREULICH and LUDWIG, 1977).

We could also see in the SC-CO$_2$ treated CalB structure enough density to place two N-acetylglucosamine (NAG) molecules attached to asparagine 74 (Figure 33), and only one NAG molecule in LPG treated CalB (Figure 35).

Figure 36 (a) shows all the CalB structures superimposed and the active site highlighted (b). Table 33 presents a summary of all CalB structures determined (untreated, SC-CO$_2$-treated and LPG-treated) comparing their main features and differences among them.

Figure 36. Structures of untreated, SC-CO$_2$ and LPG treated CalB superimposed (**A**) and the active sites (**B**).
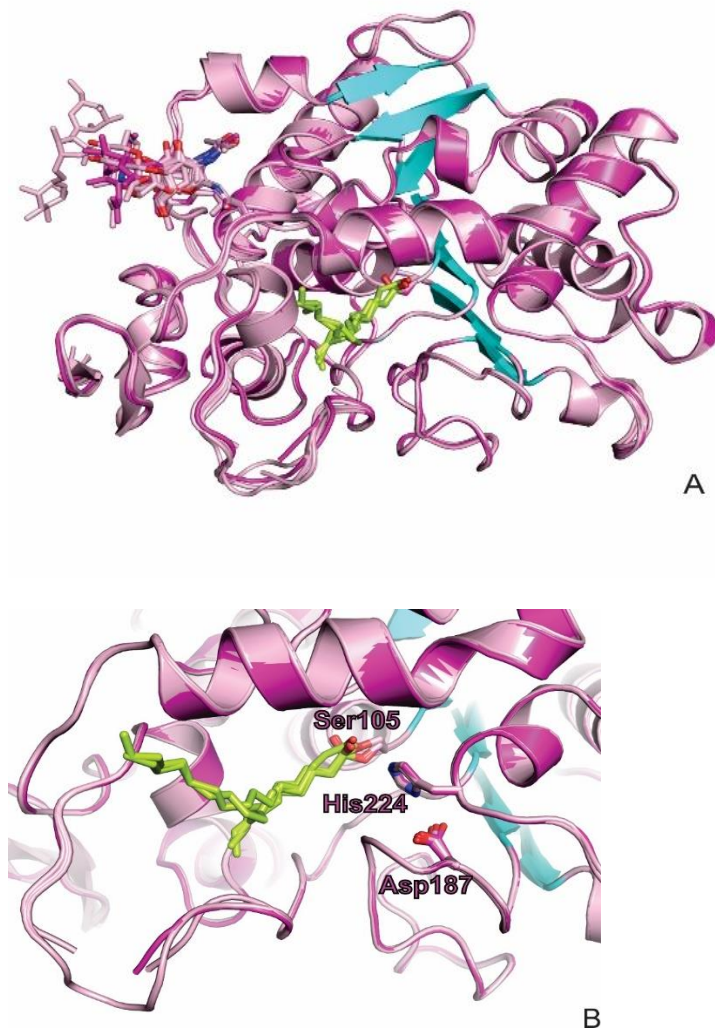
Table 33. Summary of CalB structures determined in this work.

CalB structure	Crystallization condition	Space group	Resolution (Å)	Chains	State	Residues Gap	Glycosylation-Position	Ligand-Position
Untreated	100 mM Tris pH 7; 200 mM NaCl; 29% PEG 3350; MPD	P 2_1 3	1.7	A,B	-	144-145,A 144-147,B	[2] NAG - ASN74,A,B [3] MAN, A	PLM – SER105 , A,B
SC-CO_2 treated	100 mM Tris pH 7; 200 mM NaCl; 30% PEG 3000	P 2_1 3	2.3	A,B	Closed	-	[2] NAG - ASN74 A,B	-
LPG treated	200 mM NaI; 16% PEG 3350	C 1 2 1	2.15	A,B,C, D,E,F	Closed A,B,C,E	145-146,D 142-147,F	NAG - ASN74 A,B,C,D,E,F	PLM - SER105 A,B,C

STAUCH; FISHER; CIANCI (2015) describe the residue range 140–147 (α-helix 5) corresponding to an open conformation, and same region as an unfolded loop, corresponding to a closed conformation .The residue range 140–147 presents Asp145 as the only amino acid with a charged side chain, characterizing α5 of high hydrophobicity. In the open conformation, α5 shows a series of aliphatic residues that line the channel leading to the active site with the only polar residue, Asp145, making hydrogen bonds with the side chains of Ser150 and Thr158. When closing the active site, the α-helix 5 undergoes a dramatic conformational change to an unstructured loop while bringing the carboxylic group of Asp145 close to the side chain of Lys290, thus forming a salt bridge. The spatial rearrangement of Lys290 brings α10 closer to new lid region, completing the closure of the catalytic cavity. The unfolding of α5 results in the closing of the lid over the cavity, preventing the access of any substrate to the catalytic site.

As all the three of our CalB structures were solved at comparable resolutions, we can affirm that a change, specifically related to the presence of the substrate, effectively happened after CalB treatment in SC-CO_2 and LPG. It is presently not clear if the detachment of the ligand and sugar happened during the high-pressure treatment or after the treatment, during the GF run. We know that the GF run does not displace the substrate from the untreated CalB. Therefore, we believe that the treatment rendered the enzyme more susceptible to release its ligand, either concomitantly with the treatment or during the GF run.

4.3.12. Size Exclusion Chromatography – Multi-Angle Light Scattering

SEC-MALS was performed for the previously gel-filtration purified CalB (10 mg/mL). The sample was dissolved in 0.02 M Tris pH 7.5, 0.1 M sodium chloride and 0.02% (v/v) sodium azide to a concentration of 6.66 mg/mL and a new separation was performed on a Superdex® 75 10/300 SEC column coupled to a miniDAWN TREOS three-angle light scattering detector with a laser wavelength of 660 nm (Wyatt Technology), equipped with RefractoMax520 refractive index detector (ERC Inc.) at a flow rate of 0.6 mL/min. Result of SEC-MALS for the native CalB is shown in Figure 37.

CalB started eluting after 17 minutes. The molar mass found for native CalB by SEC-MALS was $34.2 \pm 0.357\%$ kDa). The hydrodynamic radius obtained for the CalB molecule was $2.633 \pm 0.42\%$ nm.

Figure 37. SEC-MALS of native CalB.
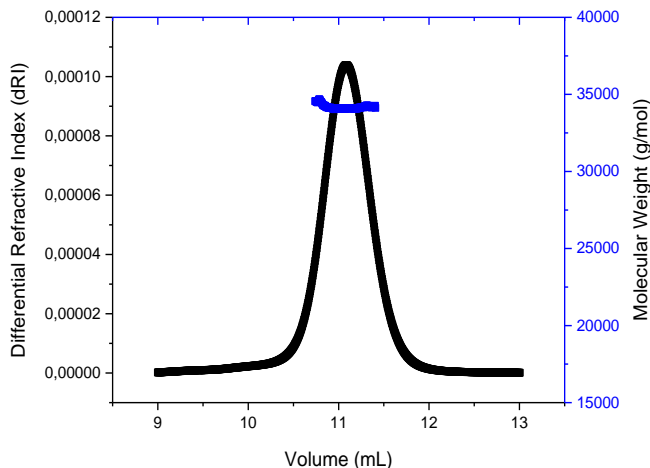
SEC-MALS measurements were also carried out by mixing the gel-filtration purified CalB at 10 mg/mL with the substrate 4-nitrophenyl palmitate (*p*-NPP) (dissolved in ethanol at 13 mM) in the molar ratio enzyme:substrate of 1:5; and by mixing the enzyme previously inhibited by 10 mM of phenylmethylsulfonyl fluoride (PMSF) with *p*-NPP (molar ratio CalB: substrate of 1:5). Figure 38 (a) presents the SEC-MALS result for CalB:*p*-NPP in the 1:5 molar ratio and (b) presents the SEC-MALS result for CalB (10 mM PMSF):*p*-NPP in the same 1:5 molar ratio.

Figure 38. SEC-MALS of CalB mixed with (**A**) *p*-NPP in the 1:5 molar ratio and (**B**) 10 mM PMSF and 1:5 molar CalB: *p*-NPP.
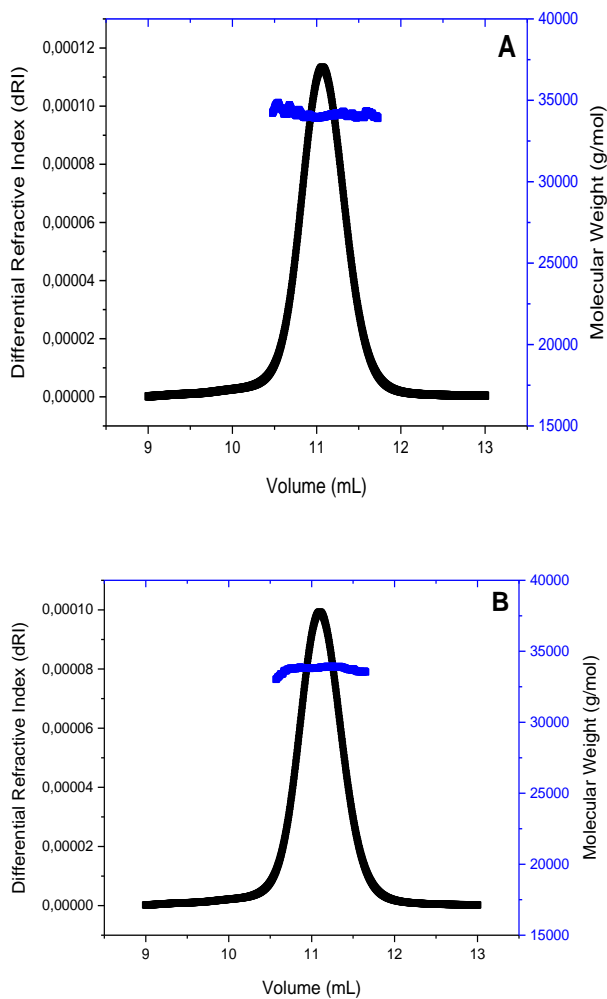
As we can see in Figure 38 (a) and (b), the molar mass obtained for the lipase in the mixture CalB + *p*-NPP and also for CalB + PMSF + *p*-NPP were both around 34 kDa (34.2 ± 0.58% and 33.8 ± 0.164%,

respectively), showing that CalB is in the monomeric state in solution even in the presence of the substrate. We conclude, therefore, that the two molecules in the asymmetric unit found in the X-ray structure are due just to crystal packing. The hydrodynamic radius was $2.649 \pm 0.432\%$ nm for the mixture 1:5 (CalB: p-NPP) and $2.519 \pm 0.418\%$ nm for the mixture CalB (10 mM PMSF):p-NPP 1:5 molar ratio.

We also performed SEC-MALS for CalB treated in CO_2 (35 ºC, 160 bar and 1 h) and LPG (65 ºC, 30 bar, 1 h), both purified after treatment as described in section 3.2.1.1. Samples were dissolved in 0.02 M Tris pH 7.5 and 0.1 M sodium chloride with 0.02% (v/v) sodium azide to a concentration of 6.66 mg/mL and a new separation was performed on a Superdex® 75 10/300 SEC column attached to a miniDAWN TREOS three-angle light scattering detector with a laser wavelength of 660 nm (Wyatt Technology), equipped with RefractoMax520 refractive index detector (ERC Inc.) at a flow rate of 0.6 mL/min. Results of SEC-MALS for CalB treated in CO_2 and LPG are shown in Figures 39 (a) and (b), respectively.

Figure 39. SEC-MALS of CalB treated with (**A**) CO_2 (35 ºC, 160 bar, 1 h) and (**B**) LPG (65 ºC, 30 bar, 1 h).
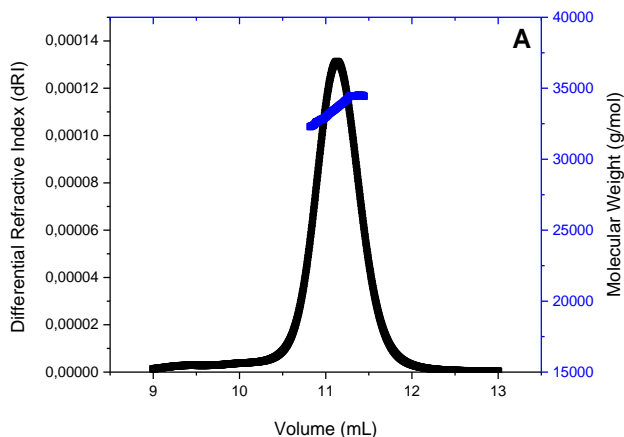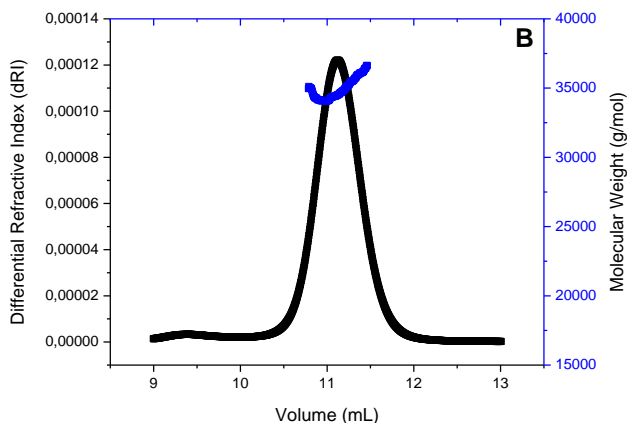
In Figure 39 (a) and (b) we can see that the high pressure treatment either with CO_2 or LPG did not change the molecular weight of CalB, meaning that CalB is still in the monomeric state in solution after the treatments, and the two and six molecules in the asymmetric unit found in the X-ray structure for the CO_2 and LPG treated CalB, respectively, are due just to crystal packing.

The shape of the molecular weight (MW) distributions (blue lines) is changing, meaning that the samples are less homogenous/monodisperse than the untreated ones. It might have occurred that the treatment slightly changed the surface of CalB, and this change is not uniform throughout the protein population. The observed effect supports our structural findings, where crystals are composed of apo and substrate bound CalB, indicating the presence of slightly different populations after treatment with LPG. Treatment with CO_2 may have resulted in a larger population of apo CalB compared to substrate bound CalB, potentially explaining the lack of substrate density in the molecules composing the crystal.

There is no distinguishable shift in molecular mass though. MW was $33.6 \pm 0.225\%$ kDa for CalB treated with CO_2, and $34.8 \pm 0.707\%$ for CalB treated in LPG; and the hydrodynamic radius was $2.64 \pm 2.35\%$ nm and $2.844 \pm 2.348\%$ nm, respectively.

148

5.   CONCLUSIONS

Untreated CalB was satisfactorily purified by size exclusion chromatography and its secondary structure elements were addressed by circular dichroism (CD). Our CD spectra confirmed that CalB is, in fact, an α/β hydrolase, mostly composed of α-helix and parallel and antiparallel β-sheets.

CalB was denatured when heated to 95 ºC, either when the far-UV spectra for the native CalB was collected at 95 ºC or when CalB was previously denatured at 95 ºC for 5 min and the spectra was collected at 20 ºC. Both data sets collected, after exposing CalB at 95 ºC, generated low α-helix contents, indicating protein unfolding, which is characterized by α-helix content reduction and random coil content increase. It was also not possible to refold the protein going from 95 ºC to 20 ºC.

Differential scanning fluorimetry (DSF) analysis indicated that CalB is more thermostable in high pH buffers (around 9), with maximum T_m in 50 mM TrisHCl pH 8.4. By investigating CalB activity in different pHs, we verified that CalB is not active in acidic pH at any temperature. We observed that CalB is more active in basic pH compared to neutral pH, and slightly more active when previously activated at 65 ºC for 1 hour.

CalB was partially inhibited by PMSF and EDTA.

CalB was successfully deglycosylated by PNGase F under denaturing conditions, but the mass spectrometry (MS) results showed that the deglycosylation under native conditions was not efficient for CalB. We can therefore not conclude if the sugars have some influence on the CalB hydrolysis activity.

We did not manage to get crystals of the unpurified CalB, most likely due to its complex buffer of undefined composition. Crystals of untreated gel-filtration purified CalB were obtained in 0.1 M Tris pH 7, 0.2 M NaCl, 29% (v/v) PEG 3350 and MPD as additive. The crystals appeared between 3 and 5 days and diffracted to 1.7 Å.

There are two molecules in the asymmetric unit of the CalB crystal and, by solving the untreated CalB structure by molecular replacement (MR), we have noticed that α5 is not present in our molecule. α5 is part of the lid and we believe that it is not present in our structure due to the presence of a ligand in the active site of CalB (Ser105). We assume that binding of the ligand at the active site

destabilizes α5, making it invisible in our electronic density. Although there are many structures of CalB deposited in the Protein Data Bank (PDB), this is the first structure showing an intermediate bound-state enzyme. It was also possible to model in the CalB structure two N-acetylglucosamine (NAG) molecules attached to Asn74, followed by three mannoses (MAN), indicating high order of branching hexoses.

We observed different CalB behavior under different experimental conditions when submitted to supercritical CO_2 (SC-CO_2) treatment. In experiment 1 (35 °C, 75 bar, 1 hour), a considerable increase in CalB residual specific activity was observed, while in other conditions the residual specific activity remained unaltered or was decreased, as in experiment 6 (65 °C, 75 bar, 6 hours), in which the largest loss of activity was observed. In general, long exposure times to mild or high pressures led to a decrease of the CalB specific hydrolysis activity.

CalB showed different behavior under different experimental conditions when exposed to pressurized LPG as well. We observed an increase of its hydrolysis activity in experiment 2 (65 °C, 30 bar, 1 hour) and the largest loss of activity was observed in experiment 8 (65 °C, 90 bar, 6 hours).

CalB treated with SC-CO_2 and LPG gradually lost activity over time at low temperatures in all three systems studied. However, the residual activity of the enzyme treated at high pressure was still above 100% until the 20th day of storage. There was no difference on the residual activity loss of CalB treated with LPG and stored at different temperatures. A greater difference was observed between CalB treated with CO_2 and flash-frozen in liquid nitrogen (-196 °C) followed by storage in the freezer (-10 °C) and CalB directly stored in the freezer at -10 °C.

Crystals of CalB purified after exposure to the experiment 5 conditions (160 bar, 35 °C, 1 hour) in SC-CO_2 at FUB were obtained in 0.1 M Tris pH 7, 0.2 M NaCl and 30% (v/v) PEG 3000 and diffracted to 2.3 Å. Crystals of CalB purified after exposure to the experiment 2 conditions (30 bar, 65 °C, 1 hour) in pressurized LPG were obtained in 16% PEG 3350 and 200mM NaI, and diffracted to 2.15 Å.

It was possible to observe some changes in the CalB structure when exposed to SC-CO_2 and LPG, followed by GF. SC-CO_2 treated CalB also showed two molecules in the asymmetric unit and same space group as the untreated CalB (P 21 3), however, the LPG treated CalB

presented six molecules in the asymmetric unit and a different space group (C 1 2 1).

We could not place a substrate bound to Ser105 in the $SC-CO_2$ treated CalB and the electronic density was only enough to place two NAG molecules attached to each Asn74. On the other hand, it was possible to place a ligand bound to Ser105 in three of the six molecules of the asymmetric unit of CalB treated with LPG. Only one NAG molecule was modeled attached to Asn74 in LPG treated CalB.

We suppose that either CalB does not have the substrate attached to Ser105 after CO_2 treatment or after gel filtration, or just very few molecules in the crystal are bound to the substrate, which does not yield a clear electron density at the active site. The ligand or the sugars could have been dissociated from the protein either because of the treatment in $SC-CO_2$ or during the gel-filtration. We also believe that the active site is not fully occupied by the substrate in all the molecules of the LPG treated CalB crystal.

Size exclusion chromatography – multi-angle light scattering (SEC-MALS) measurements revealed that CalB is in the monomeric state in solution even in the presence of the substrate or after treatment in pressurized fluids. Therefore, the two or six molecules in the asymmetric unit found in the X-ray structures are due just to crystal packing. We believe, however, that the treatments under CO_2 or LPG do change the protein conformation to the point that CalB is more prone to lose its ligand and its sugars, therefore promoting other crystal packing possibilities.

Considering the lack of studies concerning structural modifications of enzymes caused by treatment under high pressure, the investigation of CalB behavior - a lipase widely used in food, chemical and pharmaceutical industries - in pressurized fluids, and the determination of three-dimensional structure of the treated and untreated CalB via X-ray crystallography, represent such an advance in the area. There are still many questions to be addressed though, but the present results are unprecedented in the specialized literature, and may help to understand CalB activation and deactivation phenomena in $SC-CO_2$ and LPG as well as to encourage the application of such techniques to other enzymes of interest.

152

6.   OUTLOOK

During the year I developed part of my PhD thesis at the Free University of Berlin, I learned that X-ray crystallography is not only a cutting-edge technique to determine macromolecule structures, but also a very thorough technique which requires huge multidisciplinary knowledge and many experimental trials.

Taking into account the difficulties I faced during crystallization trials of CalB suspended in the commercial buffer, it is extremely relevant to point out the importance of treating the enzyme in a proper buffer, compatible to the crystallization conditions requirements and other downstream experiments.

On the other hand, major advances in describing structural changes in proteins that accompany pressure-induced denaturation have been obtained by combining high-resolution nuclear magnetic resonance (NMR) techniques with high pressure (MOZHAEV et al., 1996a; BOONYARATANAKORNKIT; PARK; CLARK, 2002).

Crystallography has also been applied under high pressure (HPMX) (KURPIEWSKA; LEWINSKI, 2010). This method of crystallization can be used for obtaining crystals of unstable intermediates or proteins that contain floppy domains or flexible loops. Briefly, the pressure is transmitted into a chamber uniformly through a pressure medium - the mother liquor crystallization solution in the case of protein crystals. The crystal is visible into the chamber, which allows centering it on the goniometer and examining sample behavior during measurements. While standard crystallographic experiments only give the structure that reflects an average structure of conformers present in the crystal, the crystallography at high pressure conditions has the ability to determine the structure of the higher energy conformers. Furthermore, high pressure might become a standard tool to improve order in macromolecular crystals, either by favoring more ordered packing or by restricting amplitudes of atomic motions in regions that are disordered at atmospheric pressure.

Thus, the ability of NMR and HPMX to obtain accurate structural information under high pressure could open a wealth of possibilities: the exploration of substrate-bound states and the mechanisms of enzymatic reactions, studies of the structural principles of organization of oligomeric proteins, the interactions between

molecules and between subunits and the detection of pressure-induced denaturation and/or activation.

REFERENCES

ADAMS, P. D., AFONINE, P. V., BUNKÓCZI, G., CHEN, V. B., DAVIS, I. W., ECHOLS, N., HEADD, J. J., HUNG, L. W., KAPRAL, G. J., GROSSE-KUNSTLEVE, R. W., McCOY, A. J., MORIARTY, N. W., OEFFNER, R., READ, R. J., RICHARDSON, D. C., TERWILLIGER, T. C., ZWART, P. H. *PHENIX*: a comprehensive **Python-based system for macromolecular structure solution.** *Acta Crystallographica Section D*, v. D66, p. 213–221, 2010.

ALMEIDA FILHO C. **Estudo experimental e teórico de coeficientes de difusão binários envolvendo componentes de óleos essenciais em dióxido de carbono supercrítico.** Tese de Doutorado em Engenharia Química, Universidade Federal de Santa Catarina - UFSC, Florianópolis, 2003.

ANDRADE, J. M.; OESTREICHER, E. G.; OLIVEIRA, J. V.; OLIVEIRA, D.; ANTUNES, O. A. C.; DARIVA, C. **Effect of treatment with compressed CO_2 and propane on D-hydantoinase activity.** *Journal of Supercritical Fluids*, v. 46, p. 342 – 350, 2008.

ASTEFANEI, A., KOK, W. T., BÄUERLEIN, P., NÚÑES, O., GALCERAN, M. T., DE VOOGT, P., SCHOENMAKERS, P. J. **Characterization of aggregates of surface modified fullerenes by asymmetrical flow field-flow fractionation with multi-angle light scattering detection.** *Journal of Chromatography A,* v. 1408, p. 197–206, 2015.

BARON, A. M. **Biocatálise em ambientes aquo-restritos: comparação de diferentes sistemas reacionais.** Dissertação de Mestrado em Química, Universidade Federal do Paraná - UFPR, Curitiba, 2003.

BAUER, C., STEINBERGER, D-J., G. SCHLAUER, GAMSE, T., MARR, R. **Activation and denaturation of hydrolases in dry and humid supercritical carbon dioxide (SC-CO_2).** *Journal of Supercritical Fluids,* v. 19, p. 79-86, 2000.

BAUER, C., GAMSE, T., MARR, R. **Quality improvement of crude porcine pancreatic lipase preparations by treatment with humid supercritical carbon dioxide.** *Biochemical Engineering Journal,* v. 9, p. 119–123, 2001.

BECKTEL, W. J. and SCHELLMAN, J. A. **Protein stability curves.** *Biopolymers*, v. 26, p. 1859-1877, 1987.

BELITZ, H. D. and GROSCH, W. **Química de los alimentos.** 2º edição. Editora Acribia, Zaragoza, 1997.

BEVILAQUA, J. V. **Estudo da catálise enzimática em meio orgânico para a produção de protótipo de fármaco antiasmático.** Tese de Doutorado em Engenharia Química, Universidade Federal do Rio de Janeiro – UFRJ, Rio de Janeiro, 2005.

BLANK, K., MORFILL, J., GUMPP, H., GAUB, H. E. **Functional expression of *Candida Antarctica* lipase B in *Eschericha coli.*** *Journal of Biotechnology*, v. 125, p. 474–483, 2006.

BÖHM, G., MUHR, R., JAENICKE, R. **CDNN: quantitative analysis of protein far UV circular dichroism spectra by neural networks.** Protein Engineering, v. 5, n. 3, p. 191 – 195, 1992.

BOONYARATANAKORNKIT, B. B.; PARK, C. B.; CLARK, D. S. **Pressure effects on intra- and intermolecular interactions within proteins.** *Biochimica et Biophysica Acta – Protein Structure and Molecular Enzymology*, v. 1595, p. 235 - 249, 2002.

BORNSCHEUER, U. T. and KAZLAUSKAS, R. J. **Hydrolases in organic synthesis – regio and stereoselective biotransformations.** Editora Wiley-VCH, Weinheim, 1999.

BORZANI, W.; SCHMIDELL, W.; LIMA, U. A.; AQUARONE, E. **Biotecnologia industrial. Volume I – Fundamentos.** Editora Edgard Blüncher Ltda., São Paulo, 2001.

BRADFORD, M. M. **A rapid and sensitive method for the quantification of microgram quantities of protein utilizing the**

principle of protein-dye binding. *Analytical Biochemistry*, v. 72, p. 248–254, 1976.

BRAGA, A. R. C.; SILVA, M. F.; OLIVEIRA, J. V.; TREICHEL, H.; KALIL, S. J. **Effect of compressed fluids treatment on β-galactosidase activity and stability.** *Bioprocess and Biosystems Engineering*, v. 35, p. 1541 – 1547, 2012.

BRUNNER, G. **Supercritical fluids: technology and application to food processing.** *Journal of Food Engineering*, v. 67, p. 21 – 33, 2005.

BRUSAMARELO, C. Z.; ROSSET, E.; DE CÉSARO, A.; TREICHEL, H.; OLIVEIRA, D.; MAZUTTI, M. A.; DI LUCCIO, M.; OLIVEIRA, J. V. **Kinetics of lipase-catalyzed synthesis of soybean fatty acid ethyl esters in pressurized propane.** *Journal of Biotechnology*, v. 147, p.108 – 115, 2010.

BUCHET, R., CARRIER, D., WONG, P. T. T., JONA, I., MARTONOSI, A. **Pressure effects on sarcoplasmic reticulum: a Fourier transform infrared spectroscopic study.** Biochimica and Biophysica Acta, v. 1023, p. 107-118, 1990.

BURKERT, J. F. M. **Otimização das condições de produção de lipase por *Geotrichum candidum* NRRL-Y552.** Tese de Doutorado em Engenharia de Alimentos, Universidade Estadual de Campinas - Unicamp, Campinas, 2002.

BURKERT J. F. M., MAUGERI F., RODRIGUES M. I. **Optimization of extracelular lipase production by *Geotrichum* sp. using factorial design.** *Bioresource Technology*, v. 91, p. 77 - 84, 2004.

CARRILHO, E.; TAVARES, M. C. H.; LANÇAS, F. M. **Fluidos supercríticos em química analítica. I. Cromatografia com fluido supercrítico: conceitos termodinâmicos.** *Química Nova*, v. 24, n. 4, p. 509 – 515, 2001.

CARVALHO, P. O.; CAMPOS, P. R. B.; NOFFS, M. D.; OLIVEIRA, J. G., SHIMIZU, M. T.; SILVA, D. M. **Aplicação de lipases**

microbianas na obtenção de concentrados de ácidos graxos poli-insaturados.** *Química Nova*, v. 26, n. 1, p. 75 - 80, 2003.

CASTRO, H. F. and ANDERSON, W. A. **Fine chemicals by biotransformation using lipases.** *Química Nova*, v. 18, p. 544 - 554, 1995.

CASTRO, H. F.; MENDES, A. A.; SANTOS, J. C.; AGUIAR, C. L. **Modificação de óleos e gorduras por biotransformação.** *Química Nova*, v. 27, n. 1, p. 146 - 156, 2004.

CELEBI, N.; YILDIZ, N.; DEMIR, A. S.; CALIMLI, A. **Enzymatic synthesis of benzoin in supercritical carbon dioxide.** *Journal of Supercritical Fluids,* v. 41, p. 386 – 390, 2007.

CHEFTEL J. C. **Review: High-pressure, microbial inactivation and food preservation.** *Food Science and Technology International*, v. 1, p. 75 - 90, 1995.

CHEN, D.; PENG, C.; ZHANG, H.; YAN, Y. **Assessment of activities and conformation of lipases treated with sub- and supercritical carbon dioxide.** *Applied Biochemistry and Biotechnology*, v. 169, p. 2189 – 2201, 2013a.

CHEN, D.; ZHANG, H.; XU, J., YAN, Y. **Effect of sub- and supercritical CO_2 treatment on the properties of *Pseudomonas cepacia* lipase.** *Enzyme and Microbial Technology,* v. 53, p. 110–117, 2013b.

CHIOU, S. H. and WU, W. T. **Immobilization of *Candida rugosa* lipase on chitosan with activation of the hydroxyl groups.** *Biomaterials*, v. 25, p. 197–204, 2004.

CHOWDHURY, S. K., KATTA, V., BEAVIS, R. C., CHAIT, B. T. **Origin and removal of adducts (molecular mass = 98 u) attached to peptide and protein ions in electrospray ionization mass spectra.** *Journal of the American Society for Mass Spectrometry*, v. 1, p. 382-388, 1990.

CIPOLATTI, E. P., VALÉRIO, A., NICOLETTI, G., THEILACKER, E., ARAÚJO, P. H. H., SAYER, C., NINOW, J. L., OLIVEIRA, D. **Immobilization of *Candida antarctica* lipase B on PEGylated poly(urea-urethane) nanoparticles by step miniemulsion polymerization.** *Journal of Molecular Catalysis B: Enzymatic*, v. 109, p. 116–121, 2014.

COELHO-SAMPAIO, T., FERREIRA, S. T., BENAIM, G., VIEYRA, A. **Dissociation of purified erythrocyte Ca^{2+}-ATPase by hydrostatic pressure.** *Journal of Biological Chemistry*, v. 266, p. 22266-22272, 1991.

COMIM, S. R. R., VENERAL, J. G., OLIVEIRA, D., FERREIRA, S. R. S., OLIVEIRA, J. V. **Enzymatic synthesis of poly(ε-caprolactone) in liquified petroleum gas and carbon dioxide.** *Journal of Supercritical Fluids*, v. 96, p. 334 – 348, 2015.

COSTA, M. A. and PERALTA, R. M. **Production of lipase by soil fung and partial characterization of lipase from a selected strain (*Penicillium wortmanii*).** *Journal of Basic Microbiology*, v. 39, p. 11 - 15, 1999.

CÔTÉ, A. and SHARECK, F. **Cloning, purification and characterization of two lipases from *Streptomyces coelicolor* A3(2).** *Enzyme and Microbial Technology*, v. 42, p. 381 - 388, 2008.

DALLA ROSA, C. **Produção de ésteres etílicos a partir de óleo de soja utilizando lipase em propano.** Dissertação de Mestrado em Engenharia de Alimentos, Universidade Regional Integrada do Alto Uruguai e das Missões – URI, Erechim, 2006.

DALLA ROSA, C.; MORANDIM M. B.; NINOW J. L.; OLIVEIRA D.; TREICHEL H.; OLIVEIRA J. **Lipase-catalyzed production of fatty acid ethyl esters from soybean oil in compressed propane.** *Journal of Supercritical Fluids*, v. 47, p. 49 – 53, 2008.

DALLA ROSA, C.; MORANDIM M. B.; NINOW J. L.; OLIVEIRA D.; TREICHEL H.; OLIVEIRA J. **Continuous lipase-catalyzed**

production of fatty acid ethyl esters from soybean oil in compressed fluids. *Bioresource Technology*, v. 100, p. 5818 – 5826, 2009.

DALLA-VECHIA, R.; NASCIMENTO, M. G.; SOLDI, V. **Aplicações de lipases imobilizadas em polímeros.** *Química Nova*, v. 27, p. 623 - 630, 2004.

DEVILLE-BONNE, D. and ELSE, A. J. **Reversible high hydrostatic pressure inactivation of phosphofructokinase from *Escherichia coli.*** *European Journal of Biochemistry*, v. 200, p. 747-750, 1991.

DIXON, M. and WEBB, E. C. **Enzymes.** Editora Academic Press, New York, 1979.

DZIEZAK, J. D. **Enzymes: catalyses for food processes.** *Food Technology*, v. 45, p. 78 - 85, 1991.

EDSALL, J. T. **Hsien Wu and the first theory of protein denaturation (1931)**. *Advances in Protein Chemistry*, v. 46, p. 1-26, 1995.

EISENMENGER, M. J. and REYES-DE-CORCUERA, J. I. **High pressure enhancement of enzymes: A review.** *Enzyme and Microbial Technology*, v. 45, p. 331 – 347, 2009.

ERIJMAN, L., LORIMER, G. H., WEBER, G. **Reversible dissociation and conformational stability of dimeric ribulose biphosphate carboxylase.** *Biochemistry,* v. 32, p. 5187-5195, 1993.

EMSLEY, P. and COWTAN, K. D. *Coot***: model-building tools for molecular graphics.** *Acta Crystallographica Section D,* v. D60, p. 2126 - 2132, 2004.

ESMELINDRO, A. F. A.; FIAMETTI, K. G.; CENI, G.; CORAZZA, M. L.; TREICHEL, H.; OLIVEIRA, D.; OLIVEIRA, J. V. **Lipase-catalyzed production of monoglycerides in compressed propane and AOT surfactante.** *Journal of Supercritical Fluids*, v. 47, p. 64 – 69, 2008.

FADILOGLU, S. and ERKMEN, O.; **Inactivation of lipase by carbon dioxide under atmospheric pressure.** *Journal of Food Engineering*, v. 52, p. 331 – 335, 2002.

FAZEKAS DE St. GROTH, S., WEBSTER, R. G., DATYNER, A. **Two new staining procedures for quantitative estimation of proteins on electrophoretic strips.** *Biochimica and Biophysica Acta*, v. 71, p. 377 - 391, 1963.

FEIHRMANN, A. F. **Avaliação da atividade enzimática de lipases imobilizadas em fluidos pressurizados.** Dissertação de Mestrado em Engenharia de Alimentos, Universidade Integrada do Alto Uruguai e das Missões – URI, Erechim, 2005.

FEITEN, M. C.; DI LUCCIO, M.; SANTOS, K. F.; OLIVEIRA, D.; OLIVEIRA, J. V. **X-ray crystallography as a tool to determine three-dimensional structures of commercial enzymes subjected to treatment in pressurized fluids.** *Applied Biochemistry and Biotechnology*, v. 182, n. 2, p. 429 – 451, 2017.

FERNANDEZ-LAFUENTE, R., ARMISEN, P., SABUQUILLO, P., FERNANDEZ-LORENTE, G., GUISAN, J. M. **Immobilization of lipases y selective adsorption on hydrophobic supports.** *Chemistry and Physics of Lipids*, v. 93, p. 185–197, 1998.

FINDRIK, Z., VASIC-RACKI, D., PRIMOZIC, M., HABULIN, M., KNEZ, Z. **Enzymatic activity of L-amino acid oxidase from snake venom *Crotalus adamanteus* in supercritical CO_2.** *Biocatalysis and Biotransformation,* v. 23, p. 315 - 321, 2005.

FRANKEN, L. P. G.; MARCON, N. S.; TREICHEL, H.; OLIVEIRA, D.; FREIRE, D. M. G.; DARIVA, C.; DESTAIN J.; OLIVEIRA, J. V. **Effect of treatment with compressed propane on lipases hydrolytic activity.** *Food and Bioprocess Technology*, v. 3, p. 511 – 520, 2010.

FRICKS, A. T.; SOUZA, D. P. B.; OESTREICHER, E. G.; ANTUNES, O. A. C.; GIRARDI, J. S.; OLIVEIRA D.; DARIVA, C. **Evaluation of radish (*Raphanus sativus* L.) peroxidase activity after high-pressure**

treatment with carbon dioxide. *Journal of Supercritical Fluids*, v. 38, p. 347 – 353, 2006.

FRICKS, A. T.; OESTREICHER, E. G.; CARDOZO FILHO, L.; FEIHRMANN, A. C.; CORDEIRO, Y.; DARIVA, C.; ANTUNES, O. A. C. **Effects of compressed fluids on the activity and structure of horseradish peroxidase.** *Journal of Supercritical Fluids*, v. 50, p. 162 – 168, 2009.

GALLAGHER, S. R. **One-dimensional SDS gel electrophoresis of proteins.** *Current Protocols in Molecular Biology*, John Wiley & Sons, 2006.

GE HEALTHCARE. **Gel Filtration - Principles and Methods.** *18-1022-18*, 2010.

GHANEM, A. and ABOUL-ENEIN, H. Y. **Application of lipase in kinetic resolution of racemates.** *Chirality*, v. 17, p. 1 - 15, 2005.

GIEβAUF, A.; MAGOR, W., STEINBERGER, D. J.; MARR, R. **A study of hydrolases stability in supercritical carbon dioxide (SC-CO$_2$).** *Enzyme and Microbial Technology*, v. 24, p. 577 – 583, 1999.

GIEβAUF, A. and GAMSE, T. **A simple process for increasing the specific activity of porcine pancreatic lipase by supercritical carbon dioxide treatment**. *Journal of Molecular Catalysis B: Enzymatic,* v. 9, p. 57 – 64, 2000.

GOETTIG, P. **Effects of glycosylation on the enzymatic activity and mechanisms of proteases.** *International Journal of Molecular Sciences*, v. 17, p. 1969 - 1993, 2016.

GONÇALVES, K. M.; BARBOSA, L. R. S.; LIMA, L. M. T. R.; CORTINES, J. R.; KALUME, D. E.; LEAL, I. C. R.; MARIZ e MIRANDA, L. S.; SOUZA, R. O. M.; CORDEIRO, Y. **Conformational dissection of *Thermomyces lanuginosus* lipase in solution.** *Biophysical Chemistry*, v. 185, p. 88 – 97, 2014.

GREULICH, K. O. and LUDWIG, H. **High pressure enzyme kinetics of dextransucrase.** *Biophysical Chemistry,* v. 6, p. 87-94, 1977.

GUPTA, R.; GUPTA, N.; RATHI, P. **Bacterial lipases: an overview of production, purification and biochemical properties.** *Applied Microbiology and Biotechnology*, v. 64, p. 763 – 781, 2004.

HABULIN, M. and KNEZ, Z. **Activity and stability of lipases from different sources in supercritical carbon dioxide and near-critical propane.** *Journal of Chemical Technology and Biotechnology*, v. 76, p. 1260 – 1266, 2001.

HABULIN, M.; PRIMOZI, M.; KNEZ, Z. **Stability of proteinase form** *Carica papaya* **latex in dense gases.** *The Journal of Supercritical Fluids*, v. 33, p. 27 – 34, 2005.

HASAN, F.; SHAH, A. A.; HAMEED, A. **Industrial applications of microbial lipases.** *Enzyme and Microbial Technology*, v. 39, p. 235 - 251, 2006.

HEI, D. J. and CLARK, D. S. **Pressure stabilization of proteins from extreme thermophiles.** *Applied and Environmental Microbiology*, v. 60, p. 932 – 939, 1994.

HENDRICKX, M.; LUDIKHUYZE, L.; VAN den BROECK, I; WEEMAES, C. **Effects of high pressure on enzymes related to food quality (review).** *Trends in Food Science & Technology*, v. 9, p. 97 - 203, 1998.

HERNANDEZ, K.; GARCIA-GALAN, C.; FERNANDEZ-LAFUENTE, R. **Simple and efficient immobilization of lipase B from** *Candida antarctica* **on porous styrene–divinylbenzene beads.** *Enzyme and Microbial Technology*, v. 49, p. 72 – 78, 2011.

HILDEBRAND, C.; FREIRE, D.; DALLA ROSA, C.; DARIVA, C.; OLIVEIRA, J. V.; OLIVEIRA, D.. **Fatty acid ethyl esters production using a non-commercial lipase in pressurized propane medium.** *Ciência e Tecnologia de Alimentos* (Online), v. 29, p. 603 - 609, 2009.

HOUSAINDOKHT, M. R.; BOZORGMEHR, M. R.; MONHEMI, H. **Structural behavior of** *Candida antarctica* **lipase B in water and**

supercritical carbon dioxide: A molecular dynamic simulation study. *Journal of Supercritical Fluids*, v. 63, p. 180 – 186, 2012.

HOUSAINDOKHT, M. R. and MONHEMI, H. **The open lid conformation of the lipase is explored in the compressed gas: New insights from molecular dynamic simulation.** *Journal of Molecular Catalysis B: Enzymatic*, v. 87, p. 135 – 138, 2013.

HU, W., ZHANG, Y., WANG, Y., ZHOU, L., LENG, X., LIAO, X. HU, X. **Aggregation and homogenization, surface charge and structural change, and inactivation of mushroom tyrosinase in an aqueous system by subcritical/supercritical carbon dioxide.** *Langmuir*, v. 27, p. 909 – 916, 2011.

IDRIS, A. and BUKHARI, A. **Immobilized *Candida antarctica* lipase B: Hydration, stripping off and application in ring opening polyester synthesis.** *Biotechnology Advances*, v. 30, p. 550 – 563, 2012.

ISO, M.; CHEN, B.; EGUCHI, M.; KUDO, T.; SHRESTHA, S. **Production of biodiesel fuel from triglycerides and alcohol using immobilized lipase.** *Journal of Molecular Catalysis B: Enzymatic*, v. 16, p. 53 – 58, 2001.

JAEGER, K. E.; RANSAC, S.; DIJKSTRA, B. W.; COLSON, C.; HEUVEL, M.; MISSET, O. **Bacterial lipases.** *FEMS Microbiology Reviews*, v. 15, p. 29 – 63, 1994.

JAEGER, K. E. and EGGERT, T. **Lipases for biotechnology.** *Current Opinion in Biotechnology*, v. 13, p. 390 – 397, 2002.

JAEGER, K. E. and REETZ, M. T. **Microbial lipases form versatile tools for biotechnology.** *Trends in Biotechnology*, v. 16, n. 9, p. 396 - 403, 1998.

JUN, C.; JEON, B. W.; JOO, J. C.; LE, Q. A. T.; GU, S. A.; BYUN, S.; CHO, D. H.; KIM, D.; SANG, B. I.; KIM, Y. H. **Thermostabilization of *Candida antarctica* lipase B by double immobilization: Adsorption on a macroporous polyacrylate carrier and R1 silaffin-mediated biosilicification.** *Process Biochemistry*, v. 48, p. 1181 – 1187, 2013.

KABSCH, W. *XDS. Acta Crystallographica Section D,* v. D66, p. 125 – 132, 2010.

KADER, R.; YOUSUF, A.; HOQ, M. M. **Optimization of lipase production by *Rhizopus MR 12* in shake culture.** *Journal of Applied Sciences*, v. 7, p. 855 - 860, 2007.

KAMAT S., CRITCHLEY G., BECKMAN E. J., RUSSELL A. J.; **Biocatalytic synthesis of acrylates in organic solvents and supercritical fluids. III. Does carbon dioxide covalently modify enzymes?** *Biotechnology and Bioengineering*, v. 46, p. 610 - 620, 1995.

KANG, J.-S. **Principles and Applications of LC-MS/MS for the Quantitative Bioanalysis of Analytes in Various Biological Samples.** Tandem Mass Spectrometry - Applications and Principles, p. 441 – 492, 2012. InTech, Available from: http://www.intechopen.com/books/tandem-massspectrometry-applications-and-principles/principles-and-applications-of-lc-ms-ms-for-the-quantitativebioanalysis-of-analytes-in-various-biol

KANWAR, S. S., KAUSHAL, R. K., JAWED, A., GUPTA, R. G., CHIMNI, S. S. **Methods for inhibition of residual lipase activity in colorimetric assay: A comparative study.** *Indian Journal of Biochemistry & Biophysics*, v. 42, p. 233 – 237, 2005.

KAO, F.-J., EKHORUTOMWEN, S. A., SAWAN, S. P. **Residual stability of lipase from *Candida rugosa* in hexane, supercritical CO_2, and supercritical SF_6.** *Biotechnology Techniques*, v. 11, p. 849 – 852, 1997.

KARMEE, K.; CASIRAGHI, L., GREINER, L. **Technical aspects of biocatalysis in non-CO_2-based supercritical fluids.** *Biotecnhnology Journal*, v. 3, p. 104 – 111, 2008.

KASCHE, V., SCHLOTHAUER, R., BRUNNER, G.; **Enzyme denaturation in supercritical CO2: stabilyzing effect of S-S bonds during the depressurization step.** *Biotechnology Letters,* v. 10, p. 569 – 573, 1998.

166

KELLY, S. M. and PRICE, N. C. **The application of circular dichroism to studies of protein folding and unfolding.** *Biochimica et Biophysica Acta*, v. 1338, n. 2, p. 161-185, 1997.

KELLY, S. M. and PRICE, N. C. **The use of circular dichroism in the investigation of protein structure and function.** *Current Protein and Peptide Science*, v. 1, p. 349 – 384, 2000.

KIM, S. K.; LEE, H. H.; PARK, Y. C.; JEON, S. T.; SON, S. H., MIN, W. K.; SEO, J. H. **Anion tags improve extracellular production of** *Candida antarctica* **lipase B in** *Escherichia coli***.** To be published. *Protein Data Bank*, 2014.

KNEZ, Z. **Enzymatic reactions in dense gases.** *The Journal of Supercritical Fluids*, v. 47, p. 357 – 372, 2009.

KNEZ, Z.; HABULIN, M.; KRMELJ, V. **Enzyme catalyzed reactions in dense gases.** *Journal of Supercritical Fluids*, v.14, p. 17 – 29, 1998.

KNEZ Z. and HABULIN M. **Compressed gases as alternative enzymatic-reaction solvents: A short review.** *Journal of Supercritical Fluids*, v. 23, p. 29 - 34, 2002.

KNUTSON, B. L. and SARKARI, M. **Processing of biological materials.** In: YORK, P. and KOMPELLA, U. **Drug Delivery and Supercritical Fluid Technology.** Editora Marcel Dekker Inc., New York, p. 411 - 460, 2004.

KRAMMER, P. and VOGEL, H. **Hydrolysis of esters in subcritical and supercritical water.** *Journal of Supercritical Fluids,* v. 16, p. 189 – 206, 2000.

KUHN, G.; MARANGONI, M.; FREIRE, D. M. G.; SOARES, V. F.; GODOY, M. G.; CASTRO, A. M.; DI LUCCIO, M.; TREICHEL, H.; MAZUTTI, M. A.; OLIVEIRA, D.; OLIVEIRA, J. V. **Esterification activities of non-commercial lipases after pre-treatment in pressurized propane.** *Journal of Chemical Technology and Biotechnology*, v. 85, p. 839 – 844, 2010.

KUHN, G. O.; COGHETTO, C.; TREICHEL, H.; OLIVEIRA, D.; OLIVEIRA, J. V. **Effect of compressed fluids treatment on the activity of inulinase from *Kluyveromyces marxianus* NRRL Y-7571 immobilized in montmorillonite.** *Process Biochemistry*, v. 46, p. 2286 – 2290, 2011.

KUHN, G. O.; DALLA ROSA, C.; SILVA, M. F.; TREICHEL, H.; OLIVEIRA, D.; OLIVEIRA, J. V. **Synthesis of fructooligosaccharides from *Aspergillus niger* commercial inulinase immobilized in montmorillonite pretreated in pressurized propane and LPG.** *Applied Biochemistry and Biotechnology*, v. 169, p. 750 – 760, 2013.

KUMAR, R.; MADRAS, S.; MADAK, J. **Enzimatic synthesis of ethyl palmitate in supercritical carbon dioxide.** *Industrial Engineering and Chemical Research*, v. 43, p. 1568 - 1573, 2004.

KUNUGI, S. **Enzyme reactions under high pressure and their applications.** *Enzyme Engineering XI*, v. 672, p. 293 – 304, 1992.

KURPIEWSKA, K.; LEWINSKI, K. **High pressure macromolecular crystallography for structural biology: a review.** *Central European Journal of Biology*, v. 5, n. 5, p 531 – 542, 2010.

LEAL, M. C. M. R.; CAMMAROTA, M. C.; FREIRE, D. M. G.; SANT'ANNA Jr., G. L. **Hydrolytic enzymes as coadjuvants in the anaerobic treatment of dairy wastewaters.** *Brazilian Journal of Chemical Engineering*, v. 19, n. 2, p. 175 - 180, 2002.

LEE, K.; FOGLIA, T. A.; CHANG, K. **Production of alkyl ester as biodiesel from fractionated lard and restaurant grease.** *Journal of the American Oil Chemists' Society*, v. 79, p. 191 - 195, 2002.

LEHNINGER, A. L; NELSON, D. L; COX, M. M. **Princípios de Bioquímica.** 2ª edição. Editora Sarvier, São Paulo, 1995.

LIAO, X., ZHANG, Y., BEI, J., HU, X., WU, J. **Alterations of molecular properties of lipoxygenase induced by dense phase carbon dioxide**. *Innovative Food Science and Emerging Technologies*, v. 10, p. 47 – 53, 2009.

LIMA, U. A.; AQUARONE, E.; BORZANI, W.; SCHMIDELL, W. **Biotecnologia industrial: Processos fermentativos e enzimáticos.** Editora Edgard Blüncher Ltda., São Paulo, 2001.

LIN, T. J.; CHEN, S. W.; CHANG, A. C. **Enrichment of n-3 PUFA contents on triglycerides of fish oil by lipase catalyzed trans-esterification under supercritical conditions**. *Biochemical Engineering Journal*, v. 29, p. 27 - 34, 2006.

LIU, Y.; CHEN, D.; XU, L.; YAN, Y. **Evaluation of structure and hydrolysis activity of *Candida rugosa* Lip7 in presence of sub-/super-critical CO_2.** *Enzyme and Microbial Technology*, v. 51, p. 354 – 358, 2012.

LIU, Y.; CHEN, D.; WANG, S. **Effect of sub- and super-critical CO_2 pretreatment on conformation and catalytic properties evaluation of two commercial enzymes of CALB and Lipase PS.** *Journal of Chemical Technology and Biotechnology*, v. 88, p. 1750 – 1756, 2013a.

LIU, Y.; CHEN, D.; YAN, Y. **Effect of ionic liquids, organic solvents and supercritical CO_2 pretreatment on the conformation and catalytic properties of *Candida rugosa* lipase.** *Journal of Molecular Catalysis B: Enzymatic*, v. 90, p. 123 – 127, 2013b.

LUTZ, S. **Engineering lipase B from *Candida antarctica*.** *Tetrahedron: Asymmetry*, v. 15, p. 2743 – 2748, 2004.

MACRAE, A. R. and HAMMOND, R. C. **Present and future applications of lipases.** *Biotechnology and Genetic Reviews*, v. 3, p. 193 – 217, 1985.

MANERA, A. P.; KUHN, G.; POLLONI, A.; MARANGONI, M.; ZABOT, G.; KALIL, S. J.; OLIVEIRA, D.; TREICHEL, H.; OLIVEIRA, J. V.; MAZUTTI, M. A.; MAUGERI, F. **Effect of compressed fluids treatment on the activity, stability and enzymatic reaction performance of β-galactosidase.** *Food Chemistry*, v. 125, p. 1235 – 1240, 2011.

MATSUDA, T. **Review: Recent progress in biocatalysis using supercritical carbon dioxide.** *Journal of Bioscience and Bioengineering*, v. 115, n. 3, p. 233 – 241, 2013.

McCABE, R. W. and TAYLOR, A. **An investigation of the acyl-binding site of *Candida antarctica* lipase B.** *Enzyme and Microbial Technology*, v. 35, p. 393 – 398, 2004.

McCOY, A. J., GROSSE-KUNSTLEVE, R. W., ADAMS, P. D., WINN, M. D., STORONI, L. C., READ, R. J. *Phaser* **crystallographic software.** *Journal of Applied Crystallography*, v. 40, p. 658 – 674, 2007.

MELGOSA, R.; SANZ, M. T.; SOLAESA, A. G.; BUCIO, S. L.; BELTRÁN, S. **Enzymatic activity and conformational and morphological studies of four commercial lipases treated with supercritical carbon dioxide.** *Journal of Supercritical Fluids,* v. 97, p. 51 – 62, 2015.

MICHELS, P. C.; HEI, D.; CLARK, D. S. **Pressure effects on enzyme activity and stability at high temperatures.** *Advances in Protein Chemistry*, v. 48, p. 341 – 376, 1996.

MONHEMI, H. and HOUSAINDOKHT, M. R. **How enzymes can remain active and stable in a compressed gas? New insights into the conformational stability of *Candida antarctica* lipase B in near-critical propane.** *Journal of Supercritical Fluids*, v. 72, p. 161 – 167, 2012.

MONHEMI, H.; HOUSAINDOKHT, M. R.; BOZORGMEHR, M. R.; GOOGHERI, M. S. S. **Enzyme is stabilized by a protection layer of ionic liquids in supercritical CO2: Insights from molecular dynamic simulation.** *Journal of Supercritical Fluids*, v. 69, p. 1 – 7, 2012.

MORAIS, M.; NUNES, J. P. M.; KARU, K.; FORTE, N.; NENNI, I.; SMITH, M. E. B.; CADDICK, S.; CHUDASAMA, V.; BAKER, J. R. **Optimisation of the dibromomaleimide (DBM) platform for native antibody conjugation by accelerated post-conjugation hydrolysis.** *Organic & Biomolecular Chemistry*, v. 15, p. 2947 - 2952, 2017. *Electronic Supplementary Information.*

MOURA, J. M. L. N.; RIBEIRO, A. P. B.; GRIMALDI, R.; GONÇALVES, L. A. G. **Reator de membrana enzimático e fluidos supercríticos: associação de processos.** *Química Nova*, v. 30, n. 4, p. 965 – 969, 2007.

MOZHAEV, V. V.; HEREMANS, K.; FRANK, J.; MASSON, P.; BALNY, C. **High pressure effects on protein structure and function.** *Proteins,* v. 24, p. 81 - 91, 1996a.

MOZHAEV, V. V.; LANGE, R.; KUDRYASHOVA, E. V.; BALNY, C. **Application of high hydrostatic pressure for increasing activity and stability of enzymes.** *Biotechnology and Bioengineering*, v. 52, p. 320 –331, 1996b.

NAKAYA, H.; MIYAWAKI, O.; NAKAMURA, K. **Determination of *log P* for pressurized carbon dioxide and its characterization as a medium for enzyme reaction.** *Enzyme and Microbial Technology*, v. 28, p. 176 – 182, 2001.

NC-IUB, Nomenclature Committee of the International Union of Biochemistry (1979) **Units of Enzyme Activity.** *European Journal of Biochemistry*, 97, 319 -320. New England BioLabs Inc., **Enzymatic removal of *N*- and *O*-glycans using PNGase F or the Protein Deglycosylation Mix.** Application Note.

NICOLETTI, G., CIPOLATTI, E. P., VALÉRIO, A., CARBONERA, N. T. G., SOARES, N. S., THEILACKER, E., NINOW, J. L., OLIVEIRA, D. **Evaluation of different methods for immobilization of *Candida antarctica* lipase B (CalB lipase) in polyurethane foam and its application in the production of geranyl propionate.** *Bioprocess and Biosystems Engineering*, v. 38, n. 9, p. 1739 – 1748, 2015.

NIESEN, F. H., BERGLUND, H., VEDADI, M. **The use of differential scanning fluorimetry to detect ligand interactions that promote protein stability.** *Nature Protocols,* v. 2, p. 2212 – 2221, 2007.

OLIVEIRA, D. **Estudo comparativo da produção enzimática de ésteres a partir de óleos vegetais em solvente orgânico e CO$_2$**

supercrítico. Tese de Doutorado em Engenharia Química, Universidade Federal do Rio de Janeiro, Rio de Janeiro, 1999.

OLIVEIRA, G. L. and MANTOVANI, M. S. **Transformações biológicas: Contribuições e perspectivas.** *Química Nova,* v. 32, n. 3, p. 742 - 756, 2009.

OLIVEIRA, J. V. and OLIVEIRA, D. **Kinetics of the enzymatic alcoholysis palm kernel oil in supercritical CO_2.** *Industrial and Engineering Chemistry Research*, v. 39, p. 4450 - 4454, 2000.

OLIVEIRA, D. and OLIVEIRA, J. V. **Enzymatic alcoholysis of palm kernel oil in n-hexane and $SC-CO_2$.** *Journal of Supercritical Fluids*, v. 19, p. 141 - 148, 2001.

OLIVEIRA, D.; FEIHRMANN, A. C.; RUBIRA, A. F.; KUNITA, M. H.; DARIVA, C.; OLIVEIRA, J. V. **Assessment of two immobilized lipases activity treated in compressed fluids**. *Journal of Supercritical Fluids*, v. 38, p. 373 – 382, 2006a.

OLIVEIRA, D.; FEIHRMANN, A. C.; DARIVA, C.; CUNHA, A. G.; BEVILAQUA, J. V.; DESTAIN, J.; OLIVEIRA, J. V.; FREIRE, D. M. G. **Influence of compressed fluids treatment on the activity of *Yarrowia lipolytica* lipase.** *Journal of Molecular Catalysis B: Enzymatic*, v. 39, p. 117 - 123, 2006b.

OTTOSSON, J., FRANSSON, L., KING, J. W., HULT, K. **Size as a parameter for solvent effects on *Candida antarctica* lipase B enantioselectivity.** *Biochimica et Biophysica Acta*, v. 1594, p. 325 – 334, 2002.

PALJEVAC, M.; PRIMOZIC, M.; HABULIN, M.; NOVAK, Z.; KNEZ, Z. **Hydrolysis of carboxymethyl cellulose catalyzed by cellulose immobilized on silica gels at low and high pressures.** *The Journal of Supercritical Fluids*, v. 43, p. 74 – 80, 2007.

PANDEY, A.; SELVAKUMAR, P.; SOCCOL, C. R.; NIGAM, P. **Solid state fermentation for the production of industrial enzymes.** *Current Science,* v. 77, p. 149 - 162, 1999.

PAQUES, F. W. and MACEDO, G. A. **Lipases de látex vegetais: Propriedades e aplicações industriais**. *Química Nova*, v. 29, p. 93 - 99, 2006.

PARK, S.Y. and LEE, H. **Structural and experimental evidences for *Candida antarctica* lipase B enantiomeric recognition towards a bulky sec-alcohol.** To be published. *Protein Data Bank*, 2017.
PATEL, R. N. **Microbial/enzymatic synthesis of chiral intermediates for pharmaceuticals.** *Enzyme and Microbial Technology*, v. 31, p. 804 - 826, 2002.

PINHEIRO, D. M. **Produção de lipase por *Penicillium restrictum*.** Dissertação de Mestrado em Ciências - Instituto de Química, Universidade Federal do Rio de Janeiro - UFRJ, Rio de Janeiro, 1992.

PIYATHEERAWONG, W., IWASAKI, Y., XU, X. B., YAMANE, T. **Dependency of water concentration on ethanolysis of trioleoylglycerol by lipases.** *Journal of Molecular Catalysis B: Enzymatic*, v. 28, p. 19 – 24, 2004.

PIZARRO, A. V. L. and PARK, E. Y. **Lipase-catalysed production of biodiesel fuel from vegetable oils contained in waste activated bleaching earth.** *Process Biochemistry*, v. 38, p. 1077 - 1082, 2003.

PRADO, G. H. C.; KHAN, M.; SALDAÑA, M. D. A.; TEMELLI, F. **Enzymatic hydrolysis of conjugated linoliec acid-enriched anhydrous milk fat in supercritical carbon dioxide.** *Journal of Supercritical Fluids*, v. 66, p. 198 - 206, 2012.

PRIMO, M. S.; CENI, G. C.; MARCON, N. S.; ANTUNES, O. A. C.; OLIVEIRA, D.; OLIVEIRA, J. V. **Effects of compressed carbon dioxide treatment on the specificity of oxidase enzymatic complexes from mate tea leaves.** *Journal of Supercritical Fluids*, v. 43, p. 283–290, 2007.

QIAN, Z.; HORTON, J. R.; CHENG, X.; LUTZ, S. **Structural redesign of lipase B from *Candida antarctica* by circular permutation and incremental truncation.** *Journal of Molecular Biology*, v. 393, p. 191 – 201, 2009.

RAZA, S.; FRANSSON, L.; HULT, K. **Enantioselectivity in *Candida antarctica* lipase B: A molecular dynamics study.** *Protein Science*, v. 10, p. 329 – 338, 2001.

REISNER, A. H., NEMES, P., BUCHOLTZ, C. **The use of Coomassie Brilliant Blue G250 perchloric acid solution for staining in electrophoresis and isoelectric focusing on polyacrylamide gels.** *Analytical Biochemistry,* v. 64, n. 2, p. 509 - 516, 1975.

REZAEI, K.; TEMELLI, F.; JENAB, E. **Effects of pressure and temperature on enzymatic reactions in supercritical fluids.** *Biotechnology Advances*, v. 25, p. 272 – 280, 2007.

ROTH, Z.; YEHEZKEL, G.; KHALAILA, I. **Identification and quantification of protein glycosylation.** *International Journal of Carbohydrate Chemistry*, Article ID 640923, v. 2012, p. 1 - 10, 2012.

RUPP, B. **Biomolecular crystallography: principles, practice, and application to structural biology.** New York: Garland Science, 2010.

SANTOS, K. F. **Structural and functional studies of the spliceosomal RNP remodeling enzyme Brr2.** Dissertation for the award of the degree "Doctor of Philosophy" at Division of Mathematics and Natural Sciences of the Georg-August-Universität Göttingen, 2012.

SAVAGE, P. E.; GOPALAN, S.; MIZAN, T. I.; MARTINO, C. J.; BROCK, E. E. **Reactions at supercritical conditions: Applications and fundamentals.** *AIChE Journal*, v. 41, p. 1723 - 1778, 1995.

SAXENA, R. K.; DAVIDSON, W. S.; SHEORAN, A.; BHOOPANDER, G. **Purification and characterization of an alkaline thermostable lipase from *Aspergillus carneus*.** *Journal Microbiology Methodology,* v. 39, p. 239 - 247, 2003a.

SAXENA, R. K.; SHEORAN, A.; GIRI, B.; DAVIDSON, S. **Purification strategies for microbial lipases.** *Journal of Microbiological Methods*, v. 52, p. 1 – 18, 2003b.

SCHERER, R. P. **Estudo da imobilização de lipase comercial de pâncreas suíno em diferentes suportes inorgânicos.** Dissertação de Mestrado em Engenharia de Alimentos, Universidade Regional Integrada do Alto Uruguai e das Missões – URI, Erechim, 2010.

SCHREIBER, A and BORTON, C. (2010) **Target and non-target screening for pesticide residues in food samples using the AB SCIEX TipleTOF™ 5600 system.** AB SCIEX. Available from: http://sciex.com/Documents/Downloads/Literature/mass-spectrometry-tripletof_pesticide_screening.pdf

SCRIBAN, E. **Biotecnologia.** Editora Malone, São Paulo, 1985.
SEDMAK, J.J.; and GROSSBERG, S.E. **A rapid, sensitive, and versatile assay for protein using Coomassie brilliant blue G250.** *Anaytical Biochemistry,* v. 79, n. 1-2, p. 544 - 552, 1977.

SENYAY-ONCEL, D. and YESIL-CELIKTAS, O. **Treatment of immobilized α-amylase under supercritical CO_2 conditions: Can activity be enhanced after consecutive enzymatic reactions?** *Journal of Molecular Catalysis B: Enzymatic*, v. 91, p. 72 – 76, 2013.

SHIN, A-K.; SIM, J-E.; KISHIMURA, H.; CHUN, B-S. **Characteristics of menhaden oil ethanolysis by immobilized lipase in supercritical carbon dioxide.** *Journal of Industrial and Engineering Chemistry*, v. 18, p. 546 - 550, 2012.

SILVA, M. F.; GOLUNSKI, S. M.; RIGO, D.; MOSSI, V.; DI LUCCIO, M.; MAZUTTI, M. A.; OLIVEIRA, D.; OLIVEIRA, J. V.; TREICHEL, H. **Pressurized propane: An alternative technique to increase inulinase activity.** *Industrial Biotechnology*, v. 8, n. 5, 2012.

SILVA, M. F.; GOLUNSKI, S. M.; RIGO, D.; MOSSI, V.; DI LUCCIO, M.; MAZUTTI, M. A.; PERGHER, S. B. C.; OLIVEIRA, D.; OLIVEIRA, J. V.; TREICHEL, H. **Liquefied petroleum gas as solvent medium for the treatment of immobilized inulinases.** *Journal of Chemical Technology and Biotechnology*, v. 88, p. 280 – 286, 2013a.

SILVA, M. F.; RIGO, D.; MOSSI, V.; DALLAGO, R. M.; DI LUCCIO, M.; HENRICK, P., KUHN, G. O.; DALLA ROSA, C.; OLIVEIRA, D.; OLIVEIRA J. V.; TREICHEL, H. **Evaluation of enzymatic activity of**

commercial inulinase from *Aspergillus niger* **immobilized in polyurethane foam.** *Food and Bioproducts Processing,* v. 91, p. 54 – 59, 2013b.

SILVA, M. F.; RIGO, D.; MOSSI, V.; GOLUNSKI, S.; KUHN, G. O.; DI LUCCIO, M.; DALLAGO, R.; OLIVEIRA, D.; OLIVEIRA J. V.; TREICHEL, H. **Enzymatic synthesis of fructooligosaccharides by inulinases from** *Aspergillus niger* **and** *Kluyveromyces marxianus* **NRRL Y-7571 in aqueous–organic médium.** *Food Chemistry*, v. 138, p. 148 – 153, 2013c.

SILVA, J. R. F.; CANTELLI, K. C.; TRES, M. V.; DALLA ROSA, C.; MEIRELLES, M. A. A.; SOARES, M. B. A.; OLIVEIRA, D.; OLIVEIRA, J. V.; TREICHEL, H.; MAZUTTI, M. A. **Treatment with compressed liquefied petroleum gas and ultrasound to improve celulase activity.** *Biocatalysis and Agricultural Biotechnology,* v. 2, p. 102 – 107, 2013d.

SKJØT, M.; DE MARIA, L.; CHATTERJEE, R.; SVENDSEN, A.; PATKAR, S. A.; ØSTERGAARD, P. R.; BRASK, J. **Understanding the plasticity of the alpha/beta hydrolase fold: lid swapping on the** *Candida antarctica* **lipase B results in chimeras with interesting biocatalytic properties.** *ChemBioChem*, v. 10, p. 520 – 527, 2009.

SOARES, C. M. F. **Otimização por planejamento experimental da imobilização de lipase em sílica de porosidade controlada na presença de estabilizantes.** Dissertação de Mestrado em Engenharia Química, Universidade Estadual de Campinas - UNICAMP, Campinas, 2000.

STAUCH, B.; FISHER, S. J.; CIANCI, M. **Open and closed states of** *Candida antarctica* **lipase B: protonation and the mechanism of interfacial activation.** *Journal of Lipid Research*, v. 56, p. 2348-2358, 2015.

STRYER, L. **Biochemistry.** Editora Freeman, New York, 1995.
STRZELCZYK, P.; BUJACZ, G. D.; KIELBASINSKI, P.; BLASZCZYK, J. **Crystal and molecular structure of hexagonal form**

of lipase B from *Candida antarctica***.** *Acta Biochimica Polonica*, v. 63, n. 1, p. 103-109, 2016.

SUBRAMANIAM, B. and McHUGH, M. **Reactions in supercritical fluids – a review.** *Industrial & Engineering Chemistry Process Design and Development*, v. 25, p. 1 - 12, 1988.

SUN, M. M. C.; TOLLIDAY, N.; VETRIANI, C.; ROBB, F. T.; CLARK, D. S. **Pressure-induced thermostabilization of glutamate dehydrogenase from the hyperthermophile *Pyrococcus furiosus***.** *Protein Science*, v. 8, p. 1056 – 1063, 1999.

SUN, M. M. C.; CAILLOT, R.; MAK, G.; ROBB, F. T.; CLARK, D. S. **Mechanism of pressure-induced thermostabilization of proteins: Studies of glutamate dehydrogenases from the hyperthermophile *Thermococcus litoralis.*** *Protein Science*, v. 10, n. 9, p. 1750 – 1757, 2001.

TANAKA, N.; IKEDA, C.; KANAORI, K.; HIRAGA, K.; KONNO, T.; KUNUGI, S. **Pressure effect on the conformational fluctuation of apomyoglobin in the native state.** *Biochemistry*, v. 39, n. 39, p. 12063 – 12068, 2000.

TANIGUCHI, Y.; SUZUKI, K. **Pressure inactivation of α-chymotrypsin.** Journal of Physical Chemistry, v. 87, p. 5185 – 5193, 1983.

TREICHEL, H.; OLIVEIRA, D.; MAZUTTI, M. A.; DI LUCCIO, M.; OLIVEIRA, V. J. **A review on microbial lipases production.** *Food and Bioprocess Technology*, v. 3, p. 182 - 196, 2010.

UPPENBERG, J.; PATKAR, S.; BERGFORS, T., JONES, T. A. **Crystallization and preliminary X-ray studies of lipase B from *Candida Antarctica.*** *Journal of Molecular Biology*, v. 235, p. 790 - 792, 1994a.

UPPENBERG, J.; HANSEN, M. T.; PATKAR, S.; JONES, T. A. **The sequence, crystal structure determination and refinement of two crystal forms of lipase B from *Candida antarctica***.** *Structure*, v. 2, p. 293 - 308, 1994b.

UPPENBERG, J.; OHNER, N.; NORIN, M.; HULT, K. KLEYWEGT, G. J.; PATKAR, S.; WAAFEN, V.; ANTHONSEN, T.; JONES, T. A. **Crystallographic and molecular-modeling studies of lipase B from *Candida antarctica* reveal a stereospecificity pocket for secondary alcohols.** *Biochemistry*, v. 34, p. 16838 - 16851, 1995.

VAGIN, A. A., STEINER, R. A., LEBEDEV, A. A., POTTERTON, L., McNICHOLAS, S., LONG, F., MURSHUDOV, G. N. **REFMAC5 dictionary: organization of prior chemical knowledge and guidelines for its use.** *Acta Crystallographica Section D - Biological crystallography*, v. 60, p. 2184 – 2195, 2004.

VALÉRIO, A., NICOLETTI, G., CIPOLATTI, E. P., NINOW, J. L., ARAÚJO, P. H. H., SAYER, C., OLIVEIRA, D. **Kinetic Study of *Candida antarctica* Lipase B Immobilization Using Poly(Methyl Methacrylate) Nanoparticles Obtained by Miniemulsion Polymerization as Support.** *Applied Biochemistry and Biotechnology*, v. 175, n. 6, p. 2961 – 2971, 2015.

VELD, M. A. J. *Candida antarctica* **Lipase B catalysis in organic, polymer and supramolecular chemistry.** Doctoral thesis for the award of the degree "Doctor of Philosophy" in Chemical Engineering at Technische Universität Eindhoven, Germany, 2010.

VEZOCNIK, V., REBOLJ, K., SITAR, S., OTA, K., TUSEK-ZNIDARIC, M., STRUS, J., SEPCIC, K., PAHOVNIK, D., MACEK, P., ZAGAR, E. **Size fractionation and size characterization of nanoemulsions of lipid droplets and large unilamellar lipid vesicles by asymmetric-flow field-flow fractionation/multi-angle light scattering and dynamic light scattering.** *Journal of Chromatography A,* v. 1418, p. 185 – 191, 2015.

VILLENEUVE, P**. Plant lipases and their applications in oils and fats modification.** *European Journal of Lipid Science and Technology,* v. 105, p. 308 - 317, 2003.

VILLENEUVE, P.; MUDERHWA, J. M.; GRAILLE, J.; HAAS, M. J. **Customizing lipases for biocatalysis: a survey of chemical, physical**

and molecular biological approaches. *Journal of Molecular Catalysis B: Enzymatic*, v. 9, p. 113 - 148, 2000.

WANG, W. **Review: Lyophilization and development of solid protein pharmaceuticals.** *International Journal of Pharmaceutics*, v. 203, p. 1 - 60, 2000.

WANG, S. S.-S., CHAO, H.-S., LIU, H.-L., LIU, H.-S. **Stability of hen egg white lysozyme during denaturation is enhanced by pretreatment with supercritical carbon dioxide.** *Journal of Bioscience and Bioengineering,* v. 107, n. 4, p. 355 - 359, 2009.

WANG, S. S.-S., LAI, J.-T., HUANG, M.-S., TAI, C. Y., LIU, H.-S. **Deactivation of isoamylase and β-amylase in the agitated reactor under supercritical carbon dioxide.** *Bioprocess and Biosystems Engineering*, v. 33, p. 1007-1015, 2010.

WEN, D.; JIANG, H.; ZHANG, K. **Supercritical fluids technology for clean biofuel production.** *Progress in Natural Science*, v. 19, p. 273 - 284, 2009.

WESCOTT, C. R. and KLIBANOV, A. M. **The solvent dependence of enzyme specificity.** *Biochimica et Biophysica Acta*, v. 1206, p. 1 – 9, 1994.

WINKLER, U. K. and STUCKMANN, M. **Glycogen, hyaluronate, and some other polysaccharides greatly enhance the formation of exolipase by** *Serratia marcescens***.** *Journal of Bacteriology*, v. 138, p. 663 – 670, 1979.

WITTGREN, B. and WAHLUND, K.-G. **Fast molecular mass and size characterization of polysaccharides using asymmetrical flow field-flow fractionation-multiangle light scattering.** *Journal of Chromatography A,* v. 760, p. 205 – 218, 1997.

WYATT, P. J. **Light scattering and the absolute characterization of macromolecules.** *Analytica Chimica Acta,* v. 272, p. 1 - 40, 1993.

XIE, Y.; AN, J.; YANG, G.; WU, G.; ZHANG, Y.; CUI, L.; FENG, Y. **Enhanced enzyme kinetic stability by increasing rigidity within the**

active site. *Journal of Biological Chemistry*, v. 289, p. 7994 - 8006, 2014.

ZALE, S. E. and KLIBANOV, A. M. **Why does ribonuclease irreversibly inactivate at high temperatures?** *Biochemistry*, v. 25, p. 5432 - 5444, 1986.

ZHOU, L., WU, J., HU, X., ZHI, X., LIAO, X. **Alterations in the activity and structure of pectin methylesterase treated by high pressure carbon dioxide.** *Journal of Agricultural and Food Chemistry*, v. 57, p. 1890 – 1895, 2009.

ZHU, K., JUTILA, A., KINNUNEN, P. K. J. **Steady state and time resolved effects of guanidine hydrochloride on the structure of** *Humicola lanuginosa* **lipase revealed by fluorescence spectroscopy.** *Protein Science*, v. 9, p. 598 – 609, 2000.